Membrane concepts for blood purification

towards improved artificial kidney devices

Marlon Tijink

MEMBRANE CONCEPTS FOR BLOOD PURIFICATION

TOWARDS IMPROVED ARTIFICIAL KIDNEY DEVICES

The research described in this thesis is financially supported by the Dutch Kidney Foundation

Promotion Committee

Prof. Dr. M. Wessling (promotor)	University of Twente
Dr. D. Stamatialis (assistant promotor)	University of Twente
Dr. T. Keller	Fresenius Medical Care, Germany
Prof. Dr. G. Catapano	University of Calabria, Italy
Prof. Dr. L. Koole	University of Maastricht
Prof. Dr. R. Lammertink	University of Twente
Prof. Dr. D. Grijpma	University of Twente
Prof. Dr. G. Van der Steenhoven (chairman)	University of Twente

Membrane concepts for blood purification – towards improved artificial kidney devices

Marlon Tijink

PhD Thesis, University of Twente, The Netherlands

ISBN: 978-90-365-3547-2

DOI: 10.3990/1.9789036535472

Cover design by Marlon Tijink

Printed by Gildeprint Drukkerijen - Enschede

MEMBRANE CONCEPTS FOR BLOOD PURIFICATION

TOWARDS IMPROVED ARTIFICIAL KIDNEY DEVICES

PROEFSCHRIFT

ter verkrijging van

de graad van doctor aan de Universiteit Twente,

op gezag van de rector magnificus,

prof. dr. H. Brinksma

volgens besluit van het College voor Promoties

in het openbaar te verdedigen op

vrijdag 24 mei 2013 om 12.45 uur

door

Marlon Susanne Liesbeth Tijink

geboren op 5 februari 1985

te Almelo

Dit proefschrift is goedgekeurd door:

promotor:

Prof. Dr. -Ing. M. Wessling

en assistent promotor:

Dr. D. Stamatialis

Table of Contents

1

General introduction

1.1. The kidneys

In general, people have two kidneys and they are located in the abdominal cavity and are approximately 11 cm long and about 160 gram each [1]. The kidneys regulate [2]:

- Body fluid osmolarity and volume
- Electrolyte balance
- Acid-base balance
- Excretion of metabolic products and foreign substances
- Production and secretion of hormones

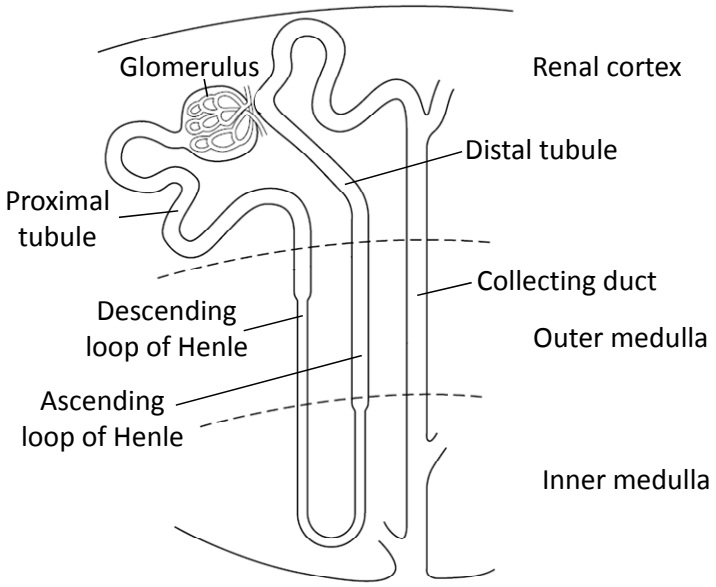

Figure 1. Schematic figure of the nephron, adapted from [3].

Each kidney contains approximately 1.2 million nephrons which are the functional units of the kidney to clear the blood and form urine (see Figure 1). Initial filtering of the blood occurs in the glomerulus to form ultrafiltrate. In the following steps, more specific clearance takes place by tubular readsorption and secretion [2]. Renal failure results in accumulation of waste products and excess fluids in the body. Transplantation of a donor kidney would generally be the best treatment, but the availability of donor kidneys is limited [4, 5]. The majority of the patients is treated with extracorporeal blood purification treatments such as hemodialysis [5].

1.2. Extracorporeal blood purification

Extracorporeal blood purification is a treatment commonly used for patients with end stage renal disease (ESRD), acute renal failure, liver failure, sepsis, multi-organ failure or poisoning. Membranes are often responsible for the purification step in extra corporeal purification treatments (see Figure 2).

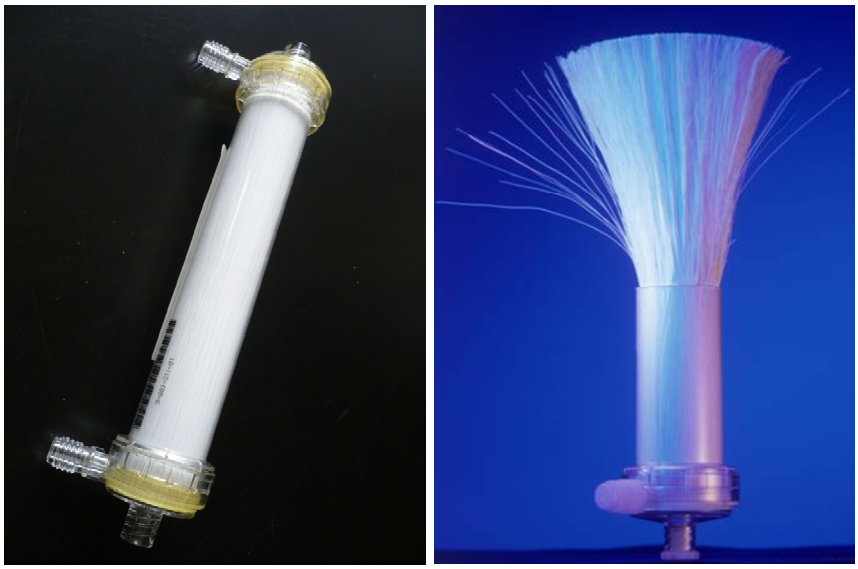

Figure 2. Pictures of hemodialyzers containing hollow fiber membranes, adapted from [1]

Kolff *et al.* saved for the first time a patient's life with a hemodialysis treatment in 1945 [6, 7]. A 67 year old woman with acute renal failure was dialyzed using the rotating drum dialyzer developed by Kolff *et al.* which contained 30 meters of cellophane membrane tubing. Many developments have been going on before and after this milestone and are well described elsewhere [8].

Risk factors such as diabetes and obesity become more and more present and the prevalence of chronic kidney disease (CKD) is increasing globally [9-11]. In the United States population, the ESRD prevalence was 1699 per million in 2008 [5]. The incidence of ESRD is around 135 per million and 336 per million in Europe and USA respectively and is expected to increase further in the future [11]. In The Netherlands 5372 patients are treated with hemodialysis and 998 with peritoneal dialysis in 2012 and the majority of these patients is older than 65 years [12]. Although considerable amounts of healthcare budgets are spent on renal replacement therapy [9, 13], the mortality of hemodialysis patients is still high [14, 15] and their health related quality of life generally low [16]. For hemodialysis patients, the 1 year mortality rates are 6.6% in Japan, 15.6% in Europe and 21.7% in the US [17]. This is also reflected in the expected remaining life years, which are 25.0 years for the general US population, 15.7 for ESRD patients with a kidney transplant and 5.6 years for ESRD patients receiving dialysis treatment [18].

1.3. Uremic retention solutes

Uremic retention solutes which would normally be excreted by the healthy kidneys are retained in the body of uremic patients. The uremic retention solutes which cause adverse biological effects are called uremic toxins [19, 20]. Uremic retention solutes are generally categorized in three groups [21, 22]. The small water-soluble molecules have a molecular weight smaller than 500 Dalton, urea and creatinine are examples of this group [21]. The middle molecules are specified with a molecular weight larger than 500 Dalton with β_2-microglobulin as prototype of this group [21, 22]. The protein-bound solutes are specified by their protein-binding with examples indoxyl sulfate and p-

cresylsulfate [21, 22]. Many of the compounds with expected biological adverse effects are difficult to remove by conventional dialysis. Either because of their size or as a consequence of protein-binding [14, 21-29]. The middle molecule β_2-microglobulin is related to hemodialysis-associated-amyloidosis and is also related to mortality in dialysis patients [26, 28]. Normally, protein-bound toxins are mainly excreted into urine by tubular secretion and for hemodialysis patients elevated levels are reported [22, 30]. Protein-bound toxins are involved in generation of reactive oxygen species and associated with cardiovascular disease and progression of chronic kidney disease [25, 27, 29, 31]. For example, indoxyl sulfate is pro-inflammatory [32] and can cause *in vitro* leukocyte adhesion [33] and cardiac fibrosis [32]. Administration of indoxyl sulfate to hypertensive rats led to aortic calcification and expression of senescence related proteins [25, 34]. Furthermore, free serum concentrations of p-cresol (which circulates in the body mainly as p-cresylsulfate) are related to mortality in hemodialysis patients [35].

Protein-bound solute clearance using current treatment strategies can be improved under certain conditions, but is still rather limited [36]. Post dilution online hemodiafiltration has shown to significantly lower the total pre-dialysis concentrations of p-cresylsulfate and 3-carboxyl-4-methyl-5-propyl-2-furanpropionic acid (CMPF), two protein-bound toxins with high protein-binding [37]. However the effect on the total concentration was only moderate and no significant effect on the free fraction (which causes biological effects) was obtained. Currently, a treatment strategy to efficiently remove protein-bound uremic toxins is still missing.

1.4. Wearable artificial kidneys (WAK)

Several wearable artificial kidneys (WAK) are in development and often based on peritoneal dialysis as well as on hemodialysis principles [38, 39]. Therefore, the removal of difficult to remove toxins will most likely not be improved compared to these conventional therapies. In contrast to the healthy kidneys which are working continuously, extracorporeal treatments like hemodialysis are

often applied 3 times a week for 4h. However, using WAK, treatment times could be prolonged. This can be advantageous, as longer treatment times are associated with improvements on survival [15]. Probably because of improved clearance of small water soluble molecules and also middle molecules, but still protein-bound toxin removal is not improved [40]. Although clearance may be improved, longer treatment times additionally imply more blood–material contact, making the material's biocompatibility a very important issue. In fact, Davenport *et al.* reported about a pilot study with a wearable artificial hemodialysis device, however, 2 out of 8 patients had clotting problems and the treatment was discontinued, emphasizing the need for materials with better biocompatibility [38]. Often adsorptive columns are used in WAK for the regeneration of the dialysate. Hence, the WAK consist out of several modalities like a membrane module and an adsorptive column etc., and combination of techniques and miniaturization of the devices seems to be an important step for the future.

1.5. Adsorption

Adsorptive techniques can improve the removal of middle molecules and protein-bound toxins [41-57]. Fractionated plasma separation and adsorption (FPSA) treatment can significantly lower p-cresylsulfate concentrations [58]. Activated carbons can adsorb p-cresylsulfate and β_2-microglobulin and other uremic toxins [48, 59, 60]. Moreover, the combination of hemodialysis with hemoperfusion can lead to improved clearance of middle molecules and a survival advantage compared to hemodialysis alone [61]. Furthermore, in WAK, a separate unit with adsorptive columns is often used for the regeneration of dialysate. The combination of membrane based transport and toxin removal by adsorption seems to be very attractive, but is often combined in separate steps [58, 61, 62].

To improve protein-bound toxin removal, the concentration of free toxin on the dialysate side should be low, so that there is a continuous driving force for the free fraction in the blood to diffuse

to the dialysate side over the whole hemodialyzer length [63]. This was illustrated by the study of Dinh *et al.* that showed that addition of powdered activated carbon into the dialysate compartment of a dialyzer can improve the clearance of protein-bound solutes compared to a hemoperfusion column [60]. Mathematical modeling predicts that the clearance of protein-bound toxins can be increased by addition of adsorptive particles to the dialysate or by increasing the dialysate flow [45]. This model was confirmed by an experimental study showing that these strategies can lead to increased clearances of protein-bound toxins while the clearance of water soluble molecules was not altered [45]. Besides, *in vivo* studies recently showed that protein-bound clearances have been improved by using higher dialysate flow rates [64]. Important to note is that dissociation rates for protein-bound solutes are fast in relation to the time spent in the artificial kidney membrane module [65, 66]. The above mentioned principle is also interesting to apply in WAKS in order to decrease the amount of necessary dialysate and improve toxin removal at the same time.

Instead of addition of activated carbon particles to the dialysate, adsorptive particles could be incorporated in the membrane itself to maintain the concentration difference driving force over the entire length of the membrane module in principle. In the 1970s so called sorbent membranes were developed [67, 68]. The concept was basically that adsorptive particles were embedded between two cuprophan membrane layers, or within a cuprophan matrix, so that this sorbent membrane could have both filtering and adsorbing capacity for uremic toxins [69]. However, cuprophan was shown to be rather bio incompatible and there was no focus on the removal of protein-bound toxins. After a clinical trial using sorbent membranes in a parallel plate dialyzer, patients rated the sorbent membrane treatment low [70], which might be due to lack of adsorbents with high purity, possible thrombus formation and because of the bio-incompatible cuprophan membrane material [71]. Later, also due to saturation and manufacturing difficulties, these membranes were removed from the market [67, 72].

1.6. Mixed matrix membrane (MMM)

In membrane science, a membrane with embedded functionalized particles, a so called mixed matrix membrane (MMM), has been proposed as an alternative concept for conventional adsorptive columns [73-75]. In conventional hemoperfusion columns it is very important that the blood or plasma flow is equally distributed within the packed bed with sorbent particles for adequately use of the adsorption capacity. Especially in case of blood which is quite viscous this becomes even more important. Furthermore, channeling can also lead to suboptimal results and even induce clotting within the cartridge. The synergistic approach of MMMs has, when compared to a chromatographic column, a very low flow resistance, and it is possible to use smaller particles leading to more optimal adsorptive capacities and kinetics [76, 77]. The MMM concept is versatile and various membrane matrix as well as embedded particles can be used [73, 74, 76]. There are several adsorptive particles in development for blood purification and also hemocompatible materials for membranes are still in development [48, 53, 56, 78-81] which are interesting to use in a MMM. It would be interesting to apply MMMs in a WAK, since problems related with columns could by avoided by the use of MMMs and the combination of adsorption with a membrane could lead to miniaturization of the device.

1.7. Scope of the thesis

In this thesis, we propose application of mixed matrix membrane (MMM) which combines membrane based removal and adsorption in one step to clear uremic toxins. Adsorptive particles are incorporated into a macro porous membrane matrix. Particles can be homogenously distributed throughout the membrane matrix, preventing cluster formation and also undesired particle release. We hypothesize that the adsorptive particles can help to clear difficult-to-remove uremic toxins such as the protein-bound toxins. Possibly, the embedded adsorptive particles can keep a concentration difference driving force over the complete membrane thereby enhancing the removal of protein-bound toxins. The MMM layer is attached to a particle free blood contacting membrane layer which can regulate solute transport from blood, prevents particle release into the blood and prevents direct blood contact with the adsorptive particles. The dual layer MMMs are also interesting for wearable artificial kidneys since two techniques are combined in one step which may lead to miniaturization. The mixed matrix membrane concept allows use of various particles as well as various membrane matrix materials. Since for longer treatment times as well as for wearable artificial kidneys, the biocompatibility of the device is very important and in this thesis we also evaluate various adsorptive particles as well as a hemocompatible membrane material for an ultimate combination in a mixed matrix membrane.

1.8. Outline of the thesis

This thesis describes preparation and characterization of membranes for blood purification. Chapter 2 and 3 focus on the development of mixed matrix membranes, whereas chapter 4 and 5 are screening potential adsorptive particles and a novel membrane material.

Chapter 2 describes the preparation of a dual layer flat sheet MMM and shows the proof of concept of combining diffusion and adsorption in one step. Addition of activated carbon particles to the polyethersulfone/polyvinylpyrrolidone membrane matrix plays an important role in the membrane formation process, and the obtained membrane morphologies and adsorptive characteristics are discussed. The combined membrane based transport and adsorptive removal are studied using a uremic retention solute.

In **chapter 3** dual layer hollow fiber mixed matrix membranes are developed using a polyethersulfone polyvinylpyrrolidone blend as membrane matrix and activated carbon as adsorptive particle. The effect of various spinning parameters on the characteristics of dual layer hollow fiber mixed matrix membranes are investigated. The removal of several protein-bound uremic toxins is evaluated using protein-bound toxin spiked human blood plasma. The role of adsorption, diffusion and convection is evaluated.

Chapter 4 presents comparison of various adsorptive particles. The activated carbon particles used in chapter 2 and 3 are here compared with two other adsorptive particles. The removal performance for several protein-bound toxins as well as small water soluble molecule creatinine and middle molecule β_2-microglobulin is tested using spiked human blood plasma.

The work in **Chapter 5** investigates membrane formation using the hemocompatible material SlipSkin^{TM} [82]. Effects of polymer composition, solvent and solvent evaporation time on membrane structure and transport properties are systematically studied. Several membranes are evaluated for biocompatibility, based on tests in the ISO categories thrombosis, coagulation, platelets, hematology and complement system.

Finally in **Chapter 6** general conclusions and reflections of the various challenges related to development and characterization of MMMs are discussed and future directions in development of blood purification membranes for improved artificial kidneys are discussed.

References

[1] Stamatialis DF, Papenburg BJ, Girones M, Saiful S, Bettahalli SNM, Schmitmeier S, Wessling M. Medical applications of membranes: Drug delivery, artificial organs and tissue engineering. Journal of Membrane Science 2008;308:1-34.

[2] Berne MNLRM. Principles of physiology. Third edition ed: Mosby; 2000.

[3] De Bruyne LKM. Mechanisms and management of diuretic resistance in congestive heart failure. Postgrad Med J 2003;79:268-71.

[4] Pauly RP, Gill JS, Rose CL, Asad RA, Chery A, Pierratos A, Chan CT. Survival among nocturnal home haemodialysis patients compared to kidney transplant recipients. Nephrology Dialysis Transplantation 2009;24:2915-9.

[5] Bethesda M. U.S. Renal Data System, USRDS 2010 Annual Data Report: Atlas of Chronic Kidney Disease and End-Stage Renal Disease in the United States National Institutes of Health, National Institute of Diabetes and Digestive and Kidney Diseases; 2010.

[6] Kolff WJ. First clinical experience with the artificial kidney. Annals of Internal Medicine 1965;62:608-19.

[7] Kolff WJ, Berk HT, ter Welle M, van der LEY AJ, van Dijk EC, van Noordwijk J. The artificial kidney: a dialyser with a great area. 1944. Journal of the American Society of Nephrology 1997;8:1959-65.

[8] Twardowski ZJ. History of hemodialyzers' designs. Hemodialysis International 2008;12:173-210.

[9] Szczech LA, Lazar IL. Projecting the United States ESRD population: Issues regarding treatment of patients with ESRD. Kidney International, Supplement 2004;66.

[10] Coresh J, et al. Prevalence of chronic kidney disease in the United States. Journal of the American Medical Association 2007;298:2038-47.

[11] Hamer RA, El Nahas AM. The burden of chronic kidney disease. British Medical Journal 2006;332:563-4.

[12] Stichting-RENINE. REgistratie NIerfunktievervanging NEderland, www.renine.nl. Leiden2012.

[13] Kerr M, Bray B, Medcalf J, O'Donoghue DJ, Matthews B. Estimating the financial cost of chronic kidney disease to the NHS in England. Nephrology Dialysis Transplantation 2012.

[14] Grooteman MPC, et al. Effect of online hemodiafiltration on all-cause mortality and cardiovascular outcomes. Journal of the American Society of Nephrology 2012;23:1087-96.

[15] Lacson Jr E, et al. Survival with three-times weekly in-center nocturnal versus conventional hemodialysis. Journal of the American Society of Nephrology 2012;23:687-95.

[16] Mazairac AHA, et al. Changes in quality of life over time-Dutch haemodialysis patients and general population compared. Nephrology Dialysis Transplantation 2011;26:1984-9.

[17] Goodkin DA, et al. Association of Comorbid Conditions and Mortality in Hemodialysis Patients in Europe, Japan, and the United States: The Dialysis Outcomes and Practice Patterns Study (DOPPS). Journal of the American Society of Nephrology 2003;14:3270-7.

[18] Bethesda M. U.S. Renal Data System, USRDS 2006 Annual Data Report: Atlas of End-Stage Renal Disease in the United States. National Institutes of Health, National Institute of Diabetes and Digestive and Kidney Diseases; 2006.

[19] Vanholder R, Glorieux G, De Smet R, Lameire N. New insights in uremic toxins. Kidney International 2003;63:S6-S10.

[20] Vanholder R, et al. Uremic toxicity: Present state of the art. International Journal of Artificial Organs 2001;24:695-725.

[21] Vanholder R, et al. Review on uremic toxins: Classification, concentration, and interindividual variability. Kidney International 2003;63:1934-43.

[22] Duranton F, Cohen G, De Smet R, Rodriguez M, Jankowski J, Vanholder R, Argiles A. Normal and pathologic concentrations of uremic toxins. Journal of the American Society of Nephrology 2012;23:1258-70.

[23] Meyer TW. The Removal of Protein-Bound Solutes by Dialysis. Journal of Renal Nutrition 2012;22:203-6.

[24] Niwa T. Update of uremic toxin research by mass spectrometry. Mass Spectrometry Reviews 2011;30:510-21.

[25] Adijiang A, Goto S, Uramoto S, Nishijima F, Niwa T. Indoxyl sulphate promotes aortic calcification with expression of osteoblast-specific proteins in hypertensive rats. Nephrology Dialysis Transplantation 2008;23:1892-901.

[26] Cheung AK, et al. Serum β-2 microglobulin levels predict mortality in dialysis patients: Results of the HEMO study. Journal of the American Society of Nephrology 2006;17:546-55.

[27] Lin CJ, et al. The role of protein-bound uremic toxins on peripheral artery disease and vascular access failure in patients on hemodialysis. Atherosclerosis 2012;225:173-9.

[28] Miyata T, et al. β 2-Microglobulin modified with advanced glycation end products is a major component of hemodialysis-associated amyloidosis. J Clin Invest 1993;92:1243-52.

[29] Wu IW, et al. P-cresyl sulphate and indoxyl sulphate predict progression of chronic kidney disease. Nephrology Dialysis Transplantation 2011;26:938-47.

[30] Deguchi T, Kusuhara H, Takadate A, Endou H, Otagiri M, Sugiyama Y. Characterization of uremic toxin transport by organic anion transporters in the kidney. Kidney International 2004;65:162-74.

[31] Itoh Y, Ezawa A, Kikuchi K, Tsuruta Y, Niwa T. Protein-bound uremic toxins in hemodialysis patients measured by liquid chromatography/tandem mass spectrometry and their effects on endothelial ROS production. Anal Bioanal Chem 2012;403:1841-50.

[32] Lekawanvijit S, Adrahtas A, Kelly DJ, Kompa AR, Wang BH, Krum H. Does indoxyl sulfate, a uraemic toxin, have direct effects on cardiac fibroblasts and myocytes? European Heart Journal 2010;31:1771-9.

[33] Ito S, Osaka M, Higuchi Y, Nishijima F, Ishii H, Yoshida M. Indoxyl Sulfate Induces Leukocyte-Endothelial Interactions through Up-regulation of E-selectin. Journal of Biological Chemistry 2010;285:38869-75.

[34] Adijiang A, Higuchi Y, Nishijima F, Shimizu H, Niwa T. Indoxyl sulfate, a uremic toxin, promotes cell senescence in aorta of hypertensive rats. Biochemical and Biophysical Research Communications 2010;399:637-41.

[35] Bammens B, Evenepoel P, Keuleers H, Verbeke K, Vanrenterghem Y. Free serum concentrations of the protein-bound retention solute p-cresol predict mortality in hemodialysis patients. Kidney International 2006;69:1081-7.

[36] Meert N, et al. Effective removal of protein-bound uraemic solutes by different convective strategies: A prospective trial. Nephrology Dialysis Transplantation 2009;24:562-70.

[37] Meert N, et al. Prospective evaluation of the change of predialysis protein-bound uremic solute concentration with postdilution online hemodiafiltration. Artificial Organs 2010;34:580-5.

[38] Davenport A, Gura V, Ronco C, Beizai M, Ezon C, Rambod E. A wearable haemodialysis device for patients with end-stage renal failure: a pilot study. Lancet 2007;370:2005-10.

[39] Ronco C, Fecondini L. The Vicenza Wearable Artificial Kidney for Peritoneal Dialysis (ViWAK PD). Blood Purification 2007;25:383-8.

[40] Basile C, et al. Removal of uraemic retention solutes in standard bicarbonate haemodialysis and long-hour slow-flow bicarbonate haemodialysis. Nephrology Dialysis Transplantation 2011;26:1296-303.

[41] Mikhalovsky SV. Emerging technologies in extracorporeal treatment: focus on adsorption. Perfusion 2003;18:47-54.

[42] Furuyoshi S, Nakatani M, Taman J, Kutsuki H, Takata S, Tani N. New Adsorption Column (Lixelle) to Eliminate ß2-Microglobulin for Direct Hemoperfusion. Therapeutic Apheresis and Dialysis 1998;2:13-7.

[43] Winchester JF, Ronco C. Sorbent hemoperfusion in end-stage renal disease: An in-depth review. Advances in Renal Replacement Therapy 2002;9:19-25.

[44] Winchester JF, Ronco C. Sorbent Augmented Hemodialysis Systems: Are We There Yet? Journal of the American Society of Nephrology 2009:in press.

[45] Meyer TW, Peattie JWT, Miller JD, Dinh DC, Recht NS, Walther JL, Hostetter TH. Increasing the clearance of protein-bound solutes by addition of a sorbent to the dialysate. Journal of the American Society of Nephrology 2007;18:868.

[46] Malik DJ, Warwick GL, Mathieson I, Hoenich NA, Streat M. Structured carbon haemoadsorbents for the removal of middle molecular weight toxins. Carbon 2005;43:2317-29.

[47] Malik DJ, Warwick GL, Venturi M, Streat M, Hellgardt K, Hoenich N, Dale JA. Preparation of novel mesoporous carbons for the adsorption of an inflammatory cytokine (IL-1). Biomaterials 2004;25:2933-40.

[48] Sandeman SR, et al. Inflammatory cytokine removal by an activated carbon device in a flowing system. Biomaterials 2008;29:1638-44.

[49] Takemoto S, Kusudo Y, Tsuru K, Hayakawa S, Osaka A, Takashima S. Selective protein adsorption and blood compatibility of hydroxy-carbonate apatites. Journal of Biomedical Materials Research 2004;69:544-51.

[50] Thümmler K, Fischer S, Feldner A, Weber V, Ettenauer M, Loth F, Falkenhagen D. Preparation and characterization of cellulose microspheres. Cellulose 2010:1-8.

[51] Weber V, et al. Functionalization and application of cellulose microparticles as adsorbents in extracorporeal blood purification. Macromolecular Symposia;294:90-5.

[52] Weber V, Hartmann J, Linsberger I, Falkenhagen D. Efficient Adsorption of Tumor Necrosis Factor with an in vitro Set-Up of the Microspheres-Based Detoxification System. Blood Purification 2007;25:169-74.

[53] Yachamaneni S, et al. Mesoporous carbide-derived carbon for cytokine removal from blood plasma. Biomaterials;31:4789-94.

[54] Yushin G, et al. Mesoporous carbide-derived carbon with porosity tuned for efficient adsorption of cytokines. Biomaterials 2006;27:5755-62.

[55] Howell CA, et al. The in vitro adsorption of cytokines by polymer-pyrolysed carbon. Biomaterials 2006;27:5286-91.

[56] Ettenauer M, Loth F, Thümmler K, Fischer S, Weber V, Falkenhagen D. Characterization and functionalization of cellulose microbeads for extracorporeal blood purification. Cellulose 2011:1-7.

[57] Costanzo JA, Ober CA, Black R, Carta G, Fernandez EJ. Evaluation of polymer matrices for an adsorptive approach to plasma detoxification. Biomaterials 2010;31:2857-65.

[58] Meijers BK, Weber V, Bammens B, Dehaen W, Verbeke K, Falkenhagen D, Evenepoel P. Removal of the uremic retention solute p-cresol using fractionated plasma separation and adsorption. Artificial Organs 2008;32:214-9.

[59] Kruse A, Tao X, Bhalani V, Handelman G, Levin NW, Kotanko P, Thijssen S. Clearance of p-cresol sulfate and β-2-microglobulin from dialysate by commercially available sorbent technology. ASAIO Journal 2011;57:219-24.

[60] Dinh DC, Recht NS, Hostetter TH, Meyer TW. Coated carbon hemoperfusion provides limited clearance of protein-bound solutes. Artificial Organs 2008;32:717-24.

[61] Chen SJ, et al. Combination of maintenance hemodialysis with hemoperfusion: A safe and effective model of artificial kidney. Int J Artif Organs 2011;34:339-47.

[62] Ronco C. Sorbents: from bench to bedside - Can we combine membrane separation processes and adsorbent based solute removal? International Journal of Artificial Organs 2006;29:819-22.

[63] Patzer J. Principles of bound solute dialysis. Therapeutic Apheresis and Dialysis 2006;10:118-24.

[64] Sirich TL, Luo FJG, Plummer NS, Hostetter TH, Meyer TW. Selectively increasing the clearance of protein-bound uremic solutes. Nephrology Dialysis Transplantation 2012;27:1574-9.

[65] Tong Z, Hage DS. Characterization of interaction kinetics between chiral solutes and human serum albumin by using high-performance affinity chromatography and peak profiling. Journal of Chromatography A 2011;1218:6892-7.

[66] Zucker SD, Goessling W, Gollan JL. Kinetics of bilirubin transfer between serum albumin and membrane vesicles. Insight into the mechanism of organic anion delivery to the hepatocyte plasma membrane. Journal of Biological Chemistry 1995;270:1074-81.

[67] Chapman GV, et al. Evaluation Of Hemodiafiltration And Sorbent Membrane Dialysis .1. Invivo And Invitro Dialyzer Performance. Dial Transplant 1982;11:758-65.

[68] Randerson DH, et al. Sorbent Membrane Dialysis In Uremia. ContribNephrol 1982;29:53-64.

[69] Henne W DG, Schmitz W, Pohle R, Lawitzki F, 4,267,047. Dialyzing membrane with adsorbent layer. United States, 1981 May 12.

[70] Chapman GV, Hone PWE, Shirlow MJ. Evaluation of hemodiafiltration and sorbent membrane dialysis: II. Clinical, nutritional, and middle molecule assessment. Dialysis and Transplantation 1982;11:871-6.

[71] Maeda K, Saito A, Kawaguchi S. Problems with activated charcoal and alumina as sorbents for medical use. Artificial Organs 1979;3:336-40.

[72] Vienken J, Diamantoglou M, Henne W, Nederlof B. Artificial dialysis membranes: From concept to large scale production. American Journal of Nephrology 1999;19:355-62.

[73] Avramescu ME, Borneman Z, Wessling M. Particle-loaded hollow-fiber membrane adsorbers for lysozyme separation. Journal of Membrane Science 2008;322:306-13.

[74] Saiful, Borneman Z, Wessling M. Enzyme capturing and concentration with mixed matrix membrane adsorbers. Journal of Membrane Science 2006;280:406-17.

[75] Borneman Z. Particle loaded membrane chromatography. Enschede: University of Twente; 2006.

[76] Avramescu ME, Gironès M, Borneman Z, Wessling M. Preparation of mixed matrix adsorber membranes for protein recovery. Journal of Membrane Science 2003;218:219-33.

[77] Tetala KKR, Stamatialis DF. Mixed matrix membranes for efficient adsorption of copper ions from aqueous solutions. Separation and Purification Technology 2013;104:214-20.

[78] Huang XJ, Guduru D, Xu ZK, Vienken J, Groth T. Blood Compatibility and Permeability of Heparin-Modified Polysulfone as Potential Membrane for Simultaneous Hemodialysis and LDL Removal. Macromolecular Bioscience;11:131-40.

[79] Mahlicli F, Altinkaya S. Surface modification of polysulfone based hemodialysis membranes with layer by layer self assembly of polyethyleneimine/alginate-heparin: a simple polyelectrolyte blend approach for heparin immobilization. Journal of Materials Science: Materials in Medicine 2012:1-14.

[80] Krause B, Storr M, Ertl T, Buck R, Hildwein H, Deppisch R, Göhl H. Polymeric membranes for medical applications. Chemie Ingenieur Technik-CIT 2003;75:1725-32.

[81] Ran F, Nie S, Zhao W, Li J, Su B, Sun S, Zhao C. Biocompatibility of modified polyethersulfone membranes by blending an amphiphilic triblock co-polymer of poly(vinyl pyrrolidone)-b-poly(methyl methacrylate)-b-poly(vinyl pyrrolidone). Acta Biomaterialia 2011;7:3370-81.

[82] Aldenhoff YBJ, Knetsch MLW, Hanssen JHL, Lindhout T, Wielders SJH, Koole LH. Coils and tubes releasing heparin. Studies on a new vascular graft prototype. Biomaterials 2004;25:3125-33.

2

A novel approach for blood purification: mixed matrix membranes combining diffusion and adsorption in one step

M. Tijink
M. Wester
J. Sun
A. Saris
L. Bolhuis-Versteegh
S. Saiful
J. Joles
Z. Borneman
M. Wessling
D. Stamatialis

This chapter has been published:

Tijink MSL, et al. A novel approach for blood purification: Mixed-matrix membranes combining diffusion and adsorption in one step. Acta Biomaterialia 2012;8:2279-87.

Abstract

Hemodialysis is a commonly used blood purification technique in patients requiring kidney replacement therapy. Sorbents could increase uremic retention solute removal efficiency but because of poor biocompatibility their use is often limited to treatment of patients with acute poisoning. This work proposes a novel membrane concept for combining diffusion and adsorption of uremic retention solutes in one step: the so called mixed matrix membrane (MMM). In this concept, adsorptive particles are incorporated in a macro porous membrane layer whereas an extra particle free membrane layer is introduced on the blood contacting side of the membrane to improve hemocompatibility and prevent particle release. These dual layer mixed matrix membranes have high clean water permeance and high creatinine adsorption from creatinine model solutions. In human plasma, the removal of creatinine and of the protein-bound solute para-aminohippuric acid (PAH) by single and dual layer membranes is in agreement with the removal achieved by the activated carbon particles alone, showing that under these experimental conditions the accessibility of the particles in the MMM is excellent. This study proves that the combination of diffusion and adsorption in a single step is possible and paves the way for development of more efficient blood purification devices excellently combining the advantages of both techniques.

2.1. Introduction

The prevalence of End Stage Renal Disease (ESRD) was about 535 000 in the United States population in 2008. Of these patients, about 355 000 were treated with hemodialysis. Despite the high health care costs of dialysis treatment (around 25 000 Euro per patient per year), hemodialysis is only partially successful in the treatment of patients with ESRD. Mortality (15-20% per year) and morbidity of these patients remain excessively high, whereas their quality of life is generally low [1]. This is reflected in the expected remaining life years, which are 25.0 years for the general U.S. population, 15.7 for ESRD patients with a kidney transplant and 5.6 years for ESRD patients receiving dialysis treatment [2].

In the last three decades, sorbent technology has been applied in treatment of severe intoxication and to increase the efficiency of hemodialysis, or replace it, and as a treatment for fulminant hepatic failure. In hemoperfusion (or plasma perfusion), blood (or plasma) is purified by extracorporeal passage through a column containing the adsorbent which can remove or neutralize the substance of interest. Hemoperfusion cannot fully substitute hemodialysis because it does not remove urea and excess fluid. Sorbents used in hemoperfusion, help to remove uremic toxins, however, direct blood contact with the adsorbent often causes hemocompatibility issues, especially on the long term [3]. Activated carbon (AC) has a long record as a sorbent in blood purification in case of intoxications, acute and chronic renal failure as well as liver failure [3-5]. Uncoated activated carbon is a strong adsorbent for uremic toxins [6] whereas polymeric coatings of activated carbon might help to improve hemocompatibility. However, coated activated carbon could still release carbon fragments, even after careful washing and a double coating process is needed to overcome this problem [7]. In conventional hemoperfusion columns, optimal distribution of blood flow within the packed sorbent bed is very important for adequately use of the adsorption capacity, especially with rather viscous and complex solutions like blood or plasma. Channelling within the column leads to suboptimal

adsorption and can induce blood coagulation. Furthermore, micro particles that can be released into the circulation and can cause emboli are always a concern related to hemoperfusion.

It is obvious that combination of the strengths of dialysis membranes with the adsorption power of high surface area sorbents can be very beneficial for the blood purification efficacy [8]. In fact, in the late 1970s so called sorbent membranes were developed. These membranes were even on the market for a certain period, produced by Enka [9-15]. However, due to their quick saturation, manufacturing difficulties, reduced patient convenience and lack of adsorbents with high purity [16-19], they were quickly abandoned. More recently, membrane filtration and adsorption columns are often combined as two separate steps in wearable artificial kidneys [20, 21].

In this work, we propose a novel membrane concept for combining diffusion and adsorption of uremic retention solutes in one step: the so called mixed matrix membrane (MMM). In this concept, adsorptive particles are incorporated in a macro porous membrane matrix. A particle free membrane layer is introduced on the blood contacting side of the membrane aiming to improve membrane hemocompatibility and prevent particle release into the circulation and hence emboli formation, see Figure 1.

Mixed matrix membranes have been proposed as an alternative for traditional chromatographic columns [22, 23]. Compared to conventional columns, they have low flow resistance, that allows using smaller particles resulting in an improved adsorption capacity and adsorption kinetics [24, 25]. Furthermore, the particles can be homogenously distributed by embedding them in the matrix, leading to optimal adsorption efficiencies and preventing quick saturation.

Here, for the proof of concept, we prepare and investigate flat sheet MMMs using materials with excellent record in blood purification. A polyethersulfone (PES) / polyvinyl pyrrolidone (PVP) polymer blend is used for the preparation of the macro porous membrane matrix (PES as a membrane forming polymer blended with PVP to improve hydrophilicity) and activated carbon is used as adsorptive particle. Creatinine, a small molecular weight uremic retention solute, often used as a

marker of kidney function, is used as model water soluble solute. The para-aminohippuric acid (PAH) which belongs to the family of hippurates, and is often used as a marker for organic anion transport because of tubular secretion, is used in this study as a model protein-bound solute [26-29].

The study investigates the combination of diffusion and adsorption in a single step which probably leads to more efficient blood purification devices and will prevent issues related to the use of conventional hemoperfusion columns.

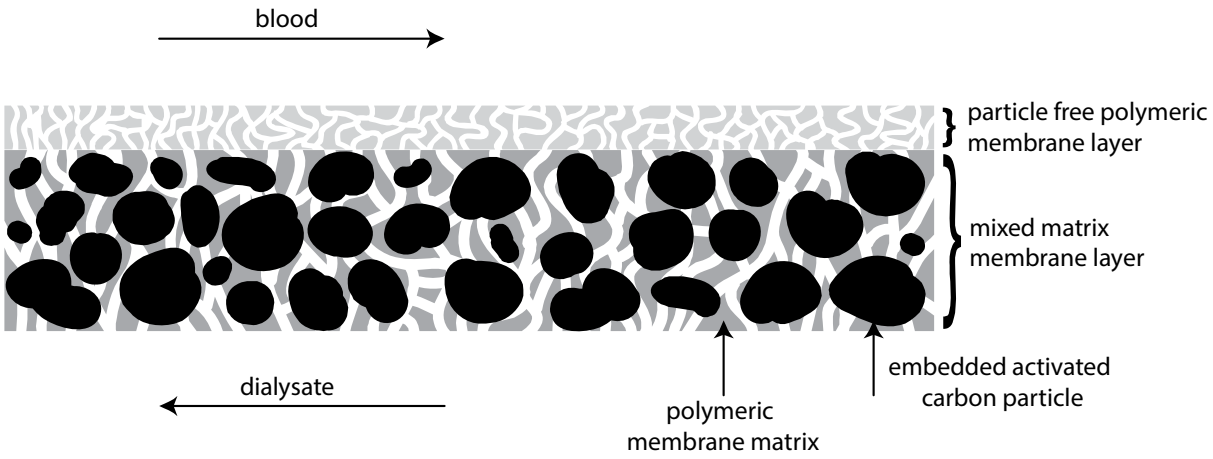

Figure 1. Concept of dual layer mixed matrix membranes for blood purification.

2.2. Materials and methods

2.2.1. Materials

Polyethersulfone (PES) (ULTRASON, E6020P, BASF, the Netherlands) was used as membrane material. Polyvinylpyrrolidone (PVP) (K90), MW≈360,000, Fluka, Sigma-Aldrich, Germany) and extra pure N-Methylpyrrolidone (NMP) (Acros organics, Belgium) were used as additive and solvent, respectively. Ultrapure water, prepared with a Millipore purification unit was used as non solvent in the coagulation bath. Activated carbon (Norit A Supra EUR, Norit Netherlands B.V., the Netherlands) was sieved with a 45µm sieve (Fritsch GmbH, Germany) and used as adsorbent particles (median size 27 µm). The following chemicals were purchased from Fluka, Sigma-Aldrich. Creatinine was dissolved in Tyrode's buffer (pH=7.4) composed of 137 mM NaCl, 5.4 mM KCl, 1.8 mM $CaCl_2$, 0.5 mM $MgCl_2$, 11.9 mM $NaHCO_3$ and 5.5 mM glucose in ultrapure water.

2.2.2. Membrane preparation

The particle free membrane layer was prepared using a 15 wt% PES and a 7 wt% PVP in NMP solution which was stirred at a roller bank over night at room temperature. For the MMM, first a mixture of 14 wt% PES and 1.4 wt% PVP in NMP solution was prepared and stirred at a roller bank overnight at room temperature, then different amounts of dry activated carbon particles were added. Loadings of 50, 60 and 70 wt% activated carbon in relation to the amount of PES in the mixed matrix membrane layer were applied, calculated as:

$$\text{Loading } (\%) = \frac{W_{AC}}{(W_{AC} + W_{PES})} \cdot 100$$

Where W_{AC} is the dry weight of activated carbon particles (g) and W_{PES} is the dry weight of PES (g). The mixtures were stirred at least overnight and ultrasound was applied for at least 15 minutes to

break down possible particle clusters. After degassing overnight, all the membranes were prepared by immersion precipitation.

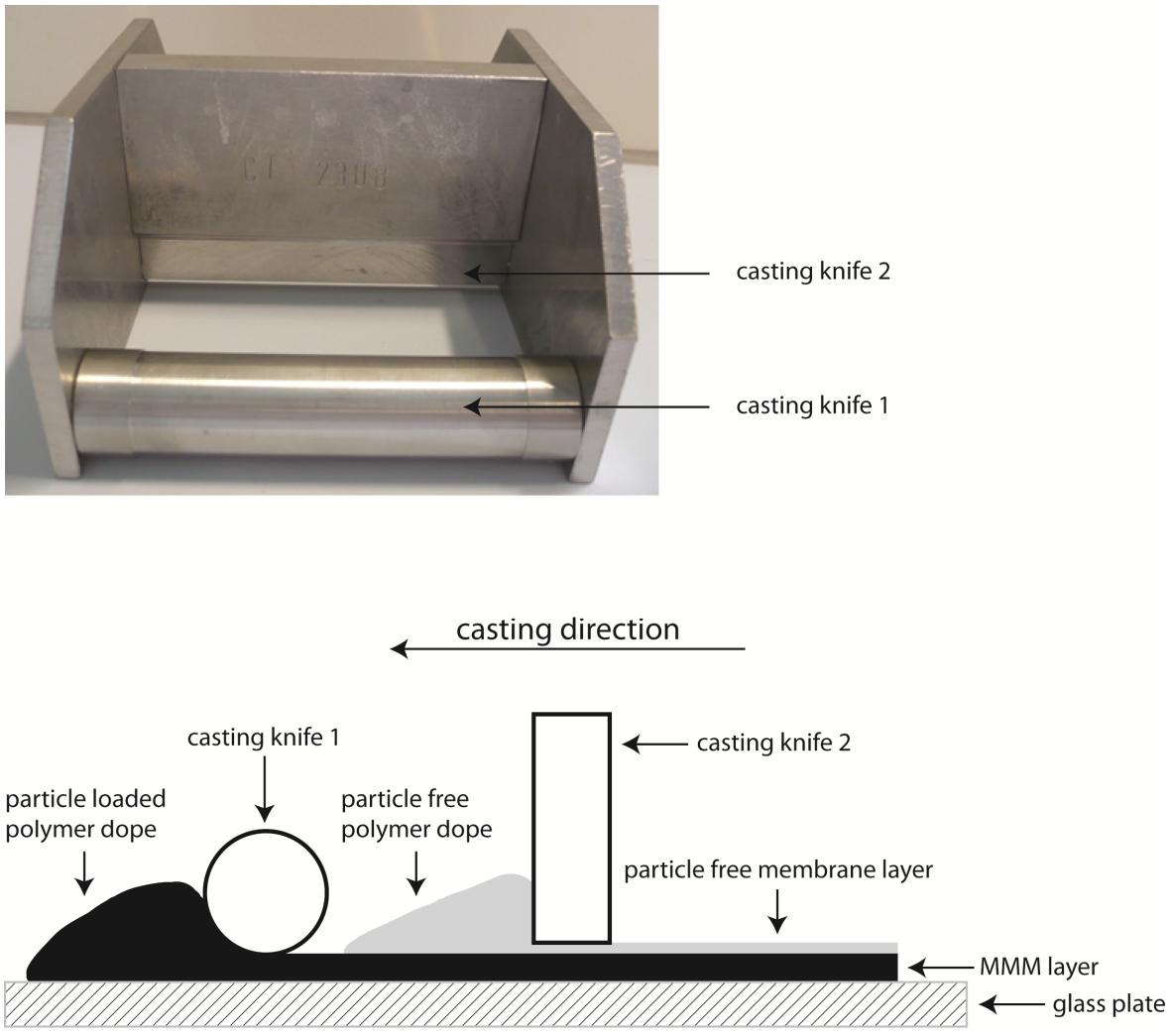

Figure 2. Picture and schematic drawing of the co-casting knife. It consists of two attached casting knifes with 300 and 450 µm slits. The particle free polymer dope is cast by casting knife 2 on top of the particle loaded polymer dope casted by casting knife 1 to form dual layer membranes.

Solutions were cast on a glass plate using a casting knife. A slit of 300 µm and 150 µm for single layer MMMs and single particle free membranes were used respectively. An adjustable co-casting knife

was used for dual layer MMMs, see Figure 2. The heights of the slits of the first and second knife were 300 and 450 µm respectively. Casting was immediately followed by immersion into the coagulation bath, containing 60 wt% NMP in ultrapure water at room temperature. After the membrane formation process, the membranes were rinsed with ultrapure water to remove residual solvent traces, and stored in ultrapure water upon further use.

2.2.3. Membrane characterization

2.2.3.1. Scanning electron microscopy

For scanning electron microscopy (SEM), membranes were dried in air at room temperature and cryogenically broken in liquid nitrogen. The obtained cross sections were dried overnight under vacuum at 30^{o}C and gold coated using a Balzers Union SCD 040 sputter coater (Oerlikon Balzers, Belgium). Coated membrane samples were examined using a JEOL JSM-5600LV scanning electron microscope (JEOL, Japan).

2.2.3.2. Membrane transport properties

Clean water fluxes of the membranes were tested at room temperature using a nitrogen pressurized dead end 'Amicon type' ultrafiltration cell and ultrapure water. Flat membranes with an active surface area of 8.04 cm^2 were used. First, membranes were pre-pressurized for at least 0.5 hour at the highest applicable pressure which was 1.00 bar. Subsequently, pressures of 0.25, 0.5, 0.75 and 1.00 bar were applied for at least 20 minutes and the clean water flux at each pressure was determined. The membrane permeance was calculated from the slope of the linear part of the flux versus transmembrane pressure relation. The BSA sieving coefficient of the single and dual layer membranes was measured at room temperature using a nitrogen pressurized dead-end Amicon ultrafiltration cell. BSA was dissolved in ultrapure water with initial concentration of 1 mg/mL and

was pressurized through the membranes (with active surface area of 12.57 cm^2) at 0.5 bar for 30 minutes. The BSA sieving coefficient (SC) was calculated using the equation:

$$SC = \frac{C_p}{C_f}$$

where C_p and C_f is the BSA concentration in the permeate and feed solution, respectively.
The BSA concentrations were determined by spectrophotometric analysis (Varian, Cary 300 Scan UV-Visible Spectrophotometer) at 278 nm. Student t-test was used for statistical testing (p<0.05).

2.2.3.3 Creatinine adsorption capacity

The creatinine adsorption capacity of the prepared membranes was determined by batch adsorption experiments with model creatinine solutions. Known amounts of dry membranes were equilibrated in solutions with different creatinine concentrations in a shaking water bath at 37°C for 24h. The equilibrium creatinine concentration (C) was determined by spectrophotometric analysis (Varian, Cary 300 Scan UV-Visible Spectrophotometer) at 230 nm with 2mm quartz cuvettes at 25°C. Via the mass balance the amount of adsorbed creatinine was calculated from the depleted amount of creatinine in the solution. The adsorption capacity (q) was expressed as mg adsorbed creatinine per gram of adsorptive particle. For this the proportion of activated carbon particles in the membrane was estimated (see appendix of this chapter and/or supplement of [30] for details). Dry membrane weight was multiplied by this proportion and the obtained amount of activated carbon particles in the membrane was used to relate with the amount of adsorbed creatinine. Origin 7.5 was used for non linear curve fitting of the isotherm in order to obtain a Langmuir fit according to the following equation:

$$q = \frac{q_m \cdot C}{K_d + C}$$

In which q is the adsorption capacity (mg/g AC), C is the equilibrium concentration of creatinine (mg/mL) in the solution, q_m is the maximum adsorption capacity (mg/g AC) and K_d is the dissociation constant (mg/mL).

2.2.3.4. Adsorption from human blood plasma

Human plasma was obtained from six patients who underwent plasma exchange because of acute renal disease. 25 mg activated carbon, MMM and dual layer MMM which contained around 25 mg activated carbon based on the proportion of activated carbon particles in them and a particle free membrane of similar size as the dual layer MMM were incubated in 4 mL of 6 different plasmas. In case of small deviations from the 25 mg sorbent weight, the amount of plasma was adjusted so that the sorbent-volume proportion would be similar to 25 mg in 4 mL. These test samples and plasmas without sorbents were incubated on a roller bank for four hours. After incubation, samples were centrifuged at 4°C for 10 minutes. The supernatant, approximately 3 ml per sample, was collected and stored in micro-cups at 4°C for analysis later. Osmolarity, pH, total protein and creatinine concentrations were measured according to the protocol of manufacturer of the kit and/or device (see Table 1) whereas the PAH concentration was measured following the protocol described elsewhere [31].

Since the initial concentrations of creatinine and PAH in plasma were different for every patient, and to avoid large variation by taking averages of the absolute concentrations, we used relative concentrations. The absolute initial creatinine concentrations in the six different plasmas were: 495.4, 1299.2, 332.6, 44.6, 276.4 and 60.9 µmole/L. For the PAH, only 2 plasmas had reasonable

baseline concentrations (49.8 and 72.4 µmole/L) therefore only 2 plasmas were used for these experiments. The relative change in concentration of the various solutes were calculated as follows:

$$Relative\ concentration = \frac{C_s}{C_b}$$

C_s is the concentration in the plasma incubated with a sample (AC or membranes) whereas C_b is the concentration in the blanc solution (plasma without sorbents or membranes). Likewise, the relative osmolarity and relative pH were calculated. Statistical differences were determined using a one-way ANOVA and Dunnett's test for the creatinine, pH, osmolarity and total protein concentrations. For PAH, due to low number of plasma samples no statistical analysis was performed.

Table 1. Test methods for analysis of blood plasma.

Parameter	Kit / device
Osmolarity	Advanced instruments osmometer model 3320
pH	Radiometer Copenhagen PHM lab pH meter
Creatinine	Bio-Rad Microplate reader Benchmark 16-channel photometer
	DiaSys Creatinine PAP FS (1 1759 99 10 026)
Total protein	Bio-Rad Laboratories GmbH Protein Assay (cat# 500-0006)
	Bio-Rad Microplate reader Benchmark 16-channel photometer

2.2.3.5 Two compartment diffusion test

A two compartment diffusion device [32] was used to measure diffusion and adsorption of creatinine onto dual layer MMMs at room temperature. Creatinine is a uremic retention solute and

is used as an indicator for solute removal by MMMs. The donor compartment was filled with 0.1 mg/mL creatinine in Tyrode's buffer, whereas the acceptor compartment was filled with pure Tyrode's buffer. The compartments were separated by a dual layer MMM, with the particle free layer facing the creatinine containing donor solution. The volume of each compartment was 65 mL and the active membrane area was 3.14 cm^2. Both solutions were stirred at room temperature. During the experiment, 600 µL samples were taken in time to determine creatinine concentrations in both compartments. The creatinine decrease in the donor compartment was considered as total removal. The amount of creatinine that appeared in the accceptor compartment was considered as creatinine which was diffused from the donor compartment. The creatinine deficiency in the mass balance was considered to be adsorbed onto the membrane. This amount was related to the dry membrane weight which was measured after the experiment.

2.3. Results and discussion

Here we describe the characterization of the prepared mixed matrix membranes in terms of morphology and transport properties. First we show the influence of the particle loading on membrane morphology followed by the clean water permeance measurements and creatinine adsorption isotherms for both the optimized single and dual layer mixed matrix membranes. Furthermore, we show adsorption from human blood plasma. Finally, we show creatinine transport results of dual layer mixed matrix membranes.

2.3.1 Membrane particle loading optimization

Different amounts of activated carbon particles were embedded in mixed matrix membranes. Particle loading is an important parameter, besides influencing membrane morphology, the amount of adsorptive sites in the MMM increases as the particle loading increases. High particle loading can result in too high viscosities for proper casting or result in membranes with low mechanical strength. Figure 3 shows cross sections of MMMs containing 50, 60 and 70 wt% of activated carbon in relation to the amount of PES. All membranes have a porous structure and no significant loss of particles was observed during membrane fabrication. Membranes loaded with 50 wt% and 60 wt% particles (Figure 3 A, B, D, E) have some macro voids which may reduce mechanical strength of the membrane and may create transport channels. Membranes loaded with 70% particles contain more adsorptive sites per gram of membrane than at lower loadings. Furthermore, membranes with 70 wt% activated carbon particles possess an open interconnected porous sponge like structure, without macro voids across the entire cross section. In fact, as the particle loading increases, the viscosity of the dope increases as well. Higher dope viscosity restricts growth of the polymer lean phase in the phase separation process, because of a higher mass flow resistance. Likewise non solvent inflow into the polymer solution is restricted, leading in turn to a slower phase separation process. The high viscosity, prevents formation of macro voids and leads to the formation of smaller pores [33].

Furthermore, the particles probably act as a nucleus in the phase inversion process, leading to sponge like structures [34]. Figure 3 G, H and I present bottom surfaces of the different membranes. Increase in particle loading can clearly be observed by the amount of particles there. Activated carbon particles are tightly held together in the porous polymer matrix and no particle clusters are observed. All the obtained membranes possess sufficient mechanical strength for handling and characterization.

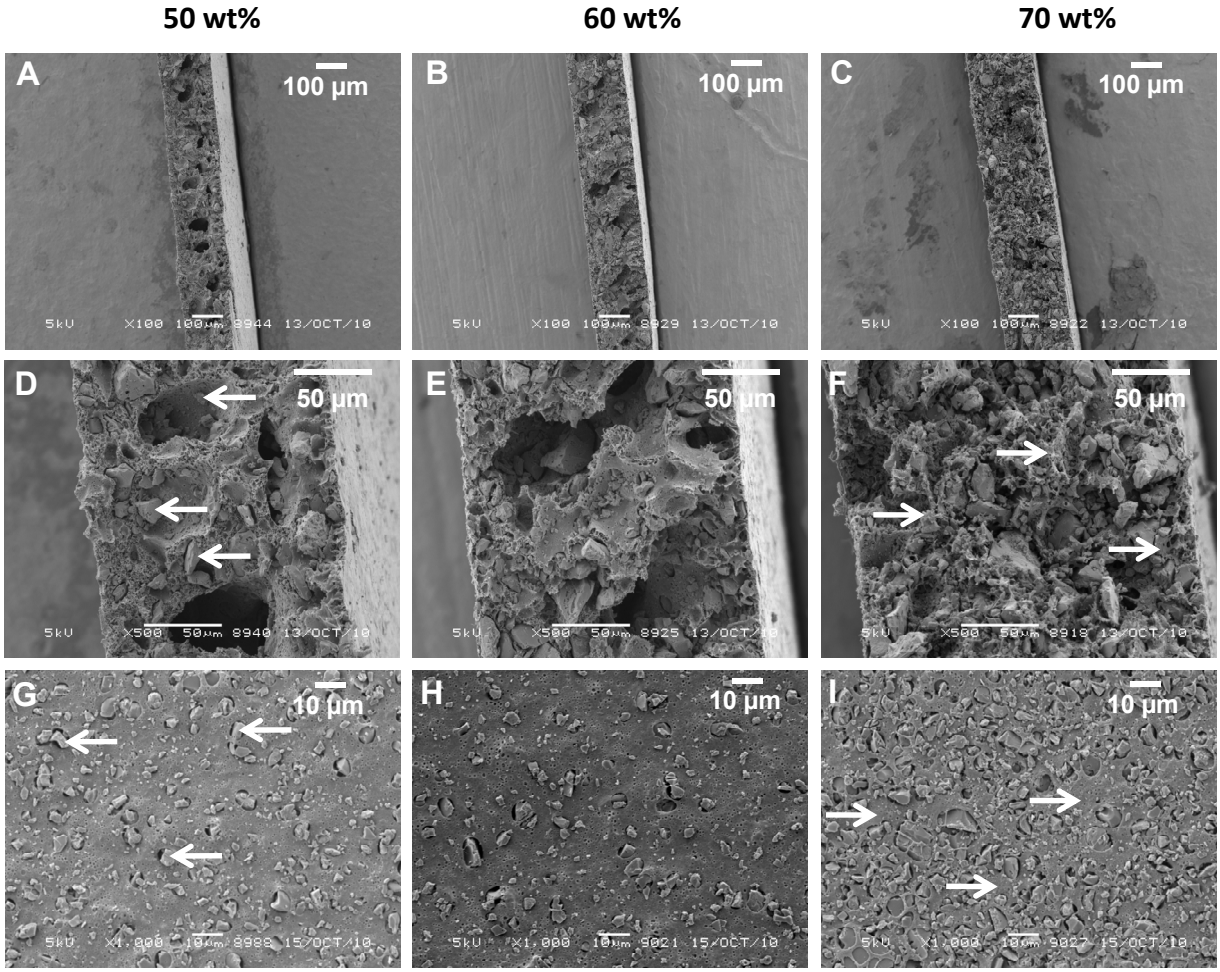

Figure 3. Scanning Electron Microscopy pictures of cross sections (A, B, C, D, E and F) and bottom surface sections (G,H and I) of single layer mixed matrix membranes with loadings of 50% (A, D, G), 60% (B, E, H) and 70% (C, F, I). The arrows in D and G indicate the activated carbon particles whereas arrows in F and I indicate the porous polymeric membrane matrix.

In conclusion, membranes loaded with 70 wt% activated carbon particles contain relatively the highest amount of adsorptive sites, show a porous interconnected structure and have sufficient mechanical strength. Therefore these membranes are selected for further characterization and development of dual layer mixed matrix membranes

2.3.2 Dual layer mixed matrix membranes

To obtain dual layer MMMs, we co-cast 70 wt% particle loaded polymer solution with a particle free polymer solution. This particle free layer will be the blood contacting membrane side to avoid direct blood contact with the embedded sorbents during blood purification. Furthermore, it will prevent particle release into the circulation and consequent emboli formation.

Figure 4A and B present a single layer MMM and dual layer MMM respectively. The dual layer MMM has a rather open interconnected porous structure. The particle loaded layer of the dual layer MMM possesses a sponge like structure. Some small round shaped voids are present in this layer but macro voids through the entire cross section are absent. The particle free layer has a dense top layer and some macro voids are present below this layer.

Figure 4C presents the single particle free membrane which was cast directly on a glass plate. This single particle free membrane has a homogenous sponge like structure whereas the particle free layer in the dual layer MMM has a dense sponge like top layer but with a more open sub layer with macro voids. Besides, the thickness of the two layers of the dual layer MMM is not in agreement with the casting thicknesses. Probably, the co-casting process, different viscosities of the dopes and different shrinkage of the two membrane layers during phase separation influence the final membrane structure of the dual layer MMM.

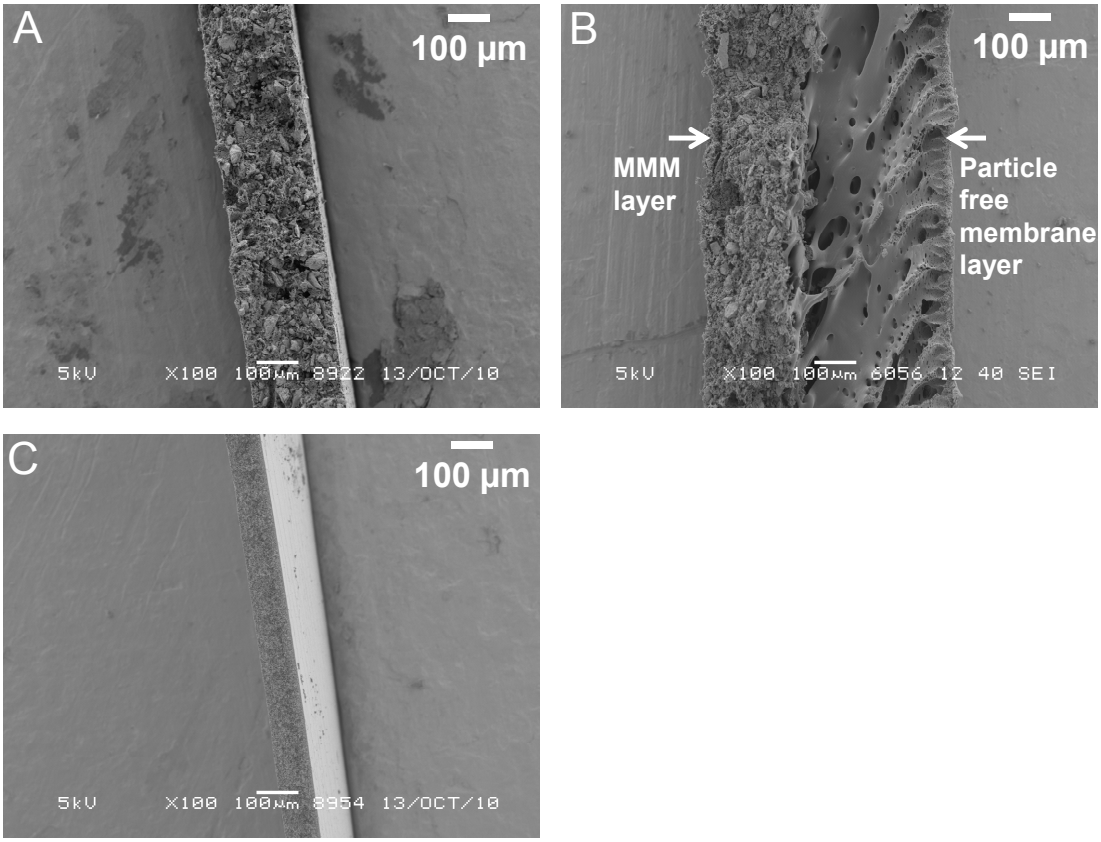

Figure 4. Scanning Electron Microscopy pictures of cross sections of a single layer MMM (A), dual layer MMM (B) and particle free membrane (C).

Figure 5A and B show photos of a single layer mixed matrix membrane and dual layer mixed matrix membrane respectively. In the dual layer MMM, the membrane layer with the particles is black and the particle free layer is white and completely covers the layer with the particles, see Figure 5B. Figure 5C shows that the layer with the particles is rather rough whereas the particle free layer has a more smooth surface and smaller pores.

In dual layer MMM, the two different layers can clearly be distinguished and are well attached to each other. In fact, no delamination of the two membrane layers was observed. These 70 wt% loaded single layer membranes and dual layer membranes are further characterized.

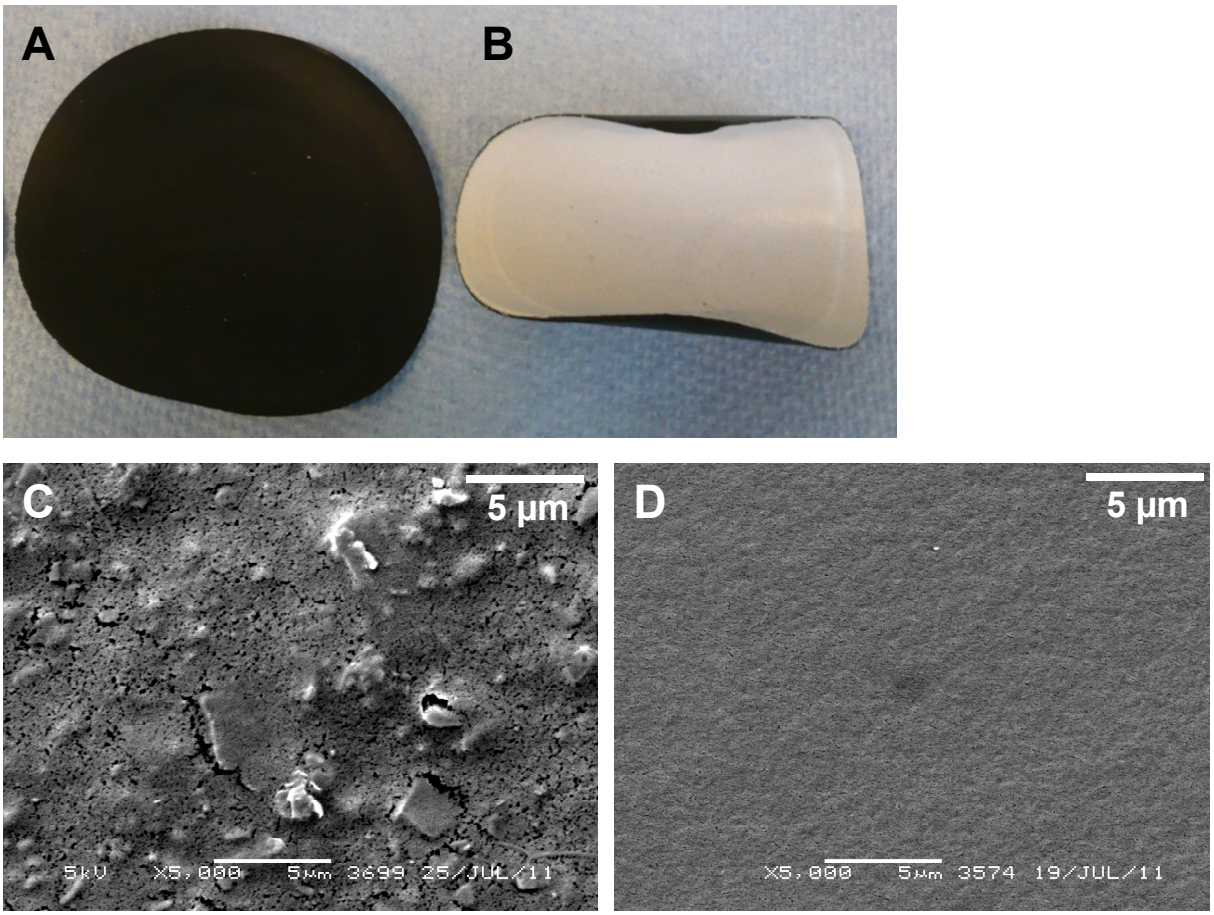

Figure 5. Surface area pictures and SEM pictures of a single layer MMM (A, C) and dual layer MMM (B, D) respectively.

2.3.3 Membrane transport properties

Figure 6 shows the clean water flux at various transmembrane pressures. For single layer MMMs, the clean water permeance is 1839 ± 55 L/m^2/h/bar based on the slope till 0.5 bar. Although these membranes were pre-pressurized before the measurement, the flux – transmembrane pressure relationship at higher pressures is not linear. This might be due to membrane compaction during the measurement or possibly relocation of the particles in the matrix which might close the bigger channels. For dual layer MMMs the permeance is significantly lower, 350.7 ± 69 L/m^2/h/bar (p<0.05) and the flux – transmembrane pressure relationship is linear in the used pressure range. The

decrease in clean water permeance for the dual layer MMMs is probably due to the additional particle free layer which has a dense sponge like skin structure.

The single layer MMMs have a BSA sieving coefficient of 0.8 ± 0.1. The dual layer MMMs have a significantly lower sieving coefficient of 0.4 ± 0.2 (p<0.05). It seems that the additional particle free layer tailors the transport through the membrane. For future applications the molecular weight cut-off of the membrane is important and can probably be tailored by optimization of the particle free layer.

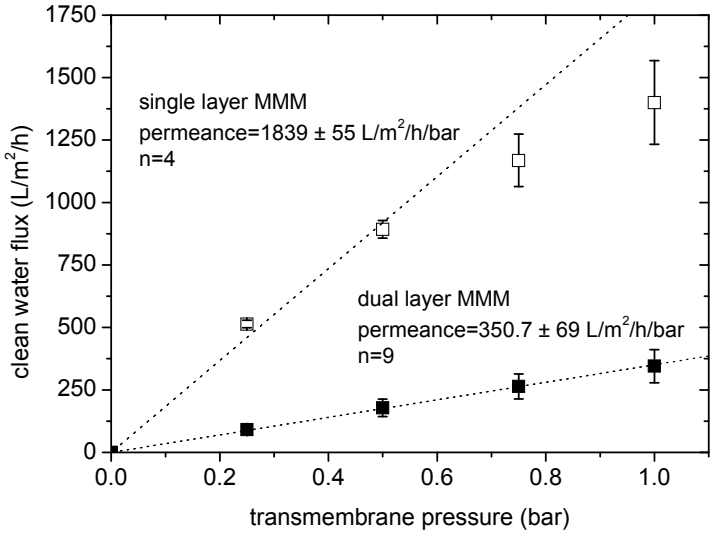

Figure 6. Average clean water flux plotted against transmembrane pressure, for single layer MMMs (□) and dual layer MMMs (■). The error bars indicate standard deviations.

2.3.4 Creatinine adsorption isotherms

For single and dual layer MMMs, the creatinine adsorption at various concentrations was measured. The adsorption capacity is expressed in mg adsorbed creatinine per gram of activated carbon. Hence the exact particle proportion in the MMM is necessary and is calculated (via the equations in the appendix) to be 0.68 and 0.53 for single and dual layer MMMs respectively.

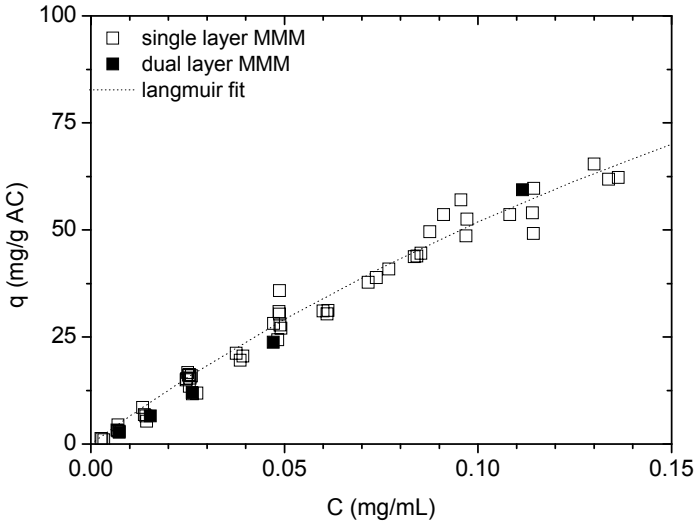

Figure 7. Creatinine isotherms for single (□) and dual layer (■) MMMs. The equilibrium adsorption capacity (q) expressed in mg adsorbed creatinine per gram of activated carbon is plotted against the equilibrium creatinine concentration (C). The dotted line represents the calculated Langmuir isotherm fit.

Figure 7 presents the results expressed in adsorption capacity (q) versus the equilibrium creatinine concentration (C). The isotherms of single and dual layer MMMs are almost identical and appear to be of Langmuir type. For the tested concentration range the best Langmuir isotherm curve fit has q_m= 234 mg/g AC and K_d = 0.351 mg/mL. The range of creatinine concentrations used here (Figure 7) is close to the levels of creatinine that is measured in uremia as the mean/median uremic creatinine concentration is 0.136 mg/mL whereas the normal level is 0.012 mg/mL [27].

Compared to other studies, the adsorption capacity of the mixed matrix membranes is high. For example at an equilibrium concentration of 0.05 mg/mL our MMMs adsorb 29 mg creatinine / g activated carbon. At the same equilibrium creatinine concentration, Deng *et al.* reported adsorption of 13 mg creatinine / g activated carbon [35] for PES and activated carbon based hybrid beads and Ye *et al.* reported adsorption of 15-20 mg creatinine / g of activated carbon or carbon nanotube [36].

In another approach using polymeric micro spheres, the creatinine adsorption was less than 10 mg/g micro sphere [37].

2.3.5 Human plasma adsorption

Figure 8A presents average relative creatinine concentrations after incubation in plasma for 4 hours, which is an average duration of a hemodialysis treatment. The particle free membrane does not significantly lower the creatinine concentration. However, more than 80% of the creatinine is removed by the single and dual layer membranes which is in excellent agreement with the removal achieved by the activated particles alone under these experimental conditions. This shows that the accessibility of the particles in the MMM is excellent. These creatinine adsorption results also fit very well to the isotherm obtained with model creatinine solutions (as presented in Figure 7) suggesting that even for the more complex human plasma the accessibility of our membranes is optimal.

The results of PAH removal by the membrane (see Figure 8B) are consistent to the results of creatinine. The particle free membrane does not seem to lower the PAH concentration whereas the single and dual layer MMMs seems to remove more that 80% of PAH similar to the removal obtained by the activated carbon particles alone. These results indicate that the developed MMMs can probably remove protein-bound compounds, and the accessibility of the particles there seem to be similar to the accessibility of the particles alone. Protein-bound solutes are thought to contribute to uremic toxicity and are hardly removed by hemodialysis [38, 39]. Adsorption has been proposed as a way to improve removal of these toxins [40, 41] and it has been shown that addition of activated carbon to the dialysate compartment of a hemodialyzer can improve protein-bound toxin removal [42, 43]. Our first results suggest that the MMM could be suitable for the improvement of protein-bound toxin removal.

It is also important to note that while under these experimental conditions our single and dual layer MMMs seem to remove more than 80% of the creatinine and PAH from the human plasma, they do

not cause any significant changes to the plasma pH, osmolarity and the total protein concentration (see Table 2). The latter indicates that undesired general protein-binding is limited.

Direct comparison of the performance of our membranes in human plasma with other literature studies is rather difficult since not all experimental conditions are the same. In this study, 25 mg of adsorbent was incubated in 4 mL plasma. This proportion can be related to the proportion used in hemoperfusion, where around 3000 mL plasma is in contact with a hemoperfusion column containing around 300 gram of activated carbon (Adsorba 300, Gambro). This gives a sorbent-volume proportion of 100 mg/mL plasma. In our experiments the sorbent-volume proportion is lower, 6 mg/mL plasma. This indicates that when we would apply a similar sorbent-volume proportion as in hemoperfusion, the obtained relative removals by our MMMs could even be higher. Perhaps the best way of comparing adsorption results is by means of isotherms at similar equilibrium concentrations of model solutions but which are unfortunately not often discussed in the literature. Nonetheless, there are a few studies with which some comparison can be done. For example, Malchesky *et al.* developed a blood purification device containing charcoal encapsulated in semi-permeable hollow tubing. A 35 Liter test solution with an initial concentration of 0.095 mg/mL creatinine was pumped through a device containing 37 mg activated carbon (sorbent-volume proportion of 0.001 mg/mL) and 30.1% of the creatinine was removed after 4h [44]. The Vicenza Wearable Artificial Kidney for peritoneal dialysis contains less than 200 gram adsorptive particles, 40% polystyrenic resins, 60% activated carbon with the latter mainly removing creatinine. A 12 L dialysate solution was pumped through the device and 94.2% of the creatinine was removed after 4h [21].

A

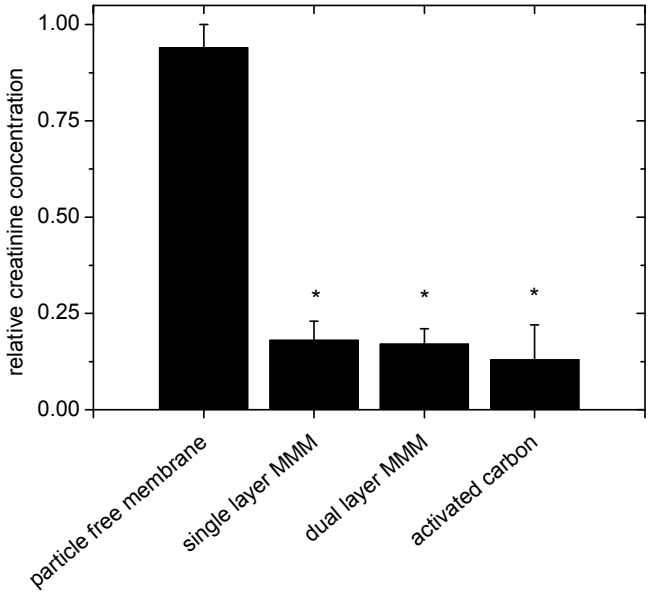

B

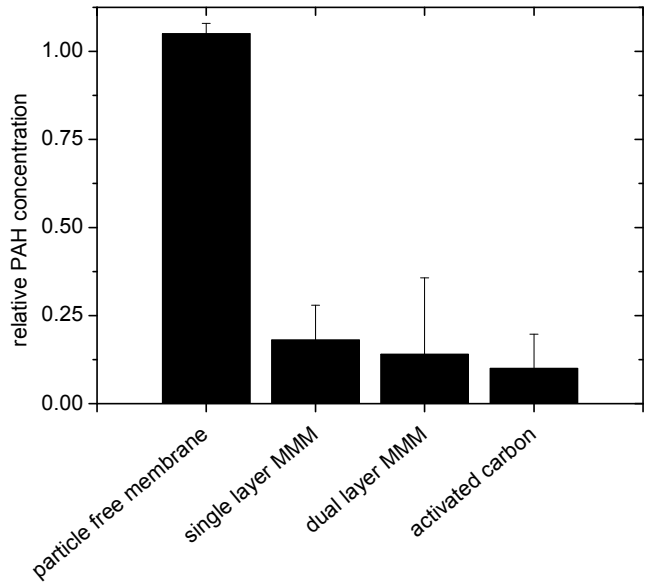

Figure 8. **A)** Average relative creatinine concentration after incubation of a particle free membrane, single layer MMMs, dual layer MMMs or pure activated carbon in plasma (n=6) for 4 hours. * indicates $p<0.05$ in comparison with a particle free membrane. **B)** Average relative PAH concentration after incubation of a particle free membrane, single layer MMM, dual layer MMM or pure activated carbon particles in plasma (n=2) for four hours.

Table 2. Relative osmolarity, pH and total protein concentration after incubation in human blood plasma (n=6) for 4 hours

Sample	Relative osmolarity	Relative pH	Relative total protein concentration
Activated carbon	0.99 ± 0.01	1.02 ± 0.04	0.93 ± 0.02
Single layer MMM	1.00 ± 0.01	1.02 ± 0.02	0.94 ± 0.05
Dual layer MMM	0.98 ± 0.01	1.00 ± 0.01	1.01 ± 0.07
Particle free membrane	1.01 ± 0.01	1.03 ± 0.02	1.03 ± 0.06

2.3.6 Creatinine diffusion through MMMs

For estimating the transport of uremic retention solutes through our membranes, we tested diffusion through and adsorption onto dual layer MMMs using a two compartment diffusion device with a 0.1 mg/mL creatinine feed solution. This concentration is clinically relevant as it is very close to the mean/median uremic creatinine concentration measured in uremia of 0.136 mg/mL [27]. Figure 9 shows that after some time the diffused creatinine starts increasing and continues in time. Adsorption of creatinine starts almost immediately, and after more than 24 hours seems to reach a plateau. The contribution of creatinine removal after 7 hours by adsorption is over 80% of the total creatinine removal. No quick saturation occurs for the developed MMMs under these experimental conditions. The MMM combines uremic retention solute removal via both diffusion as well as adsorption in one single step. This is a novel and promising approach in the extracorporeal blood purification technology. In this paper we showed the first proof of concept, in the future, we foresee several opportunities for MMMs in the use of blood purification. MMMs could be used in a wearable artificial kidney (WAK). The MMM combines two methods of blood purification in one step (adsorption and membrane based removal). This could enhance the miniaturization of the device.

Besides, MMMs might be useful for dialysis with less dialysate (in a WAK), making sure that sufficient amounts of toxins can be removed. Or MMMs could be placed in a separate circuit for regeneration of the dialysate which could be useful for a WAK system. Furthermore, the MMM may function as an adsorptive barrier for endotoxins thereby preventing endotoxins from the dialysate entering the patients circulation.

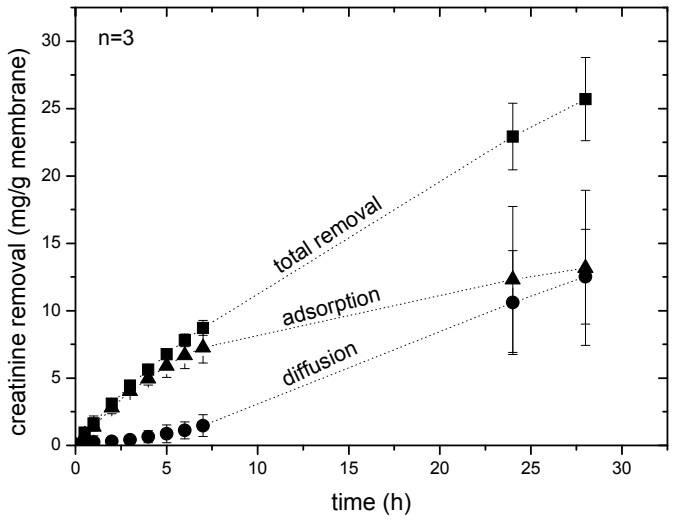

Figure 9. Average creatinine total removal, diffusion and adsorption plotted versus time, n=3. Total removal (■) is the amount of creatinine removed from the donor compartment. This removal is mediated by diffusion (●) and adsorption (▲) of creatinine. Error bars indicate standard deviations. The dotted lines are plotted to guide the eye.

2.4. Conclusions and outlook

This work presents a novel approach for uremic retention solute removal combining diffusion and adsorption. Dual layer MMMs were formed consisting of a particle free membrane layer and a mixed matrix membrane layer containing activated carbon. The dual layer MMMs have a clean water permeance of around 350 L/m^2/h/bar, and show rather high creatinine adsorption of around 29 mg creatinine / g activated carbon at equilibrium concentration of 0.05 mg/mL. Moreover, both single and dual layer MMMs significantly reduce the creatinine concentration in human blood plasma, without general effects on osmolarity, pH and total protein concentration.

Our future plans will focus on removal of a broad range of uremic toxins including other protein-bound toxins and middle molecules since these are difficult to remove with current hemodialysis. Adsorption based removal with MMMs might improve the clearances of these toxins as well.

We will also fabricate and optimize dual layer mixed matrix hollow fiber membranes with a thin particle free inner layer. Recent literature studies have shown that it is possible to prepare dual layer membranes and dual layer MMMs with different characteristics (material, layer thickness, particle type etc.) [45-50]. Our focus will be on tailoring the membrane structure by parameters like spinneret design, pumping speeds and polymer and bore liquid compositions to achieve optimal toxin removal.

Acknowledgements

M. Tijink would like to thank the Dutch Kidney Foundation for financial support.

The Dutch Kidney Foundation had no involvement in study design, collection and analysis of the data and interpretation of the results.

References

[1] Bethesda M. U.S. Renal Data System, USRDS 2010 Annual Data Report: Atlas of Chronic Kidney Disease and End-Stage Renal Disease in the United States National Institutes of Health, National Institute of Diabetes and Digestive and Kidney Diseases; 2010.

[2] Bethesda M. U.S. Renal Data System, USRDS 2006 Annual Data Report: Atlas of End-Stage Renal Disease in the United States. National Institutes of Health, National Institute of Diabetes and Digestive and Kidney Diseases; 2006.

[3] Mydlik M, Bucek J, Derzsiova K. Influence of charcoal haemoperfusion on platelet count in acute poisoning and during regular dialysis treatment. International Urology and Nephrology 1981;13:387-9.

[4] Ash SR, Sullivan TA, Carr DJ. Sorbent suspensions vs. sorbent columns for extracorporeal detoxification in hepatic failure. Therapeutic Apheresis and Dialysis 2006;10:145-53.

[5] Winchester JF, et al. Sorbents in Acute Renal Failure and End-Stage Renal Disease: Middle Molecule and Cytokine Removal. Blood Purification 2004;22:73-7.

[6] La Greca G, Brendolan A, Ghezzi PM, De Smet R, Tetta C, Gervasio R, Ronco C. The concept of sorbent in hemodialysis. International Journal of Artificial Organs 1998;21:303-8.

[7] Nakabayashi NM, E. Preparation of Poly-Hema Coated Spherical Activated Charcoal for Direct Hemoperfusion. Hemoperfusion: kidney and liver support and detoxification 1980:57-61.

[8] Davankov VA, Pavlova LA, Tsyurupa MP, Tur DR. Novel polymeric solid-phase extraction material for complex biological matrices; Portable and disposable artificial kidney. Journal of Chromatography B: Biomedical Sciences and Applications 1997;689:117-22.

[9] Malchesky PS, Varnes W, Piatkiewicz W, Nose Y. Membranes Containing Sorbents For Blood Detoxification. Transactions American Society for Artificial Internal Organs 1977;23:659-66.

[10] Denti E, Walker JM, Brancaccio D, Tessore V. Evaluation of novel sorbent systems for joint hemodialysis and hemoperfusion. Medical Instrumentation 1977;11:212-6.

[11] Malchesky PS, Piatkiewicz W, Nakamoto S, Nose Y. Haemoperfusion made safe with sorbent membranes. Proc Eur Dial Transplant Assoc 1978;15:591-2.

[12] Malchesky PS, Piatkiewicz W, Varnes WG, Ondercin L, Nose Y. Sorbent Membranes - Device Designs, Evaluations And Potential Applications. Artificial Organs 1978;2:367-71.

[13] Klein E, Holland FF, Eberle K. Sorbent-filled hollow fibers for hemopurification. Transactions of the American Society for Artificial Organs 1978;VOL.24:127-30.

[14] Gurland HJ, Castro LA, Samtleben W, Fernandez JC. Combination of hemodialysis and hemoperfusion in a single unit for treatment of uremia. Clinical Nephrology 1979;11:167-72.

[15] Henne W DG, Schmitz W, Pohle R, Lawitzki F, 4,267,047. Dialyzing membrane with adsorbent layer. United States, 1981 May 12.

[16] Chapman GV, et al. Evaluation Of Hemodiafiltration And Sorbent Membrane Dialysis .1. Invivo And Invitro Dialyzer Performance. Dial Transplant 1982;11:758-65.

[17] Chapman GV, Hone PWE, Shirlow MJ. Evaluation of hemodiafiltration and sorbent membrane dialysis: II. Clinical, nutritional, and middle molecule assessment. Dialysis and Transplantation 1982;11:871-6.

[18] Maeda K, Saito A, Kawaguchi S. Problems with activated charcoal and alumina as sorbents for medical use. Artificial Organs 1979;3:336-40.

[19] Randerson DH, et al. Sorbent Membrane Dialysis In Uremia. ContribNephrol 1982;29:53-64.

[20] Davenport A, Gura V, Ronco C, Beizai M, Ezon C, Rambod E. A wearable haemodialysis device for patients with end-stage renal failure: a pilot study. Lancet 2007;370:2005-10.

[21] Ronco C, Fecondini L. The Vicenza Wearable Artificial Kidney for Peritoneal Dialysis (ViWAK PD). Blood Purification 2007;25:383-8.

[22] Avramescu ME, Borneman Z, Wessling M. Particle-loaded hollow-fiber membrane adsorbers for lysozyme separation. Journal of Membrane Science 2008;322:306-13.

[23] Saiful, Borneman Z, Wessling M. Enzyme capturing and concentration with mixed matrix membrane adsorbers. Journal of Membrane Science 2006;280:406-17.

[24] Avramescu ME, Borneman Z, Wessling M. Dynamic Behavior of Adsorber Membranes for Protein Recovery. Biotechnology and Bioengineering 2003;84:564-72.

[25] Avramescu ME, Gironès M, Borneman Z, Wessling M. Preparation of mixed matrix adsorber membranes for protein recovery. Journal of Membrane Science 2003;218:219-33.

[26] Smith HW, Finkelstein N, Aliminosa L, Crawford B, Graber M. The renal clearances of substituted hippuric acid derivatives and other aromatic acids in dog and man. J Clin Invest 1945;24:388-404.

[27] Vanholder R, et al. Review on uremic toxins: Classification, concentration, and interindividual variability. Kidney International 2003;63:1934-43.

[28] Van Aubel RAMH, Masereeuw R, Russel FGM. Molecular pharmacology of renal organic anion transporters. American Journal of Physiology - Renal Physiology 2000;279:F216-F32.

[29] Besseghir K, Mosig D, Roch-Ramel F. Facilitation by serum albumin of renal tubular secretion of organic anions. American Journal of Physiology - Renal Fluid and Electrolyte Physiology 1989;256.

[30] Tijink MSL, et al. A novel approach for blood purification: Mixed-matrix membranes combining diffusion and adsorption in one step. Acta Biomaterialia 2012;8:2279-87.

[31] Waugh WH, Beall PT. Simplified measurement of p aminohippurate and other arylamines in plasma and urine. Kidney International 1974;5:429-36.

[32] Papenburg BJ, Vogelaar L, Bolhuis-Versteeg LAM, Lammertink RGH, Stamatialis D, Wessling M. One-step fabrication of porous micropatterned scaffolds to control cell behavior. Biomaterials 2007;28:1998-2009.

[33] Smolders CA, Reuvers AJ, Boom RM, Wienk IM. Microstructures in phase-inversion membranes. Part 1. Formation of macrovoids. Journal of Membrane Science 1992;73:259-75.

[34] Husain S, Koros WJ. Macrovoids in hybrid organic/inorganic hollow fiber membranes. Industrial and Engineering Chemistry Research 2009;48:2372-9.

[35] Deng X, Wang T, Zhao F, Li L, Zhao C. Poly(ether sulfone)/activated carbon hybrid beads for creatinine adsorption. Journal of Applied Polymer Science 2007;103:1085-92.

[36] Ye C, Gong QM, Lu FP, Liang J. Adsorption of uraemic toxins on carbon nanotubes. Separation and Purification Technology 2007;58:2-6.

[37] Gao B, Yang Y, Wang J, Zhang Y. Preparation and adsorption characteristic of polymeric microsphere with strong adsorbability for creatinine. Journal of Biochemical and Molecular Toxicology 2008;22:166-74.

[38] Bammens B, Evenepoel P, Keuleers H, Verbeke K, Vanrenterghem Y. Free serum concentrations of the protein-bound retention solute p-cresol predict mortality in hemodialysis patients. Kidney International 2006;69:1081-7.

[39] Vanholder R, De Smet R, Lameire N. Protein-bound uremic solutes: The forgotten toxins. Kidney International, Supplement 2001;59:S266-S70.

[40] Winchester JF, Amerling R, Dubrow A, Feinfeld DA, Gruber SJ, Harbord N, Kuntsevich V. Dialysis desiderata. Hemodialysis International 2007;11.

[41] Ronco C. Sorbents: from bench to bedside - Can we combine membrane separation processes and adsorbent based solute removal? International Journal of Artificial Organs 2006;29:819-22.

[42] Dinh DC, Recht NS, Hostetter TH, Meyer TW. Coated carbon hemoperfusion provides limited clearance of protein-bound solutes. Artificial Organs 2008;32:717-24.

[43] Meyer TW, Peattie JWT, Miller JD, Dinh DC, Recht NS, Walther JL, Hostetter TH. Increasing the clearance of protein-bound solutes by addition of a sorbent to the dialysate. Journal of the American Society of Nephrology 2007;18:868.

[44] Malchesky PS, Nose Y. Device and method for effecting fluid interchange functions. US: Japan Foundation for Artifical Organs, Cleveland, Ohio; 1978. p. 10.

[45] Li D, Chung TS, Wang R. Morphological aspects and structure control of dual-layer asymmetric hollow fiber membranes formed by a simultaneous co-extrusion approach. Journal of Membrane Science 2004;243:155-75.

[46] Albrecht W, Weigel T, Groth T, Hilke R, Paul D. Formation of porous bilayer hollow fibre membranes. Macromolecular Symposia 2002;188:131-41.

[47] Andre JMdS. Mixed matrix membranes, a new platform for enzymatic reactions. Enschede: University of Twente; 2009.

[48] Borneman Z. Particle loaded membrane chromatography. Enschede: University of Twente; 2006.

[49] Widjojo N, Chung TS, Kulprathipanja S. The fabrication of hollow fiber membranes with double-layer mixed-matrix materials for gas separation. Journal of Membrane Science 2008;325:326-35.

[50] Widjojo N, Zhang SD, Chung TS, Liu Y. Enhanced gas separation performance of dual-layer hollow fiber membranes via substructure resistance reduction using mixed matrix materials. Journal of Membrane Science 2007;306:147-58.

Appendix of Chapter 2

The formulas below are used for the calculation of the proportion of activated carbon particles in single layer and dual layer MMM.

$$P_{SL\,MMM} = \frac{W_{AC}}{W_{SL\,MMM}} = \frac{W_{AC}}{(W_{AC} + W_{PES} + W_{PVP})}$$

$$P_{DL\,MMM} = \frac{W_{AC}}{W_{DL\,MMM}} = \frac{W_{AC}}{(W_{MMM} + W_{PFL})} = \frac{P_{SL\,MMM} \cdot \rho_{MMM} \cdot F_{MMM} \cdot V_{MMM}}{(\rho_{MMM} \cdot F_{MMM} \cdot V_{MMM} + \rho_{PFL} \cdot F_{PFL} \cdot V_{PFL})}$$

$$F_{MMM} = \frac{(W_{PES} + W_{PVP} + W_{AC})}{(W_{PES}+W_{PVP}+W_{AC} + W_{NMP})}$$

$$F_{PFL} = \frac{(W_{PES} + W_{PVP})}{(W_{PES}+W_{PVP} + W_{NMP})}$$

$P_{SL\,MMM}$ = Proportion of activated carbon particles in the single layer MMM

W_{AC} = Weight of activated carbon (g)

$W_{SL\,MMM}$ = Weight of single layer MMM (g)

W_{PES} = Weight of PES (g)

W_{PVP} = Weight of PVP (g)

$P_{DL\,MMM}$ = Proportion of activated carbon particles in the dual layer MMM

$W_{DL\,MMM}$ = Weight of dual layer MMM (g)

W_{PFL} = Weight of particle free membrane layer (g)

W_{MMM} = Weight of MMM layer (g)

ρ_{MMM} = Density of MMM dope (g/mL) = 1.12 g/mL

F_{MMM} = Weight factor of MMM layer

V_{MMM} = Volume of a 1x1 cm casted MMM film layer (mL)

ρ_{PFL} = Density of particle free polymer dope (g/mL) = 1.04 g/mL

F_{PFL} = Weight factor of particle free membrane layer

V_{PFL} = Volume of a 1x1 cm casted particle free film layer (mL)

W_{NMP} = Weight of NMP (g)

3

Hollow fiber mixed matrix membranes for removal of protein-bound toxins

M. Tijink
M. Wester
G. Glorieux
K. Gerritsen
J. Sun
R. Sousa
P. Swart
Z. Borneman
M. Wessling
R. Vanholder
J. Joles
D. Stamatialis

This chapter is in preparation for publication

Abstract

In case of renal failure uremic retention solutes accumulate in the patient's body. Despite the significant efforts, the removal of protein bound solutes using current renal replacement therapies is especially challenging. Here we investigate the application of a hollow fiber mixed matrix membrane (MMM) for removal of these toxins. The MMM hollow fiber consists of porous macro-void free polymeric inner membrane layer well attached to the activated carbon containing outer MMM layer. The new membranes have permeation properties in the ultrafiltration range and can adsorb 57%, 82% and 94% of p-cresylsulfate, indoxyl sulfate and hippuric acid respectively, from spiked human plasma in 4h. Besides static adsorption the dual layer hollow fiber MMM can also remove these protein bound toxins under dynamic conditions (cross flow experiments under diffusion and convection modes). Our results indicate potential for these novel membranes for clearance of difficult to remove protein bound toxins.

3.1. Introduction

Prevalence of chronic kidney disease (CKD) increases globally [1, 2] due to the aging population and increasing incidence of risk factors such as diabetes mellitus [3]. Despite considerable amounts of healthcare budgets spent on renal replacement therapy [3, 4], mortality of dialysis patients remains high [5, 6] and their overall health related quality of life low [7]. In fact, the accumulation of uremic retention solutes plays an important role in CKD related morbidity and mortality [8-11]. Small water soluble molecules can be removed by dialysis, but middle molecules and protein bound toxins are difficult to remove with conventional renal replacement therapies. Protein bound toxins are involved in generation of reactive oxygen species and associated with cardiovascular disease, progression of CKD and mortality [9, 11-17]. Although improved uremic toxin removal has been achieved by extending the duration of dialysis, and this is associated with lower mortality rates [18], the removal of protein bound toxins is not improved by extended treatment if the total blood and dialysate fluid crossing the dialyzer is kept constant, [19] or by high-flux dialysis [20]. Convective therapies such as hemodiafiltration can improve removal of the middle molecule ß2-microglobulin [6]. Post dilution online hemodiafiltration has shown to significantly lower total pre-dialysis concentrations of p-cresylsulfate and 3-carboxyl-4-methyl-5-propyl-2-furanpropionic acid (CMPF), two protein bound toxins with high protein binding. However, the effect on their total concentration was only moderate [21].

To improve protein bound toxin removal, the concentration of free toxin on the dialysate side should be low, so that there is a continuous driving force for the free fraction in the blood to diffuse to the dialysate side over the whole hemodialyzer length [22, 23]. Indeed, Dinh *et al.* showed that adding powdered activated carbon into the dialysate compartment, improved the clearance of protein bound solutes by continuous binding of the diffused free fraction [24]. Furthermore, raising the dialysate flow can have a similar effect [22] and Sirich *et al.* showed *in vivo* that removal of protein bound solutes increased by raising the dialysate flow rates [25]. Another way of maintaining a high

concentration gradient over the entire length of a hemodialyzer membrane, thereby probably enhancing protein bound toxin removal, could be incorporation of adsorptive particles in the membrane itself. In fact, more than 30 years ago, so called sorbent membranes were developed, in which adsorptive particles were embedded between two cuprophan membrane layers, or within a cuprophan matrix, to combine both filtering and adsorbing capacity for uremic toxins [26]. However, removal of protein bound toxins was not addressed. After a clinical trial with sorbent membranes, patients rated the treatment low and complained about increased lethargy [27]. This might be due to lack of adsorbents with high purity [28]. In addition, manufacturing difficulties and rapid saturation caused these membranes to be removed from the market [29, 30].

Previously, we showed the concept of a membrane with embedded adsorptive particles, a so-called porous mixed matrix membrane (MMM) [31]. These flat sheet MMMs consisted of a porous particle free layer attached to the mixed matrix membrane layer with embedded particles and showed high adsorption capacity of creatinine and could combine diffusion and adsorption of creatinine in one step [31]. Here, we develop a dual layer hollow fiber MMM to remove protein bound uremic toxins. Polyethersulfone (PES) was used as a membrane forming material, blended with the hydrophilic additive polyvinylpyrrolidone (PVP). This polymer blend is often used for hemodialysis membranes [32, 33]. Activated carbon was selected as adsorptive particle because it adsorbs a broad range of solutes, including protein bound toxins, and it has a long track record in blood purification [24, 34]. A special triple layer spinneret is designed for the spinning of a polymeric inner layer and a thicker outer MMM layer. The influence of spinning parameters such as bore liquid composition and pumping speeds are investigated. Fabricated fibers are characterized in terms of adsorptive capacities and transport properties. Creatinine, a small molecular weight uremic retention solute, often used as a marker of kidney function, was used as a model for water soluble solute. Hippuric acid, indoxyl sulphate and p-cresylsulphate, often used as representatives for the protein bound uremic toxins and associated with negative effects [12-15], are used as model for the protein bound

uremic toxins. Static adsorption experiments as well as experiments under flow conditions are performed to estimate the transport properties of the new hollow fiber MMMs. We investigate here whether these hollow fiber MMMs can clear protein bound toxins. Ultimately this membrane might maintain a concentration difference and thereby a diffusion driving force over the entire membrane length, leading to improved protein bound toxin removal.

3.2. Materials and methods

3.2.1. Materials

Ultrason E 6020 polyethersulfone (PES), obtained from BASF (Ludwigshafen, Germany), and polyvinylpyrrolidone (PVP) K90 (360 000 g/mole) (Fluka, Sigma-Aldrich Chemie Gmbh Munich, Germany) were used as membrane forming materials. N-methylpyrrolidone (NMP) (Acros Organics, Geel, Belgium) was used as solvent. Ultra-pure water was used as non-solvent in the bore liquid and distilled water was used as non-solvent in the coagulation bath. Norit A Supra EUR (European pharmacopoeia grade) (Norit Netherlands BV, Amersfoort, The Netherlands) was sieved in a 45 µm sieve (Fritsch GmbH, Idar-Oberstein, Germany) to a median particle size of 27 µm and were used as activated carbon (AC) particles for incorporation in the MMM and tested separately as pure particles.

The chemicals needed for Tyrode's buffer and the dialysate solution were obtained from Fluka, Sigma Aldrich: 5.4 mM KCl, 137 mM NaCl, 1.8 mM $CaCl_2$, 0.5 mM $MgCl_2$, 11.9 mM $NaHCO_3$ and 5.5 mM glucose were dissolved in ultra-pure water to obtain Tyrode's buffer (pH 7.4). For the dialysate solution, 2 mM KCL, 140 mM NaCl, 1.5 mM $CaCl_2$, 0.25 mM $MgCl_2$, 35 mM $NaHCO_3$ and 5.5 mM glucose were dissolved in ultra-pure water. Creatinine, indoxyl sulfate (IS) and hippuric acid (HA) were purchased from Sigma Aldrich. p-cresylsulfate (PCS) is not commercially available and was synthesized as described before [35].

Polyethylene tubes (Rubber BV, Hilversum, The Netherlands) were used for module fabrication and two component glue (Bison kombi snel rapide, Eriks, Almelo, The Netherlands) was used for potting of the modules. Single fiber modules were applied for the creatinine diffusion experiment, while four fiber modules were used for the plasma diffusion and plasma convection experiments.

Uremic human plasma was obtained from six patients who received a plasma exchange treatment because of acute kidney injury and human blood plasma was obtained from six healthy donors from Sanquin (Amsterdam, The Netherlands) in compliance with local ethical guidelines.

3.2.2. Hollow fiber MMM fabrication

For the adsorptive layer, a dope solution (MMM1) was prepared containing 14 wt% PES and 1.4 wt% PVP K90 dissolved in NMP. The AC particles were added to this dope and after mixing on a roller bank for at least 48 hours, a homogenous dope was obtained with a loading of 60 wt% activated carbon particles in relation to the amount of PES. This solution was degassed for at least 48 hours. The polymer dope of the particle free inner layer (IL1) consisted of 15 wt% PES and 10 wt% PVP dissolved in NMP. After 24 hour mixing on a roller bank the solution was filtered using a Bekipor ST AL3 15 µm filter (Bekaert, Kortrijk, Belgium) and allowed to degas for at least 24h. The following bore liquids were prepared by 24h mixing: B1) 5 wt% PVP in ultra-pure water, B2) 5 wt% PVP and 60 wt% NMP in ultra-pure water and allowed to degas for at least 24h. For the single layer MMM spinneret 1 was used and for the dual layer HF MMM, spinneret 2 was designed (see Table 1 and the appendix of this chapter). The dimensions of the spinnerets were chosen because of practical reasons so that dual layer hollow fibers could be spun for the proof of concept of this study.

Table 1. Spinneret dimensions

	Spinneret 1	Spinneret 2
Inner diameter needle (mm)	0.12	0.26
Outer diameter needle (mm)	0.15	0.46
Inner diameter first orifice (mm)	0.22	0.66
Outer diameter first orifice (mm)		0.96
Inner diameter second orifice (mm)		1.66

All hollow fiber membranes were fabricated by dry wet spinning via immersion precipitation. The MMM dope was pressurized, while the particle free inner layer dope and the bore liquid were pumped through the spinneret. After a 3 cm air gap, the nascent hollow fiber was immersed into a water coagulation bath at room temperature and the hollow fiber was formed by phase separation.

Table 2. Spinning conditions

	SL	DL1	DL2	DL3
Bore liquid	B1	B1	B1	B2
Inner layer polymer dope	-	IL1	IL1	IL1
Mixed matrix membrane layer dope	MMM1	MMM1	MMM1	MMM1
Bore liquid pumping speed (mL/min)	2.7	2.7	2.7	2.7
Inner layer dope pumping speed (mL/min)	-	2.03	0.9	0.9
Pressurized mixed matrix membrane dope speed (mL/min)	8.4	3.9	3.9	3.2
Pulling wheel speed (m/min)	-	4.4	4.4	7
Spinneret	1	2	2	2

Bore liquid B1 contains 5 wt% PVP in ultra pure water, bore liquid B2 contains 5 wt% PVP and 60 wt% NMP in ultra pure water. Inner layer polymer dope IL 1 contains 15 wt% PES and 10 wt% PVP in NMP. Mixed matrix membrane layer dope MMM1 contains 14 wt% PES, 1.4 wt% PVP in NMP and 60 wt% AC in relation to the amount of PES.

During hollow fiber spinning, several parameters were varied, Table 2 describes the spinning conditions. For the single layer MMM (SL), the pulling wheel was not constantly used to collect the hollow fiber, for the other fibers the applicable pulling wheel speeds are presented in Table 2. The pulling wheel speed was adjusted so that the fiber was continuously picked up by the wheel. The

pressurized MMM dope speed was aimed to be the same in DL1, DL2, and DL3. But because of practical difficulties with the pressure regulator the pressurized MMM dope speeds was a little bit lower for DL3. Dual layer HF MMMs were collected during at least three succeeding periods of five minutes of spinning. The collected fibers were washed in ultra-pure water to remove any remaining solvent, and stored in ultra-pure water upon further use. The AC proportion in the membrane was estimated using the content of AC particles, PES and PVP in de dopes, density and pumping speeds of the dopes similar as described before [31].

3.2.3. Membrane characterization

3.2.3.1. Scanning electron microscopy (SEM)

To investigate their surface, the fibers were cut open to expose the inner surface and glued on a sample holder. To examine cross sections, the hollow fiber membranes were dried in air followed by fracturing in liquid nitrogen and were clamped in a cross section sample holder. Then, the samples were dried under vacuum at 30^{o}C and subsequently gold coated using a BalzersUnion SCD 040 sputter coater (OerlikonBalzers, Balzers, Liechtenstein) and examined using a JEOL JSM-5600LV Scanning Electron Microscope (JEOL, Tokyo, Japan). Cross sections of fibers DL1, DL2 and DL3 collected in succeeding periods of five minutes during the spinning were examined. Inner diameter (I.D.), outer diameter (O.D.) and membrane layer thicknesses were determined using SEM pictures originating from all collecting periods.

3.2.3.2. Clean water permeance

Hollow fiber membranes were dried in air and single fiber modules were prepared by gluing the fiber in a tube with a Festo T-connection (Eriks, The Netherlands). After potting, both ends were cut open. The modules were equilibrated in ultra-pure water for at least seven days. Before testing, modules were pre-pressurized at 2 bar for 1 hour, then trans membrane pressures of 0.5, 1.0, 1.5 and 2.0 bar

were applied and the amount of permeated ultra-pure water was measured over time. The clean water permeance (L_p) ($L/m^2/h/bar$) was determined by calculating the slope of a linear fit of the flux versus pressure graph. Fibers from each succeeding five minute period during the spinning were tested for clean water permeance.

3.2.3.3. Adsorption isotherms

Air dried hollow fiber membranes were cut in pieces of 4 cm length and were incubated in 5 mL solutions containing different concentrations of creatinine, IS or HA in Tyrode's buffer in a shaking water bath at 37°C. The range of creatinine concentrations was close to the creatinine levels present in the normal (0.012 mg/mL) and uremic state (0.136 mg/mL) [36]. Also the range of IS and HA concentrations were close to the average uremic concentrations 0.053 mg/mL and 0.247 mg/mL and highest reported uremic concentrations 0.236 mg/mL and 0.471 mg/mL respectively [36], although recent data suggests lower concentrations [8].

After a 72, 48 or 24 hour incubation period, the creatinine, IS and HA concentrations were measured by photo spectrometric analysis at 230, 278 and 228 nm at 25°C in a 2, 2 and 10 mm quartz cuvette respectively. The adsorptive capacity for each uremic retention solute is expressed in mg adsorbed per gram of embedded activated carbon. For the isotherms, the equilibrium adsorption capacity (q) is plotted against the equilibrium concentration of the component (C). The exact particle proportion in DL3 is necessary for this and is calculated to be 0.47. A Langmuir curve fit was obtained as described before [31] and the maximum adsorption capacity (q_m) and dissociation constant (K_d) were estimated.

3.2.3.4. Static adsorption from human blood plasma

Uremic plasma was used for measurements on creatinine, osmolarity, pH, and total protein. Frozen human plasma from three healthy donors was thawed and spiked with PCS, IS and HA to obtain

either similar total concentrations as in uremic patients [8] or higher total concentrations. The spiked plasma solutions were allowed to mix for 10 minutes prior to the start of the experiment. This plasma was tested for concentrations of PCS, IS, HA, creatinine, urea, total protein, Na^+, K^+, Ca^2 and osmolarity and pH.

A PES/PVP particle free flat sheet membrane was used as reference (was made as described before as a single particle free membrane [31]). Approximately 25 mg activated carbon particles, DL3 containing approximately 25 mg activated carbon and approximately 25 mg flat sheet home-made PES/PVP particle free membrane were incubated in approximately 4 mL of different plasmas. The amount of added plasma was adjusted to the amount of incubated material so that the material – plasma relation was always similar to 25 mg material in 4 mL plasma.

All tubes were incubated on a roller bank. After the incubation time, tubes were centrifuged at 3500 rpm for 10 min, and supernatant was collected and one part was stored at 4^{o}C and another part was directly frozen and stored in -80^{o}C. Osmolarity, pH, Na^+, K^+, Ca^{2+}, total protein, urea and creatinine concentrations are measured using the techniques described in Table 3. Furthermore, free and total PCS, IS and HA concentrations were analyzed as described before [37, 38]. The absolute value of a sample was always related to the value of the control plasma at that time point as follows:

$$Relative\ concentration = \frac{C_t}{C_0}$$

Where C_t is the concentration in the plasma incubated with a sample (AC, DL3 or PES/PVP membranes) at that time point, and C_0 is the concentration in the blanc (plasma without sorbents or membranes). Relative osmolarities and pH were calculated in a similar way. Statistical differences were determined using a one-way ANOVA and a post-hoc Tukey test for PCS, IS, HA, osmolarity, pH, and Na^+, K^+, Ca^{2+}, total protein, urea and creatinine concentrations.

Table 3. Test methods for analysis of blood plasma

Parameter	Kit / Device
Osmolarity	Advanced instruments osmometer model 3320
pH	Radiometer Copenhagen PHM lab pH meter
Sodium	Corning 480 Flame Photometer
Potassium	Corning 480 Flame Photometer
Calcium	Bio-Rad Microplate reader Benchmark 16-channel photometer
	DiaSys Calcium CPC FS (1 1121 99 10 021)
Total protein	Bio-Rad Microplate reader Benchmark 16-channel photometer
	Bio-Rad Laboratories GmbH Protein Assay (cat# 500-0006)
Urea	Starrcol standard SC-60-S photometer
	DiaSys Urea CT FS (1 3115 99 10 026)
Creatinine	Bio-Rad Microplate reader Benchmark 16-channel photometer
	DiaSys Creatinine PAP FS (1 1759 99 10 026)

3.2.3.5. Cross flow measurements

Figure 1a and b show the schematic representations of the experimental set up used for the diffusion and convection cross flow experiments respectively. Membrane modules containing one or four hollow fibers were prepared from 8 mm tubes and two Kartell T connections (VWR, Amsterdam, The Netherlands) for the experiments with model solutions and spiked human plasma respectively. Both ends were cut open after potting. Modules were equilibrated in water for at least seven days.

a

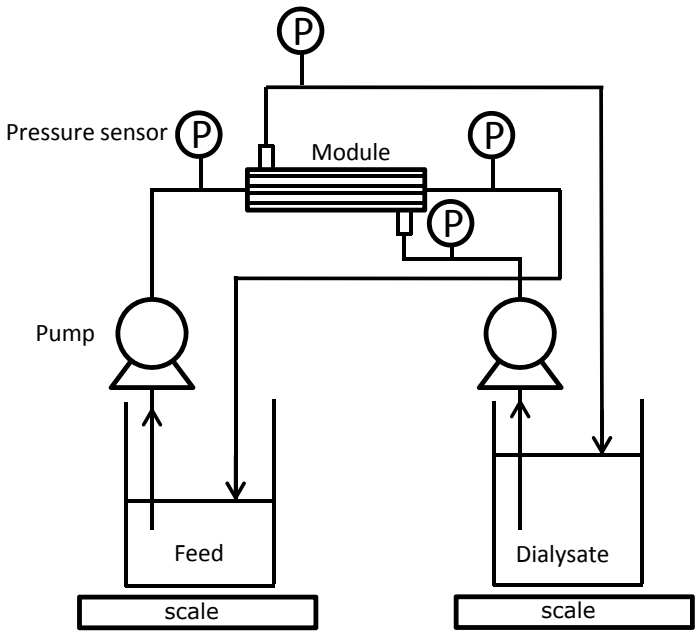

b

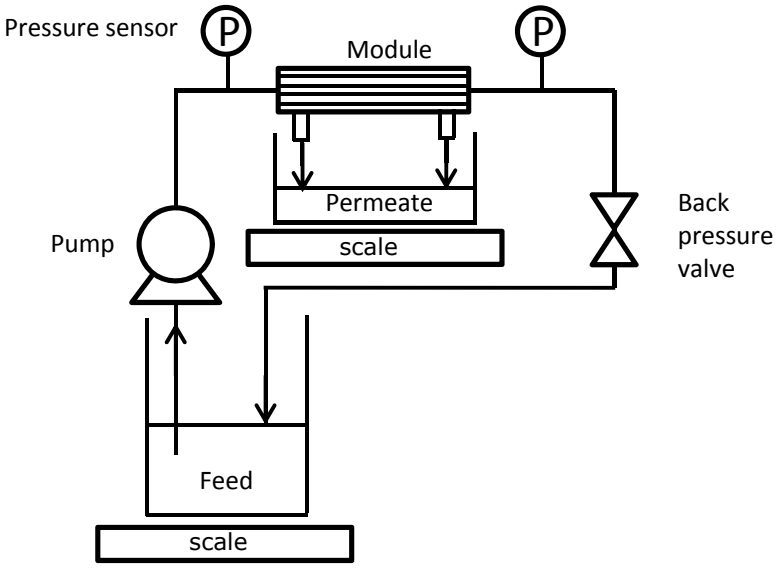

Figure 1. Schematic representations of experimental set up for **a**) diffusion experiments, **b**) convection experiments.

Before the start of the experiment with human plasma, clean water was pressurized through the membranes at 1 bar for at least 1 hour to check if all hollow fiber membranes were open. The modules for the diffusion and convection experiments with human plasma contained on average 96.1 ± 4.1 mg DL3. For the model solution diffusion experiment, the feed consisted of 50 mL 0.1 mg/mL creatinine in ultra-pure water solution (close to mean uremic creatinine concentration [36]) and dialysate was 100 mL ultra-pure water, while for the spiked plasma diffusion experiment the feed consisted of 50 mL spiked human plasma (spiked as described in section 3.2.3.4.) and the dialysate was 100 mL dialysate buffer. For the diffusion experiments, the feed was pumped through the lumen of the hollow fiber, while the dialysate was pumped around the fibers in the counter current direction. The feed and dialysate solutions were pumped at 5 mL/min and 31.4 mL/min respectively. Using these flow rates no transmembrane pressure could be detected.

For the spiked human plasma convection experiment the Spectrumlabs Kross Flo Research IIi system and a back pressure valve (SpectrumLabs automatic back pressure valve, JM separations, Tilburg, The Netherlands) was used in order to obtain constant trans membrane pressures during the whole experiment. The 50 mL spiked human plasma (see section 3.2.3.4.) was pumped through the hollow fiber membranes at 15 mL/min and the transmembrane pressure was set at 0.25 bar.

For all cross flow experiments, at the indicated time points the pressures and the weight of the feed and dialysate or permeate compartments were measured and 2 mL samples were taken from both compartments. After the model solution diffusion experiment, creatinine concentrations were measured using photo spectrometric analysis as described in section 3.2.3.3. The amount of creatinine removed from the feed solution was defined as total removal. The amount of creatinine that appeared in the dialysate solution was considered as creatinine which was diffused from the feed solution. The creatinine deficiency in the mass balance was considered to be adsorbed onto the MMM. These amounts were related to the dry membrane weight which was estimated based on the measured active fiber length in the modules.

Plasma samples were immediately frozen in liquid nitrogen and kept at -80^{o}C until analysis. Total protein concentration, PCS, IS and HA were analyzed as described in section 3.2.3.4. The relative total protein concentrations were calculated as described in section 3.2.3.4. In this case, the value of plasma at the start of the experiment was taken as blanc (C_0).

3.3. Results and discussion

3.3.1. Hollow fiber membrane fabrication and morphology

Figure 2a shows a photograph of membrane DL1. The two membrane layers can clearly be distinguished because of the black and white colors of the MMM layer with embedded black activated carbon particles and the white particle free porous polymeric inner layer, respectively.

Figure 2b shows SEM images of several fabricated hollow fiber mixed matrix membranes. In the round single layer hollow fiber MMM (SL), the AC particles are well distributed in the porous membrane matrix, no cluster formation is observed. Relatively big pores are present in the middle of the membrane structure, while close to the lumen and close to the outside surface, smaller pores are visible. No macro-voids through the complete cross section of the membrane wall are found.

a

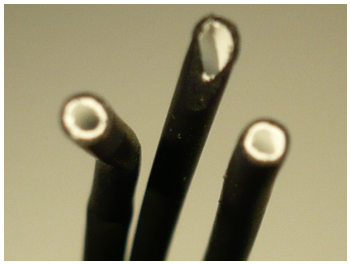

Figure 2. a) Photograph of dual layer hollow fiber MMMs DL1.

b

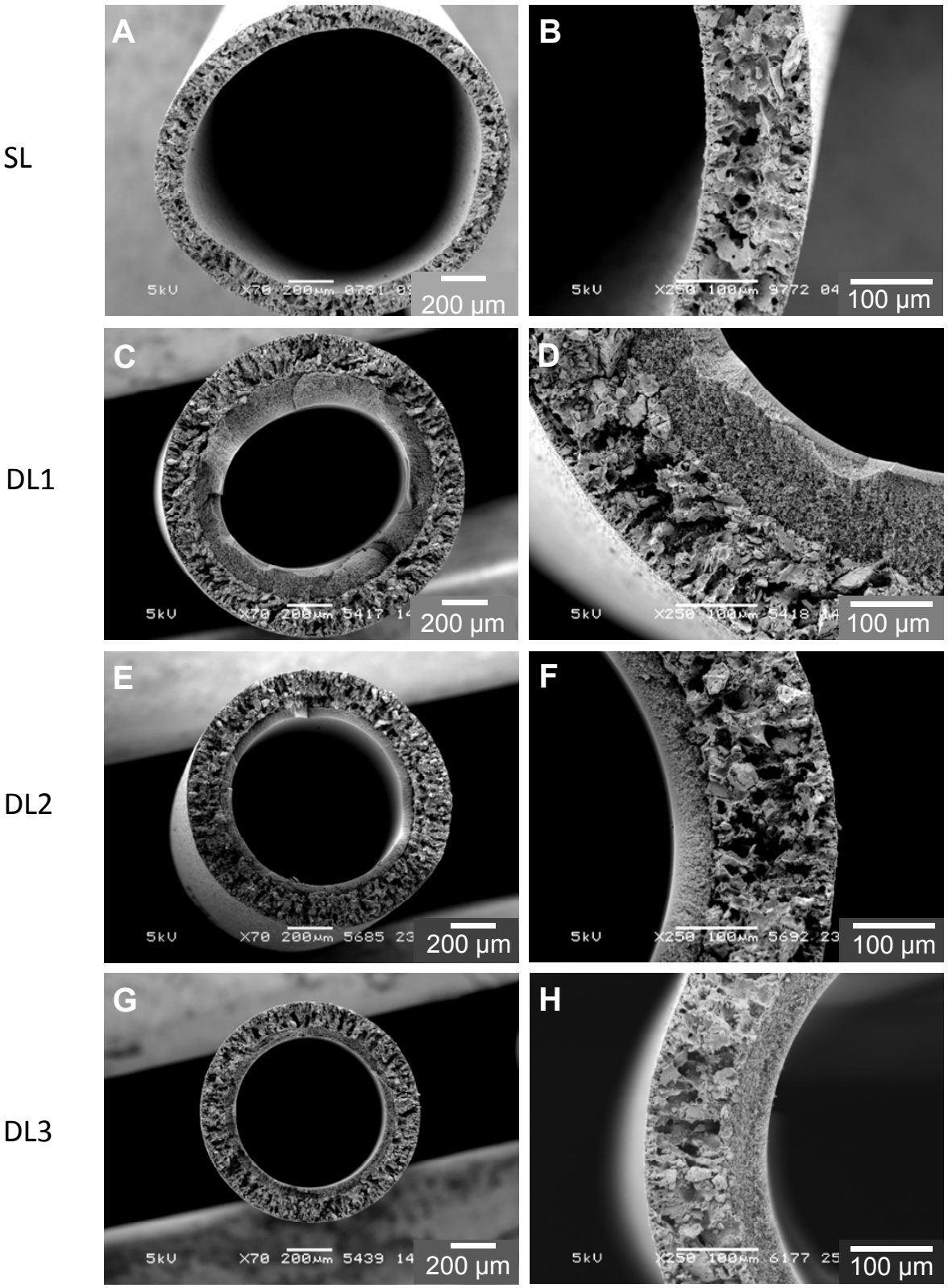

Figure 2 b) Scanning electron microscopy images of single layer hollow fiber MMM SL (A, B) and dual layer hollow fiber MMMs DL1 (C, D), DL2 (E, F), and DL3 (G, H).

c

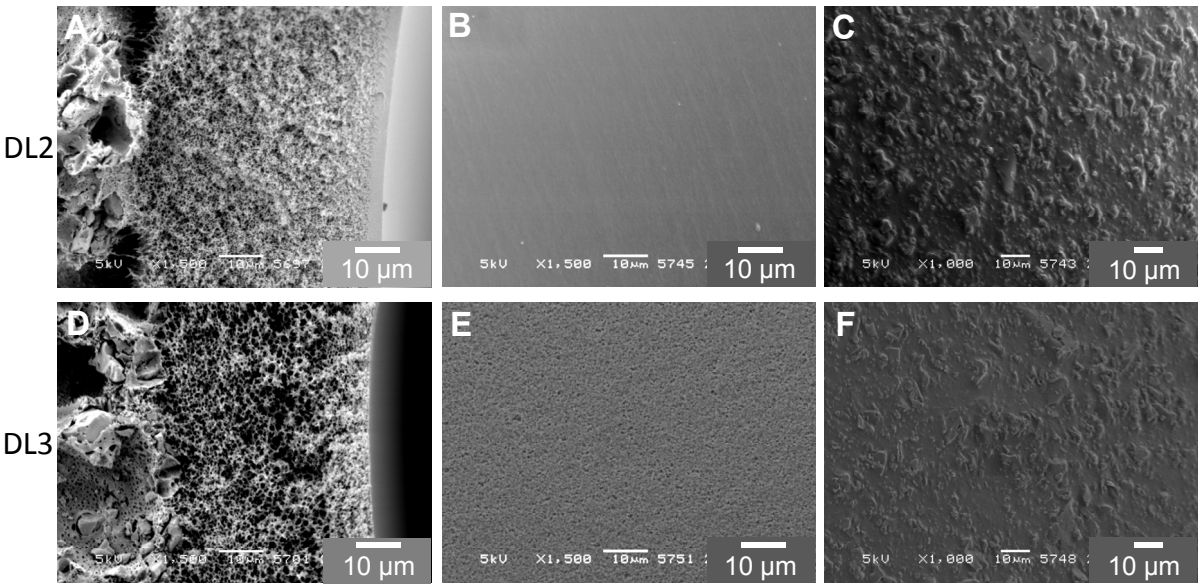

Figure 2 c) Scanning electron microscopy images of fiber DL2 (A, B, C) and DL3 (D, E, F) of cross section (A, D), inner surface (B, E) and outside surface (C, F) with magnifications of 1500x (A, B, D, E) and 1000x (C, F)

Using 5% PVP in the bore liquid and a high bore liquid pumping speed ensured formation of a fiber with a circular bore. Water as bore liquid and/or lower pumping speeds often resulted in the formation of an irregular shape of the inner contour of the fiber (data not shown). The amounts of PES and PVP in the dopes and composition of coagulation fluids were based on the literature [39] and previous experience in our lab with flat sheet membranes [31] and hollow fiber membranes (data not shown). PVP K90 is often used for hemodialysis membranes. Because of its relatively high molecular weight the viscosity of the dope solution was high, promoting formation of macro-void free membranes. Moreover this type of PVP has shown to give biocompatible macro-void free membranes with high solute permeability [40, 41].

Figure 2b also presents SEM pictures of DL1, a dual layer hollow fiber MMM. The two membrane layers can be clearly distinguished, and are well attached to each other. The inner layer is a porous sponge like particle free membrane layer and seems to have a dense skin layer on the inside,

whereas pores become bigger towards the outside. The outside MMM layer has a similar structure as the SL membrane. The particle free membrane layer and the MMM layer have almost the same thickness of around 140 ± 20 µm and 155 ± 20 µm (Table 4). To avoid mass transfer limitations, a thinner particle free membrane layer is desirable. Therefore, the inner layer polymer dope pumping speed was decreased and DL2 was obtained (Figure 2b) having a much thinner inner membrane layer of 52 ± 3 µm. The MMM layer thickness and membrane structure is similar as in DL1. However, still a rather dense skin layer is observed on the lumen of the hollow fiber membrane.

Table 4. Average ± SD dimensions of hollow fiber mixed matrix membranes.

	SL	DL1	DL2	DL3
Outer diameter (O.D.) (µm)	1487 ± 38	1339 ± 14	1186 ± 37	984 ± 11
Inner diameter (I.D.) (µm)	1247 ± 21	776 ± 80	774 ± 29	669 ± 9
Inner layer thickness (µm)	-	140 ± 20	52 ± 3	49 ± 5
Mixed matrix membrane layer thickness (µm)	112 ± 4	155 ± 20	154 ± 8	111 ± 4

In general, by using bore liquids with high amounts of solvent, slower phase separation can be obtained leading to bigger pore sizes [42]. Therefore we changed the composition of the bore liquid from solvent free to a 60% solvent containing bore liquid, also based on previous experiences in flat sheet membranes [31, 39]. Dual layer hollow fiber DL3 was obtained (Figure 2b), and the inside layer seems to have a thinner skin layer than DL2. This can also be seen in Figure 2c, no pores are visible at the inner surface of DL2 while on the inner surface of DL3 pores can be observed. The MMM layer structure of DL3 is similar as in the other dual layer hollow fiber MMM, however, the two layers seem to be better connected in DL3. Probably due to solvent containing bore liquid, slower phase

separation occurs, allowing more time for the separate layers to connect. The pulling wheel speed was higher for this fiber than for DL1 and DL2. Probably, due to the slower phase separation, the nascent fiber became more extended by the pulling. This might explain the smaller dimensions of DL3 compared to DL2, see Table 4. Besides, the little decrease in pumping speed of the MMM dope may have played a role in this. The outer surfaces in Figure 2c show that the particles are well distributed in the MMM matrix.

3.3.2. Clean water permeance

Figure 3 presents a linear clean water flux vs. pressure relationship for DL3 with a clean water permeance of 58.4 ± 9.3 L/m^2/h/bar. Lower as well as higher clean water permeances have been described for polyethersulfone based hollow fibers used for hemodialysis [43, 44].

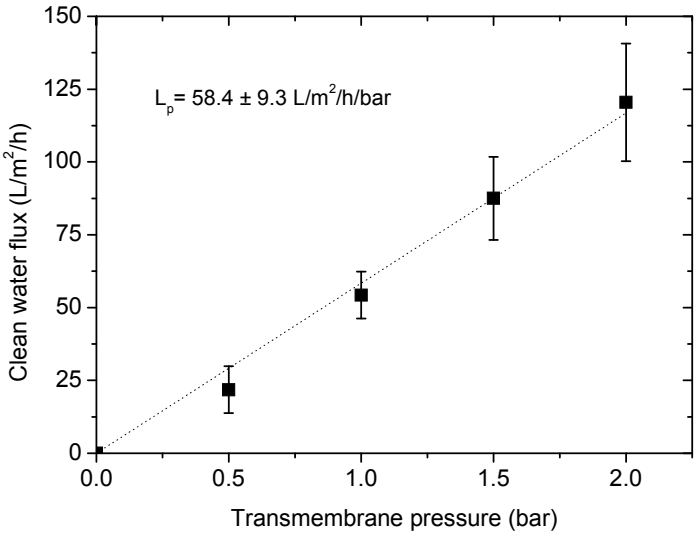

Figure 3. Average clean water flux versus transmembrane pressure for DL3 (n=6). Error bars indicate standard deviations.

Neither particle loss during the experiment nor delamination of the two membrane layers was observed. DL1 and DL2 show a clean water permeance of less than 3 L/m^2/h/bar. For all hollow fibers DL 1, 2 and 3 the clean water permeance was measured for fiber samples from different collection periods and show constant clean water permeances in all cases. Because of higher water permeance, DL3 was selected for further characterization in this paper.

3.3.3 Static adsorption

Adsorption isotherms

DL3 adsorbs creatinine, IS and HA, which is illustrated by the adsorption isotherms in Figure 4. Langmuir isotherm curve fits have been performed, even though for the tested concentration range a plateau was not reached yet in all cases. For creatinine, IS and HA, q_m= 3064 mg/g AC and K_d = 1.433 mg/mL, q_m= 350 mg/g AC and K_d=0.023 mg/mL, q_m= 134 mg/g AC and K_d=0.0195 mg/mL were obtained respectively. DL3 has much higher adsorption capacity for creatinine in comparison to flat sheet dual layer MMMs developed earlier [31]. For example, at a creatinine equilibrium concentration of 0.05 mg/mL the flat sheet dual layer MMM adsorbed approximately 29 mg creatinine per gram of activated carbon while the DL3 adsorbed around 100 mg/g AC. It is rather difficult to directly compare our results to other studies because of different experimental conditions and limited availability of *in vitro* adsorption data. In any case, we will discuss here some examples where comparison is possible. For example for creatinine adsorption, other publications with different approaches but using activated carbon as sorbent, report lower adsorption values at similar equilibrium concentrations [45-47]. Furthermore, granular and powdered carbons have been tested for adsorption of several compounds including IS. Using a sorbent/volume ratio of 2 mg/mL and an initial concentration of 0.03 mg/mL IS in a protein free solution, removal of more than 90% of the free IS was obtained after 24h. For our isotherm experiment we also used a protein free solution and free IS. Using a lower sorbent/volume ratio of 1.2 mg/mL but a longer incubation time (48h) we

obtained removal of 95% at a similar initial concentration. Thus, IS adsorption by DL3 is in the same range as a commercial activated carbon [24].

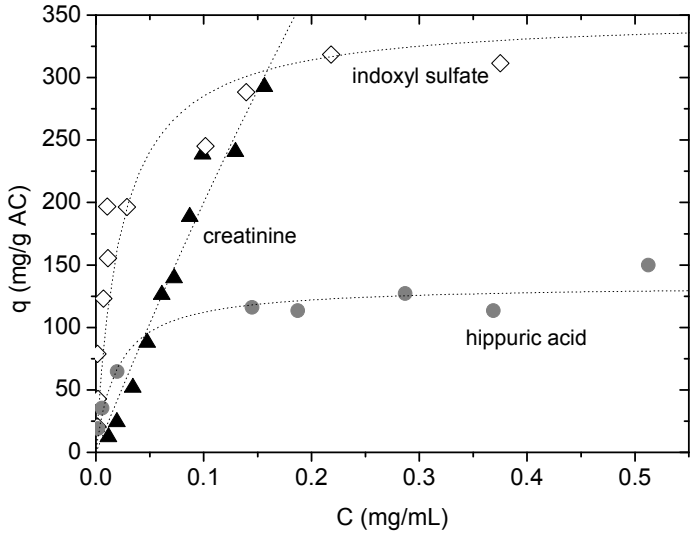

Figure 4. Adsorption isotherms at 37 °C for DL3. The equilibrium adsorption capacity (q) expressed in mg adsorbed creatinine (▲), indoxyl sulfate (◊) or hippuric acid (●) per gram of activated carbon (AC) embedded in DL3 is plotted against the equilibrium concentration (C) of creatinine, indoxyl sulfate and hippuric acid. The dotted lines represent the calculated Langmuir isotherm fits.

Adsorption from human blood plasma

Figure 5 shows the average relative creatinine concentrations after incubation in uremic plasma. The DL3 significantly removes creatinine compared to the particle free PES/PVP membrane, up to 83 ± 4 % is adsorbed after 4h. This approaches the creatinine removal by activated carbon particles alone, which suggests a good creatinine accessibility of the particles embedded in DL3. Relative plasma pH and osmolarity did not change significantly during the test duration. The total protein concentration is unchanged indicating that undesired protein binding is also limited (data not shown).

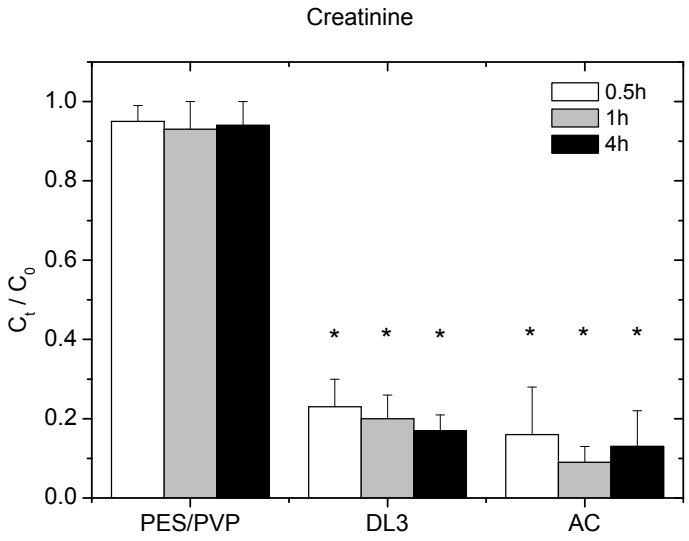

Figure 5. Average relative creatinine concentrations (C_t / C_0) after incubation of a PES/PVP membrane, dual layer hollow fiber mixed matrix membrane DL3 or pure activated carbon (AC) in plasma (n=6) for 0.5, 1 or 4h. * indicates a significant difference compared to particle free PES/PVP membrane (p<0.05). Error bars indicate standard deviations.

The amount of PCS, IS and HA bound to protein was on average 98%, 97% and 53% respectively and this was constant for the duration of the experiments (data not shown). Figure 6 shows the average relative PCS, IS and HA concentrations after 1h and 4h incubation with a PES/PVP membrane, DL3 or activated carbon particles for both initial spiked concentrations. DL 3 and AC both remove PCS, IS and HA significantly compared to the PES/PVP membrane. For the plasma which was spiked for uremia relevant concentrations, the relative PCS concentration is lowered to an average of 0.43 and 0.16 by DL3 and AC respectively after 4h. IS is also removed by DL3 and AC and after 4h average relative IS concentrations of 0.17 and 0.03 are obtained, respectively. For HA, the DL3 membrane and AC decrease the average relative concentrations after 4h to 0.05 and 0.01, respectively. The PES/PVP membrane does not adsorb PCS, IS and HA. Thus, even in these experimental conditions with a relatively low sorbent – plasma ratio 6.25 mg/mL (compared to ~100 mg/mL in hemoperfusion) the majority of PCS, IS and HA can be removed from the plasma within 4h by DL3.

However, the activated carbon particles decreased the relative concentrations significantly more (p<0.05) than DL3 in all cases which may be due to some diffusion limitations, or reduction in adsorption capacity introduced by the membrane matrix.

a

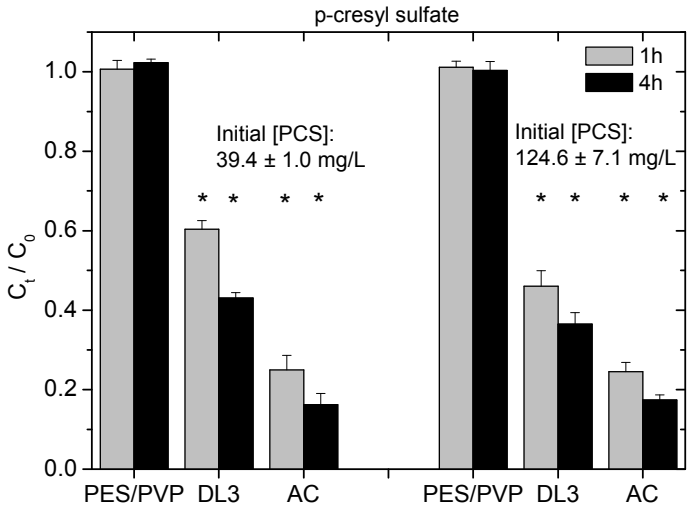

Figure 6. Relative concentrations after incubation of a particle free PES/PVP membrane, dual layer hollow fiber MMM DL3 and pure activated carbon particles (AC) in spiked plasma with 2 different initial concentrations for 1 or 4h. **a**) p-cresylsulfate. * indicates a significant difference compared to the particle free PES/PVP membrane (p<0.05)

b

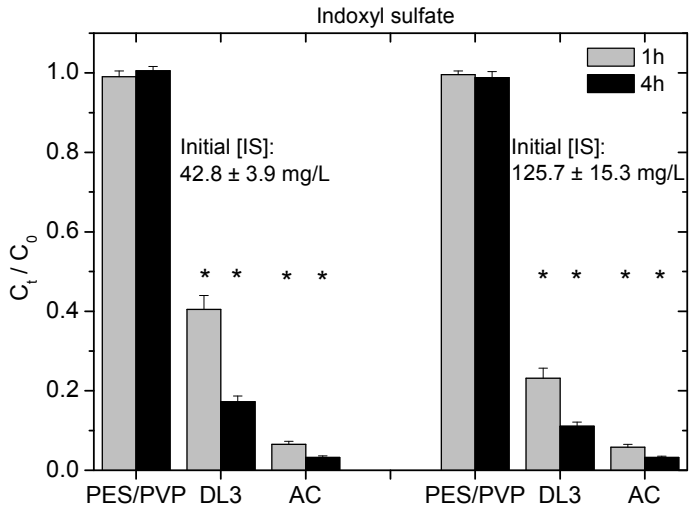

c

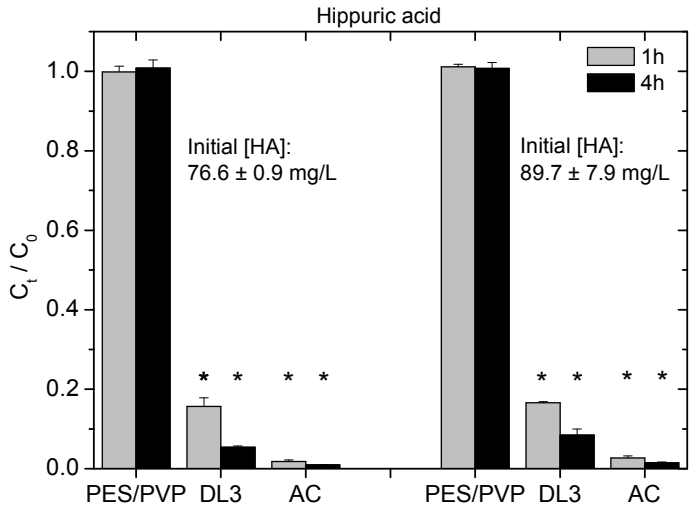

Figure 6. Relative concentrations after incubation of a particle free PES/PVP membrane, dual layer hollow fiber MMM DL3 and pure activated carbon particles (AC) in spiked plasma with 2 different initial concentrations for 1 or 4h **b**) Indoxyl sulfate, **c**) Hippuric acid. * indicates a significant difference compared to the particle free PES/PVP membrane (p<0.05)

One should remember however, that in this work we use small particles (median size 27 μm) which although seem to have sub optimal accessibility in the membrane matrix, but probably cannot be applied in adsorption columns which commonly have much larger particles for removal of solutes from blood or plasma. Small particles in columns could introduce high pressure drop into the system, as shown in [48], possibly resulting in protein denaturation, and leakage of particle fragments into the patient's blood circulation. In contrast to adsorptive columns, in MMMs small particles can be used without a high pressure drop and channeling since particles are well distributed into the polymeric matrix [48]. In any case, in the future we plan to develop improved dual layer membranes with improved pore connectivity and higher particle loading.

Table 5. Average relative plasma values ± sd after incubation in human blood plasma of three donors for 4h. The plasma is incubated with a PES/PVP membrane, dual layer hollow fiber MMM DL3 or pure activated carbon (AC) particles alone

	PES/PVP	DL3	AC
Relative osmolarity	1.008 ± 0.01	0.963 ± 0.01*	0.984 ± 0.01
Relative pH	1.004 ± 0.01	1.041 ± 0.07	1.046 ± 0.06
Relative Na^+ concentration	0.965 ± 0.07	0.952 ± 0.07	1.003 ± 0.02
Relative K^+ concentration	0.959 ± 0.08	0.935 ± 0.07	0.983 ± 0.01
Relative Ca^{2+} concentration	1.008 ± 0.04	1.040 ± 0.10	0.981 ± 0.07
Relative total protein concentration	1.002 ± 0.03	0.982 ± 0.05	0.996 ± 0.02
Relative urea concentration	0.986 ± 0.03	0.959 ± 0.06	0.957 ± 0.02
Relative creatinine concentration	0.946 ± 0.02	0.000 ± 0.00*	0.000 ± 0.00*

* indicates a significant difference compared with PES/PVP (p<0.05)

Table 5 presents average relative plasma values after incubation in plasma. Low levels of creatinine (compared to an uremic situation) are present in this plasma from healthy donors, and DL3 and AC completely remove creatinine within 4h (p<0.05), indicating the good adsorptive power even at low solute concentrations. There is no effect on pH or concentrations of Na^+, K^+, Ca^{2+}, total protein and urea (see Table 5) by DL3 or AC. DL3 lowered osmolarity (p<0.05 versus PES/PVP membrane), although this was not observed in the previous experiment using plasma exchange plasma.

3.3.4 Cross flow measurements

Creatinine diffusion cross flow measurements

As we showed before [31], dual layer MMMs can combine diffusion and adsorption in one step. Figure 7 shows that a lot of creatinine is adsorbed in the beginning and DL3 becomes more or less saturated. Whereas the diffusion of creatinine continues during the whole experiment. After 4h, which is a common duration of a hemodialysis treatment, both diffusion and adsorption equally contributed to the total creatinine removal. Almost 40 mg/g membrane creatinine was removed after 4h. Although this data cannot be directly compared to the *in vivo* situation, a rather crude comparison can be done. Assuming *in vivo* removal to be similar as in this experiment, one would require 45 gram (or 0.6 m^2) MMM to remove the daily creatinine production (~1800mg), which seems to be in a realistic range.

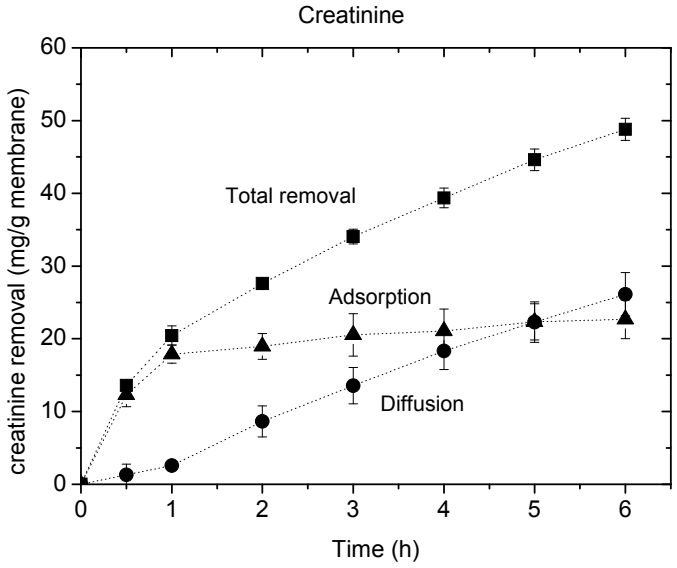

Figure 7. Average creatinine total removal (■), diffusion (●) and adsorption (▲) plotted vs. time, (n=3). Total removal is the amount of creatinine removed from the feed solution. This removal is mediated by diffusion and adsorption of creatinine. Error bars indicate standard deviations. The dotted lines are plotted to guide the eye.

Plasma cross flow measurements

For testing the removal of protein bound toxins PCS, IS and HA from spiked plasma, cross flow experiments were performed either in diffusion (Figure 1a) or convection mode (Figure 1b). The amount of PCS, IS and HA bound to protein was on average 90.0%, 86.6% and 38.1% respectively at the start of the experiments. In the diffusion experiments, albumin is retained by the membrane (relative total protein concentration in plasma after 6h: 1.000 ± 0.02) equivalent to membranes in hemodialysis. In the convection experiments, albumin partially passed through the membrane (together with a lot of fluid) with a relative total protein concentration of 2.224 ± 0.49 in the feed and 0.306 ± 0.18 in the permeate at the end of the experiment, respectively.

a

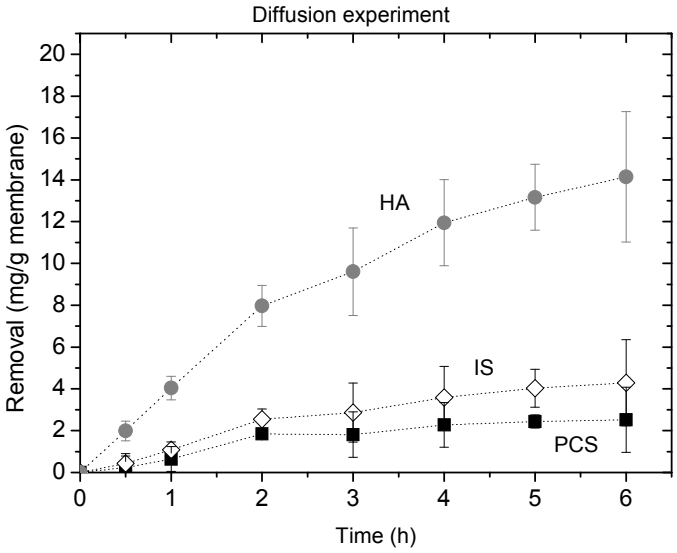

b

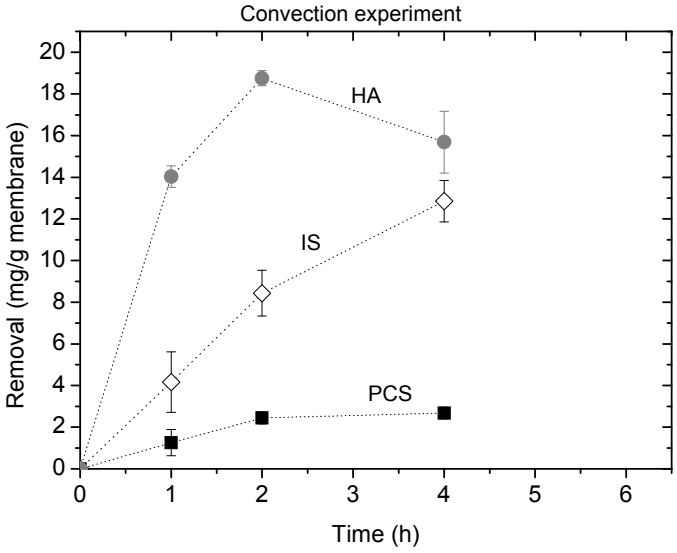

Figure 8. Removal of p-cresylsulfate (PCS) (■), indoxyl sulfate (IS) (◊) and hippuric acid (HA) (●) plotted over the time.

a) Diffusion experiment (n=3). **b**) Convection experiment (n=3). Dotted lines are plotted to guide the eye.

Figure 8a presents the results of toxin removal in the diffusion experiments. The removal presented there corresponds to the amount of toxin depleted from the feed plasma in time. In most cases the toxin concentration in the dialysate was very low or below the HPLC detection limit. Therefore we can reasonably assume that the toxin removal here is mostly due to adsorption on the MMM. Figure 8b presents the results of toxin adsorption onto the hollow fiber MMMs during the convection experiments. This was estimated based on the amount of toxin depleted from the feed plasma and from the collected permeate based on the mass balance. In both cases, the adsorption of the toxins on the MMMs increases in time. It seems that the amount adsorbed in the convection experiments is higher than in the diffusion experiments, probably due to higher transport of the toxins due to the pressure difference. The removal of these hard to remove protein bound toxins by the DL3 in diffusion and convection cross flow experiments with spiked human plasma shows the potential for further development of this type of membranes. Direct comparisons of our work with other studies are rather difficult because of different experimental conditions. However, we could make a rather crude extrapolation to see if we are in a feasible range. Healthy subjects excrete 78 mg PCS and 69 mg IS in their urine in 24h [49]. Our membranes removed on average 2.27 mg PCS/g membrane and 3.58 mg IS /g membrane in 4h in the diffusion experiment and 2.68 mg/g membrane PCS and 12.85 mg/g membrane IS in the convection experiment. Assuming similar removal in the *in vivo* situation, one would need 5-35 gram (0.07-0.5 m^2) MMM for daily removal of these toxins. Comparing to hemoperfusion columns containing around 300 grams of particles, or hemodialyzers containing 1-2 m^2 membrane, these values show the good potential of our membrane. Further membrane optimization may improve the adsorption capacity of the hollow fiber membrane and its transport characteristics.

3.4. Conclusions and outlook

In this work we fabricated a dual layer hollow fiber MMM with a porous macro-void free inner membrane layer that was well attached to the MMM outer layer containing AC particles. Spinning parameter as spinneret type, bore liquid composition and pumping speed of the dope solutions influence the final membrane structure of the MMM. This dual layer hollow fiber MMM adsorbs both creatinine and difficult-to-remove protein bound toxins from human plasma solutions. Furthermore, in cross flow experiments with human spiked plasma, the MMM removes protein bound toxins, indicating great potential of this new concept for removal of these difficult-to-remove type of toxins.

Future research could be focused on further membrane optimization. The inner layer thickness may be further reduced to minimize mass transport limitations. Porosity can be optimized to obtain a sharp cut off and possibly designed to avoid albumin loss and achieve optimal particle accessibility. Furthermore, the overall particle proportion of the membrane may be further increased and also other dimensions of the fiber may enhance transport properties. It would be interesting to fabricate modules of dual layer hollow fiber membranes on a bigger scale, for example comparable to hemodialysis modules in size, or comparable in terms of activated carbon content to commercially available adsorptive columns and test removal capacity of several uremic retention solutes.

Acknowledgements

M. Tijink would like to acknowledge the Dutch Kidney Foundation for the financial support of this project. J. Sun would like to thank National Natural Science Foundation of China (51203020) and Shanghai Nature Science Foundation (11ZR1400500). K. Gerritsen would like to acknowledge the ERA-EDTA for their financial support. Andre Eppingbroek, Erik Rolevink and Herman Teunis are acknowledged for their support with the design of the novel spinneret.

References

[1] Coresh J, et al. Prevalence of chronic kidney disease in the United States. Journal of the American Medical Association 2007;298:2038-47.

[2] Hamer RA, El Nahas AM. The burden of chronic kidney disease. British Medical Journal 2006;332:563-4.

[3] Szczech LA, Lazar IL. Projecting the United States ESRD population: Issues regarding treatment of patients with ESRD. Kidney International, Supplement 2004;66.

[4] Kerr M, Bray B, Medcalf J, O'Donoghue DJ, Matthews B. Estimating the financial cost of chronic kidney disease to the NHS in England. Nephrology Dialysis Transplantation 2012.

[5] Lacson Jr E, et al. Survival with three-times weekly in-center nocturnal versus conventional hemodialysis. Journal of the American Society of Nephrology 2012;23:687-95.

[6] Grooteman MPC, et al. Effect of online hemodiafiltration on all-cause mortality and cardiovascular outcomes. Journal of the American Society of Nephrology 2012;23:1087-96.

[7] Mazairac AHA, et al. Changes in quality of life over time-Dutch haemodialysis patients and general population compared. Nephrology Dialysis Transplantation 2011;26:1984-9.

[8] Duranton F, Cohen G, De Smet R, Rodriguez M, Jankowski J, Vanholder R, Argiles A. Normal and pathologic concentrations of uremic toxins. Journal of the American Society of Nephrology 2012;23:1258-70.

[9] Bammens B, Evenepoel P, Keuleers H, Verbeke K, Vanrenterghem Y. Free serum concentrations of the protein-bound retention solute p-cresol predict mortality in hemodialysis patients. Kidney International 2006;69:1081-7.

[10] Cheung AK, et al. Serum β-2 microglobulin levels predict mortality in dialysis patients: Results of the HEMO study. Journal of the American Society of Nephrology 2006;17:546-55.

[11] Ito S, Osaka M, Higuchi Y, Nishijima F, Ishii H, Yoshida M. Indoxyl Sulfate Induces Leukocyte-Endothelial Interactions through Up-regulation of E-selectin. Journal of Biological Chemistry 2010;285:38869-75.

[12] Adijiang A, Goto S, Uramoto S, Nishijima F, Niwa T. Indoxyl sulphate promotes aortic calcification with expression of osteoblast-specific proteins in hypertensive rats. Nephrology Dialysis Transplantation 2008;23:1892-901.

[13] Lin CJ, et al. The role of protein-bound uremic toxins on peripheral artery disease and vascular access failure in patients on hemodialysis. Atherosclerosis 2012;225:173-9.

[14] Wu IW, et al. P-cresyl sulphate and indoxyl sulphate predict progression of chronic kidney disease. Nephrology Dialysis Transplantation 2011;26:938-47.

[15] Itoh Y, Ezawa A, Kikuchi K, Tsuruta Y, Niwa T. Protein-bound uremic toxins in hemodialysis patients measured by liquid chromatography/tandem mass spectrometry and their effects on endothelial ROS production. Anal Bioanal Chem 2012;403:1841-50.

[16] Lekawanvijit S, Adrahtas A, Kelly DJ, Kompa AR, Wang BH, Krum H. Does indoxyl sulfate, a uraemic toxin, have direct effects on cardiac fibroblasts and myocytes? European Heart Journal 2010;31:1771-9.

[17] Adijiang A, Higuchi Y, Nishijima F, Shimizu H, Niwa T. Indoxyl sulfate, a uremic toxin, promotes cell senescence in aorta of hypertensive rats. Biochemical and Biophysical Research Communications 2010;399:637-41.

[18] Saran R, et al. Longer treatment time and slower ultrafiltration in hemodialysis: Associations with reduced mortality in the DOPPS. Kidney International 2006;69:1222-8.

[19] Basile C, et al. Removal of uraemic retention solutes in standard bicarbonate haemodialysis and long-hour slow-flow bicarbonate haemodialysis. Nephrology Dialysis Transplantation 2011;26:1296-303.

[20] Dhondt A, Vanholder R, Van Biesen W, Lameire N. The removal of uremic toxins. Kidney International, Supplement 2000;58:S47-S59.

[21] Meert N, et al. Prospective evaluation of the change of predialysis protein-bound uremic solute concentration with postdilution online hemodiafiltration. Artificial Organs 2010;34:580-5.

[22] Meyer TW, Peattie JWT, Miller JD, Dinh DC, Recht NS, Walther JL, Hostetter TH. Increasing the clearance of protein-bound solutes by addition of a sorbent to the dialysate. Journal of the American Society of Nephrology 2007;18:868.

[23] Patzer J. Principles of bound solute dialysis. Therapeutic Apheresis and Dialysis 2006;10:118-24.

[24] Dinh DC, Recht NS, Hostetter TH, Meyer TW. Coated carbon hemoperfusion provides limited clearance of protein-bound solutes. Artificial Organs 2008;32:717-24.

[25] Sirich TL, Luo FJG, Plummer NS, Hostetter TH, Meyer TW. Selectively increasing the clearance of protein-bound uremic solutes. Nephrology Dialysis Transplantation 2012;27:1574-9.

[26] Henne W DG, Schmitz W, Pohle R, Lawitzki F, 4,267,047. Dialyzing membrane with adsorbent layer. United States, 1981 May 12.

[27] Chapman GV, Hone PWE, Shirlow MJ. Evaluation of hemodiafiltration and sorbent membrane dialysis: II. Clinical, nutritional, and middle molecule assessment. Dialysis and Transplantation 1982;11:871-6.

[28] Maeda K, Saito A, Kawaguchi S. Problems with activated charcoal and alumina as sorbents for medical use. Artificial Organs 1979;3:336-40.

[29] Chapman GV, et al. Evaluation Of Hemodiafiltration And Sorbent Membrane Dialysis .1. Invivo And Invitro Dialyzer Performance. Dial Transplant 1982;11:758-65.

[30] Vienken J, Diamantoglou M, Henne W, Nederlof B. Artificial dialysis membranes: From concept to large scale production. American Journal of Nephrology 1999;19:355-62.

[31] Tijink MSL, et al. A novel approach for blood purification: Mixed-matrix membranes combining diffusion and adsorption in one step. Acta Biomaterialia 2012;8:2279-87.

[32] Su BH, Fu P, Li Q, Tao Y, Li Z, Zao HS, Zhao CS. Evaluation of polyethersulfone highflux hemodialysis membrane in vitro and in vivo. Journal of Materials Science: Materials in Medicine 2008;19:745-51.

[33] Zweigart C, Neubauer M, Storr M, Böhler T, Krause B. 2.13 - Progress in the Development of Membranes for Kidney-Replacement Therapy. In: Editor-in-Chief: Enrico D, Lidietta G, editors. Comprehensive Membrane Science and Engineering. Oxford: Elsevier; 2010. p. 351-90.

[34] Ash SR. Sorbents in treatment of uremia: A short history and a great future. Seminars in Dialysis 2009;22:615-22.

[35] Feigenbaum J, Neuberg CA. Simplified method for the preparation of aromatic sulfuric acid esters. Journal of the American Chemical Society 1941;63:3529-30.

[36] Vanholder R, et al. Review on uremic toxins: Classification, concentration, and interindividual variability. Kidney International 2003;63:1934-43.

[37] Meert N, et al. Effective removal of protein-bound uraemic solutes by different convective strategies: A prospective trial. Nephrology Dialysis Transplantation 2009;24:562-70.

[38] Meert N, et al. Novel method for simultaneous determination of p-cresylsulphate and p-cresylglucuronide: Clinical data and pathophysiological implications. Nephrology Dialysis Transplantation 2012;27:2388-96.

[39] Boom RM. Membrane formation by immersion precipitation: the role of a polymeric additive [PhD Thesis]. Enschede: University of Twente; 1992.

[40] Xu ZL, Qusay FA. Polyethersulfone (PES) hollow fiber ultrafiltration membranes prepared by PES/non-solvent/NMP solution. Journal of Membrane Science 2004;233:101-11.

[41] Yang Q, Chung TS, Weber M. Microscopic behavior of polyvinylpyrrolidone hydrophilizing agents on phase inversion polyethersulfone hollow fiber membranes for hemofiltration. Journal of Membrane Science 2009;326:322-31.

[42] Liu Y, Koops GH, Strathmann H. Characterization of morphology controlled polyethersulfone hollow fiber membranes by the addition of polyethylene glycol to the dope and bore liquid solution. Journal of Membrane Science 2003;223:187-99.

[43] Barzin J, Feng C, Khulbe KC, Matsuura T, Madaeni SS, Mirzadeh H. Characterization of polyethersulfone hemodialysis membrane by ultrafiltration and atomic force microscopy. Journal of Membrane Science 2004;237:77-85.

[44] Liao Z, Klein E, Poh CK, Huang Z, Lu J, Hardy PA, Gao D. Measurement of hollow fiber membrane transport properties in hemodialyzers. Journal of Membrane Science 2005;256:176-83.

[45] Deng X, Wang T, Zhao F, Li L, Zhao C. Poly(ether sulfone)/activated carbon hybrid beads for creatinine adsorption. Journal of Applied Polymer Science 2007;103:1085-92.

[46] Ye C, Gong QM, Lu FP, Liang J. Adsorption of uraemic toxins on carbon nanotubes. Separation and Purification Technology 2007;58:2-6.

[47] Gao B, Yang Y, Wang J, Zhang Y. Preparation and adsorption characteristic of polymeric microsphere with strong adsorbability for creatinine. Journal of Biochemical and Molecular Toxicology 2008;22:166-74.

[48] Tetala KKR, Stamatialis DF. Mixed matrix membranes for efficient adsorption of copper ions from aqueous solutions. Separation and Purification Technology 2013;104:214-20.

[49] Martinez AW, Recht NS, Hostetter TH, Meyer TW. Removal of P-cresol sulfate by hemodialysis. Journal of the American Society of Nephrology 2005;16:3430-6.

Appendix of Chapter 3

A triple spinneret was designed so that fibers with a thin inner layer and thicker outer layer could be fabricated. The channels for the bore liquid and inner layer polymer dope are connected as usual in spinnerets, whereas for the outer layer MMM dope a special distribution ring was designed, see Figure 1 and 2.

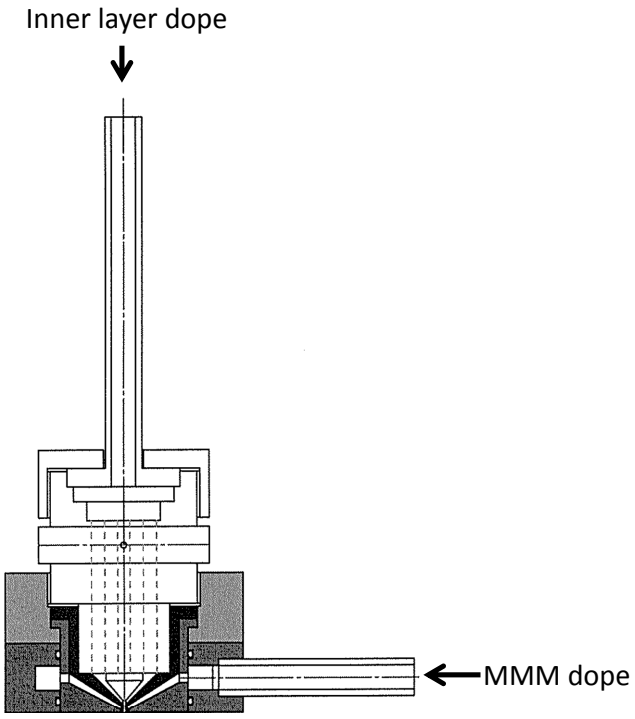

Figure 1. Schematic representation of triple spinneret 2

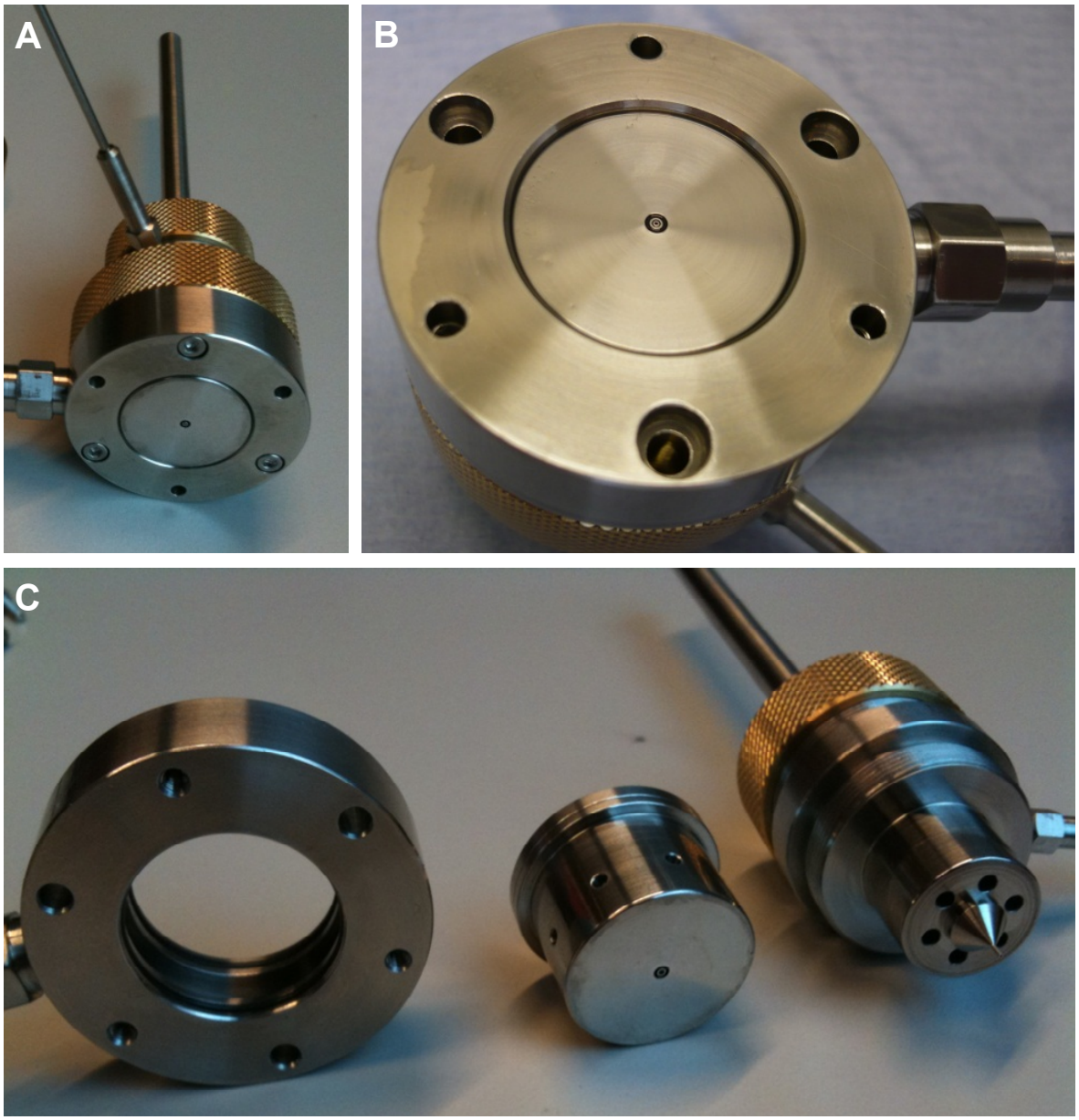

Figure 2. Photographs of triple spinneret 2, A) spinneret with distribution ring. B) bottom of the spinneret with distribution ring. C) Disassembled spinneret, with the distribution ring separately on the left.

4

Screening of adsorptive particles for uremic toxin removal

M. Tijink
M. Wester
G. Glorieux
K. Gerritsen
R. Vanholder
J. Joles
M. Wessling
D. Stamatialis

Abstract

Uremic retention solutes accumulate in uremic patients and this is associated with mortality. Middle molecules and protein-bound toxins are poorly removed using conventional hemodialysis treatment and adsorption may help to remove these molecules. In this work three types of adsorptive particles are investigated. Norit activated carbon, Mast carbon and Y-carbon show adsorption of small water soluble molecule creatinine, middle molecule β_2-microglobulin and protein-bound toxins p-cresylsulfate, indoxyl sulfate and hippuric acid. Thus, a broad spectrum of uremic toxins can be removed using adsorptive particles. Y-carbon seems to adsorb more β_2-microglobulin per gram of adsorbent than Mast carbon and Norit activated carbon, while for removal of protein-bound toxins the latter two seem to be a bit better. For the future it would be interesting to investigate these particles further and incorporate in a mixed matrix membrane structure.

4.1. Introduction

In uremic patients, various retention solutes accumulate in their body which would, under normal condition, be excreted by the kidneys. Those compounds that interact negatively with biologic functions are called uremic toxins [1]. Uremic retention solutes are generally categorized into three categories [2, 3]. The small water-soluble molecules have a molecular weight smaller than 500 Dalton, urea and creatinine are examples from this group [2]. The middle molecules are specified with a molecular weight larger than 500 Dalton with β_2-microglobulin as prototype [2, 3]. The protein-bound solutes, specified by their protein-binding with examples indoxyl sulfate and p-cresylsulfate [2, 3]. Accumulation of these types of uremic toxins is associated with adverse effects and mortality [4-9].

Protein-bound toxins and middle molecules are poorly removed by conventional hemodialysis [2, 3, 10-12]. Some convective strategies can improve the β_2-microglobulin clearance, but protein-bound toxin removal hardly enhanced [13]. Post dilution online hemodiafiltration has shown to significantly lower the total pre-dialysis concentrations of p-cresylsulfate and 3-carboxyl-4-methyl-5-propyl-2-furanpropionic acid (CMPF), two protein-bound toxins with high protein-binding [14]. However the effect on the total concentration was only moderate and no significant effect on the free fraction (which causes biological effects) was obtained. Currently, a treatment strategy to efficiently remove protein-bound uremic toxins is still missing. It is suggested that adsorptive techniques may improve their removal [15-19]. In fact, various particles for the adsorption of toxins from blood are in development [20-31]. However, most of the particles are not yet commercially available. Furthermore, many of them are tested for cytokine removal, and it is not clear which particles are suitable for uremic toxin removal.

In this chapter we investigate if adsorptive particles are suitable for uremic toxin removal, including small water soluble molecules, as well as the hard-to-remove middle molecules and protein-bound uremic toxins. Ultimately, we would like to embed particles in a mixed matrix membrane (MMM), as

described earlier in this thesis and which has shown to be a concept with potential to improve the clearance of uremic toxins which are difficult to remove.

In chapter 2 and 3 of this thesis, the Norit activated carbon (AC) was used for embedding in a MMM. This type of particle is commercially available and comes in a powdered form, which is suitable for embedding in a membrane. Norit A Supra Eur which is a steam activated carbon made of natural origin adsorbs many biomolecules according to the manufacturer. Furthermore it meets the requirements of the US Food Chemical Codex and European Pharmacopoeia requirements.

Besides Norit AC, we selected two more adsorptive particles based on their availability, particle size and price. Mast Carbon are polymer pyrolysed carbon granules with mesoporosity which are biocompatible and can adsorb cytokines from human plasma [23, 24, 32]. Furthermore we selected Y-carbon, which is a powdered carbide-derived-carbon (CDC) with controlled porosity suitable for uremic toxin removal according to the supplier. Carbide-derived-carbons have been shown to remove cytokines from human blood plasma [21, 22]. The selected particles are tested for adsorption of molecules from the three uremic retention solute classes using creatinine as water soluble molecule, β_2-microglobulin as middle molecule and p-cresylsulfate, indoxyl sulfate and hippuric acid as protein-bound toxins.

4.2. Materials and methods

4.2.1. Materials

Norit A Supra Eur was obtained from Norit Netherlands BV, The Netherlands and sieved in a in a 45 µm sieve (Fritsch GmbH, Germany) to an median particle size of 27 µm. Mesoporous mast carbon granules (125-259 µm) were obtained from MAST Carbon International Ltd (Basingstoke, UK). Y-carbon particles are smaller than 40 µm and were kindly provided by Y-carbon (Bristol, US). Creatinine, indoxyl sulfate and hippuric acid were purchased from Sigma Aldrich (Zwijndrecht, The Netherlands). P-cresylsulfate is not commercially available and was synthesized as described before [33].

4.2.2. Scanning electron microscopy

Norit activated carbon, Mast carbon and Y-carbon were glued on a SEM holder. After application of a gold coating using a BalzersUnion SCD 040 sputter coater (OerlikonBalzers, Belgium), the particles were examined using a JEOL JSM-5600LV scanning electron microscopy (SEM) (JEOL, Japan).

4.2.3. Plasma adsorption

Frozen human blood plasma from healthy donors was obtained from Sanquin (The Netherlands) in compliance with local ethical guidelines. Plasma from 3 donors was thawed and in the first case spiked with creatinine, p-cresylsulfate, indoxyl sulfate and hippuric acid to levels of 131.5 mg/L, 40.7 mg/L, 40.2 mg/L, 80.9 mg/L respectively. These concentrations were based on the reported total concentrations of these compounds in uremic patients [2, 3]. In the second case, the plasma was spiked to higher concentrations of the protein-bound toxins with: 131.5 mg/L creatinine, 116.6 mg/L p-cresylsulfate, 125.4 mg/L indoxyl sulfate and 90.3 mg/L hippuric acid. In a separate experiment for β_2-microglobulin adsorption, plasma from 2 donors was used and spiked to 84.7 mg/L.

All the spiked plasma solutions were allowed to mix for 10 minutes prior to the start of the experiment. In one experiment, the protein-binding was investigated and samples were taken from the plasma at t=0 and t=6 h.

Pure particles of ~25 mg, and flat sheet home-made PES/PVP particle free membranes (taken as control and fabricated as described before [34]) were incubated in ~4 mL plasma of three different donors. Also 4 mL blanc plasma (without sorbents or membranes) was used as control. The amount of added plasma was adjusted to the amount of incubated material so that the material – plasma relation was always similar to 25 mg material in 4 mL plasma. For β_2-microglobulin, only the blanc solution was used as control. All tubes were incubated on a roller bank for 4 hours. After the incubation time, they were centrifuged at 3500 rpm from 10 min, the supernatant was collected and a part was stored at 4^{o}C for analysis of osmolarity, pH, Na^+, K^+, Ca^{2+}, total protein, urea and creatinine concentrations which were measured according to the protocol of manufacturer of the kit and/or device (see Table 1). The rest of the supernatant of the samples was frozen at -80^{o}C for analysis of the plasma of one donor for p-cresylsulfate, indoxyl sulfate, hippuric acid as using HPLC analysis as described before [13, 35]. β_2-microglobulin concentrations were measured by means of ELISA as described before [13]. The absolute value of the solute was always related to the value of control plasma at that time point as follows:

$$Relative\ concentration = \frac{C_s}{C_b}$$

Where C_s is the concentration in the indicating plasma sample, and C_b is the concentration in the blanc (plasma without adsorptive particles or membranes). Relative osmolarities and pH were calculated in a similar way. Statistical differences were determined for relative osmolarity, pH, Na^+, K^+, Ca^{2+}, total protein, urea and creatinine concentrations using a one-way ANOVA and post-hoc Tukey test.

Table 1. Test methods for analysis of blood plasma

Parameter	Kit / Device
Osmolarity	Advanced instruments osmometer model 3320
pH	Radiometer Copenhagen PHM lab pH meter
Sodium	Corning 480 Flame Photometer
Calcium	Bio-Rad Microplate reader Benchmark 16-channel photometer
	DiaSys Calcium CPC FS (1 1121 99 10 021)
Total protein	Bio-Rad Microplate reader Benchmark 16-channel photometer
	Bio-Rad Laboratories GmbH Protein Assay (cat# 500-0006)
Urea	Starrcol standard SC-60-S photometer
	DiaSys Urea CT FS (1 3115 99 10 026)
Creatinine	Bio-Rad Microplate reader Benchmark 16-channel photometer
	DiaSys Creatinine PAP FS (1 1759 99 10 026)

4.3. Results and discussion

4.3.1. Scanning electron microscopy

Figure 1 shows scanning electron microscopy (SEM) images of the particles. The Norit and Y-carbon particles are in powdered form (Figure 1A, D, C, F). Mast carbon is a granular form of carbon and small spheres are observed on the SEM images. The spheres are porous with a gradient of larger pore sizes towards the middle of the sphere (Figure 1 B, E).

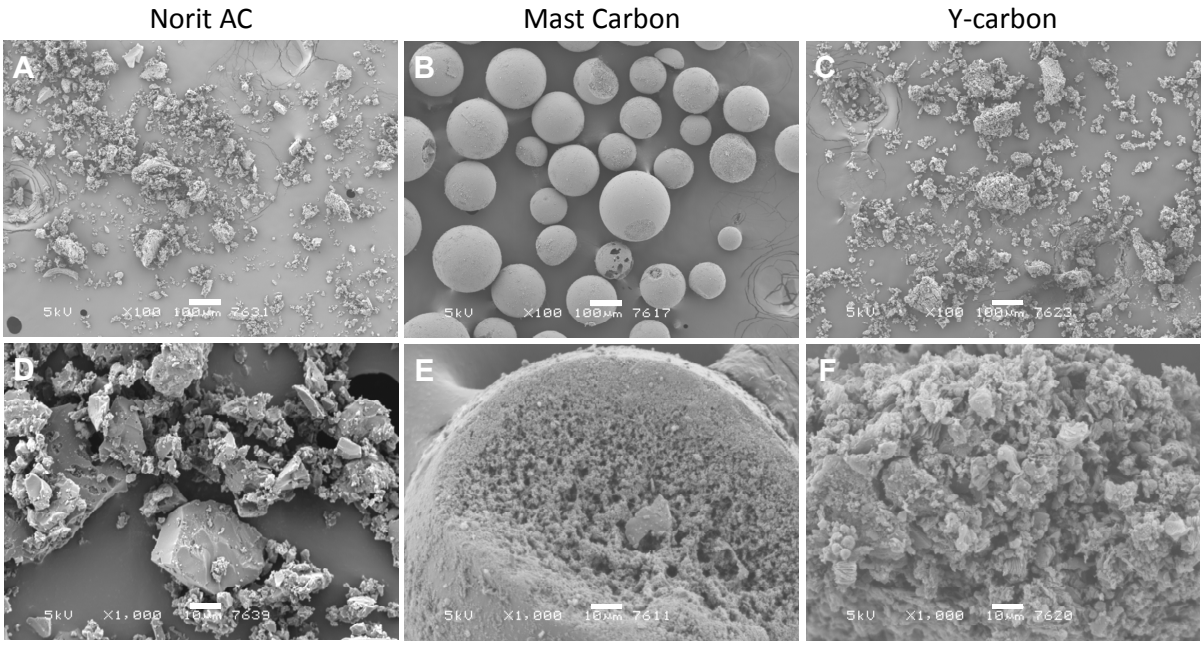

Figure 1. Scanning electron microscopy images of Norit Activated carbon, Mast Carbon and Y-Carbon. Magnifications of 100x (Figure 1 A, B, C) and 1000x (Figure 1 D, E, F). Scale bars indicate 100 µm in Figure 1A, B, C and 10 µm in Figure 1D, E, F.

4.3.2. Adsorption from human plasma

Figure 2 presents the average relative creatinine concentrations of plasma (from 3 donors) incubated with the various materials. Norit AC and Mast carbon adsorb most of the creatinine and significantly lower the relative creatinine concentration to 0.07 and 0.08 ($p < 0.001$) while Y-carbon adsorbs less creatinine (relative concentration reaches 0.24) ($p < 0.01$).

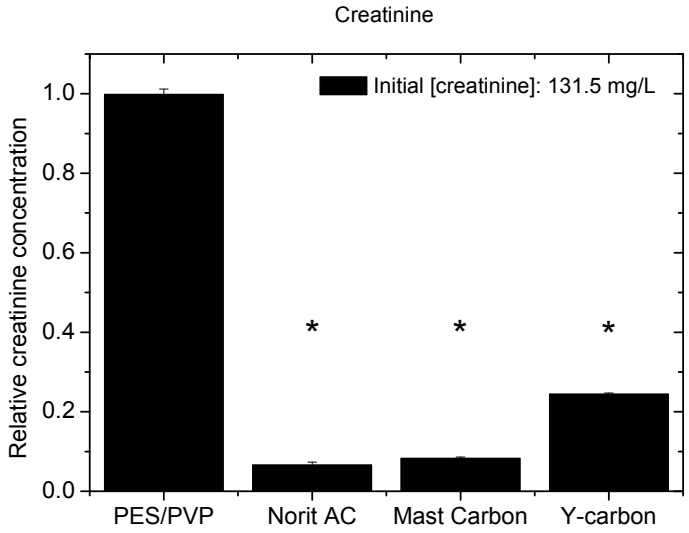

Figure 2. Average relative creatinine concentrations after incubation of a PES/PVP membrane, Norit activated carbon, Mast carbon or Y-carbon in spiked human plasma (n=3) for 4h. Error bars indicate standard deviations. * indicate a significant decrease in comparison with the PES/PVP membrane.

The free fraction of p-cresylsulfate, indoxyl sulfate, and hippuric acid are constant for the duration of at least 6h (data not shown). Figure 3 presents the relative p-cresylsulfate (a), indoxyl sulfate (b) and hippuric acid (c) concentrations in human spiked blood plasma after incubation with the tested materials at 2 initial spiked concentrations. Figure 3a shows that the majority of p-cresylsulfate is adsorbed by the particles. Norit AC and Mast Carbon lower the relative p-cresylsulfate concentration to less than 0.2.

a

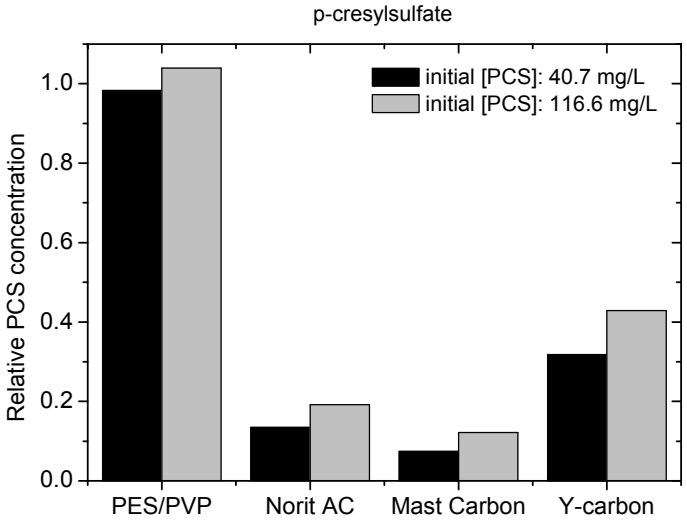

b

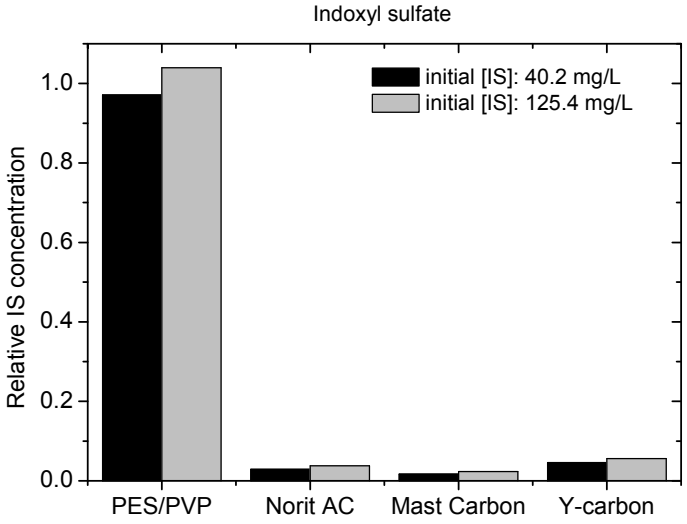

Figure 3. Relative concentrations after incubation of a PES/PVP membrane, Norit activated carbon, Mast carbon or Y-carbon in spiked human plasma with 2 different initial concentrations for 4h. **a**) p-cresylsulfate (PCS), **b**) indoxyl sulfate (IS),

c

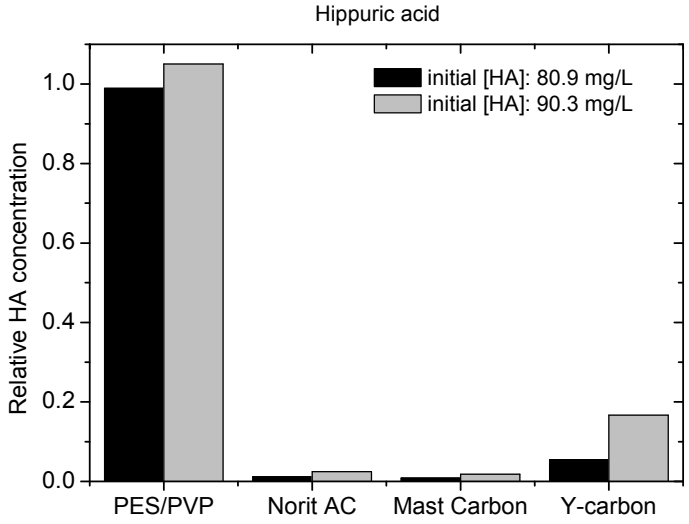

Figure 3. Relative concentrations after incubation of a PES/PVP membrane, Norit activated carbon, Mast carbon or Y-carbon in spiked human plasma with 2 different initial concentrations for 4h. **c**) hippuric acid (HA)

Figure 3b shows that all particles remove in 4h most of the indoxyl sulfate to relative concentrations less than 0.06. Figure 3c shows that after incubation with Norit AC and Mast Carbon the relative concentration are less than 0.025. Y-carbon also removes the majority of the hippuric acid (relative concentration less than 0.17). In all cases, the PES/PVP membrane does not adsorb any of the toxins, whereas the majority of the p-cresylsulfate, indoxyl sulfate and hippuric acid is removed by Norit AC, Mast Carbon and Y-Carbon. Even in these experimental conditions with low sorbent – plasma relation of 6.25 mg/mL (compared to ~100 mg/mL in hemoperfusion) the majority of the protein-bound toxins can be removed within 4h by all the particles. Y-carbon seems to lower the relative concentrations of the protein-bound toxins in a smaller extend than Norit AC and MAST carbon. It is hard to directly compare the adsorption results to other studies. Although some data can roughly be extrapolated. 78 mg p-cresylsulfate and 69 mg indoxyl sulfate is excreted by healthy subjects in their 24h urine [36]. Based on our results, using the total uremic concentrations of the protein-bound

toxins, we would need the following amount of sorbents to remove these amounts each day: for p-cresylsulfate 14, 13 and 18 gram of Norit AC, Mast carbon or Y-carbon would be necessary, while based on indoxyl sulfate 11 gram of each particle would be enough. Compared to hemoperfusion columns which often contain hundreds of grams adsorptive particles, the estimated amounts seems to be in a good range.

Figure 4 presents the relative β_2-microglobulin concentrations after 4 hour incubation in spiked plasma with the adsorptive particles. Y-carbon removes the majority of β_2-microglobulin and lowers the relative concentration to 0.14. Norit activated carbon and Y-carbon decreased the relative concentration to 0.86 and 0.62 after 4h incubation.

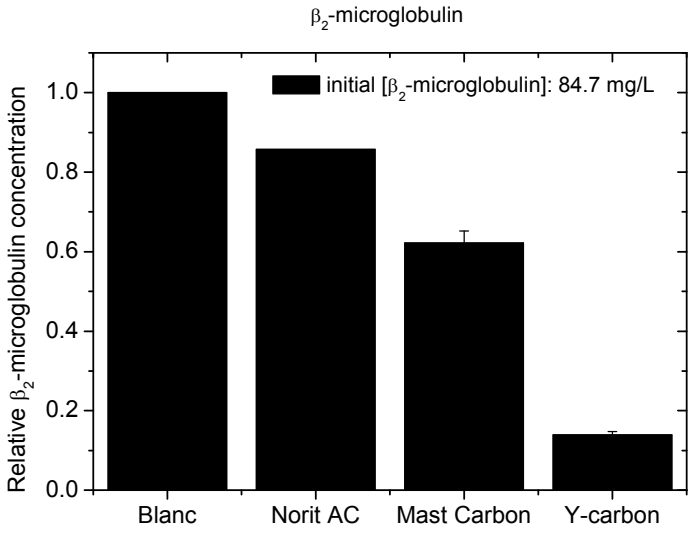

Figure 4. Average relative β_2-microglobulin concentrations after incubation of human spiked plasma (blanc), or Norit activated carbon (1 donor), Mast carbon (2 donors), Y-carbon (2 donors) with spiked human plasma for 4h. Error bars indicate standard deviations

While creatinine, protein-bound toxins and β_2-microglobulin can be removed from the plasma by Norit AC, Mast carbon and Y-carbon, there is no significant effect on relative osmolarity, relative pH

or relative concentrations of Na^+, K^+, Ca^{2+}, total protein and urea (see Table 2). Generally, activated carbons do not adsorb urea, and that seems also to be the case for the three carbon types tested here. Y-carbon seems to adsorb more β_2-microglobulin than Mast carbon and Norit AC, while for removal of protein-bound toxins the latter two seem to be a bit better. In industrial applications of activated carbon, micropores (< 2 nm) seem to be most important. However, for medical applications, mesopores (2-50 nm) are very important since not all substances can access micropores and can then hardly be adsorbed [15]. For example, β_2-microglobulin has a size of approximately 4.5 · 2.5 · 2 nm [37, 38]. It could be that the Y-carbon contains more mesopores compared to Norit AC and Mast carbon and therefore the β_2-microglobulin fits more easily, while the surface area per gram of particles could be smaller so that there is somewhat lower adsorption for the smaller protein-bound toxins.

Table 2. Average relative plasma values ± sd after incubation in human blood plasma of three donors for 4h. The plasma is incubated with a PES/PVP membrane, Norit activated carbon, Mast carbon or Y-carbon.

	PES/PVP	Norit AC	Mast carbon	Y-carbon
Relative osmolarity	0.994 ± 0.01	0.970 ± 0.01	0.983 ± 0.02	0.993 ± 0.02
Relative pH	1.005 ± 0.01	0.973 ± 0.06	1.007 ± 0.00	0.981 ± 0.00
Relative Na^+ concentration	1.010 ± 0.01	1.003 ± 0.02	0.997 ± 0.05	0.999 ± 0.00
Relative K^+ concentration	1.038 ± 0.03	1.039 ± 0.04	0.983 ± 0.04	0.989 ± 0.04
Relative Ca^{2+} concentration	0.995 ± 0.00	0.915 ± 0.07	0.976 ± 0.03	1.017 ± 0.01
Relative total protein concentration	1.013 ± 0.03	1.011 ± 0.07	0.985 ± 0.03	0.944 ± 0.00
Relative urea concentration	1.014 ± 0.03	0.986 ± 0.03	0.965 ± 0.03	1.034 ± 0.05

4.4. Conclusions and outlook

This study screened three types of particles for the adsorption of three types of uremic retention solutes namely the small molecular weight water soluble molecules, middle molecules and protein-bound solutes. Norit AC, Mast carbon and Y-carbon can all adsorb all the three types of uremic retention solutes, although in different amounts. Y-carbon adsorbs the most β_2-microglobulin per gram of adsorbent, but Mast carbon and Norit AC seem to adsorb more creatinine and protein-bound toxins.

Ultimately, we would like to embed a good uremic toxin adsorbing particle in a porous MMM, and this may be more feasible using powdered carbons rather than granules. Besides, the use of smaller adsorptive particles such as Y-carbon have advantages compared to granules for rapid uptake of protein-bound toxins at low concentrations [39]. Based on the results obtained in this study, Y-carbon is an interesting candidate for embedding in a membrane matrix. The majority of creatinine, protein-bound toxins and β_2-microglobulin are removed by Y-carbon. Norit activated carbon and Mast carbon seem to perform a bit better on creatinine and protein-bound solute adsorption but do not adsorb the majority of β_2-microglobulin. It would be interesting to further investigate the surface area of the particles, and adsorption kinetics and this may also be used to compare these particles with each other and ultimately incorporate them in a mixed matrix membrane.

Acknowledgements

M. Tijink would like to thank the Dutch Kidney Foundation for financial support of the project.

References

[1] Vanholder R, et al. Uremic toxicity: Present state of the art. International Journal of Artificial Organs 2001;24:695-725.

[2] Vanholder R, et al. Review on uremic toxins: Classification, concentration, and interindividual variability. Kidney International 2003;63:1934-43.

[3] Duranton F, Cohen G, De Smet R, Rodriguez M, Jankowski J, Vanholder R, Argiles A. Normal and pathologic concentrations of uremic toxins. Journal of the American Society of Nephrology 2012;23:1258-70.

[4] Adijiang A, Goto S, Uramoto S, Nishijima F, Niwa T. Indoxyl sulphate promotes aortic calcification with expression of osteoblast-specific proteins in hypertensive rats. Nephrology Dialysis Transplantation 2008;23:1892-901.

[5] Lin CJ, et al. The role of protein-bound uremic toxins on peripheral artery disease and vascular access failure in patients on hemodialysis. Atherosclerosis 2012;225:173-9.

[6] Wu IW, et al. P-cresyl sulphate and indoxyl sulphate predict progression of chronic kidney disease. Nephrology Dialysis Transplantation 2011;26:938-47.

[7] Miyata T, et al. β 2-Microglobulin modified with advanced glycation end products is a major component of hemodialysis-associated amyloidosis. J Clin Invest 1993;92:1243-52.

[8] Cheung AK, et al. Serum β-2 microglobulin levels predict mortality in dialysis patients: Results of the HEMO study. Journal of the American Society of Nephrology 2006;17:546-55.

[9] Bammens B, Evenepoel P, Keuleers H, Verbeke K, Vanrenterghem Y. Free serum concentrations of the protein-bound retention solute p-cresol predict mortality in hemodialysis patients. Kidney International 2006;69:1081-7.

[10] Meyer TW. The Removal of Protein-Bound Solutes by Dialysis. Journal of Renal Nutrition 2012;22:203-6.

[11] Niwa T. Update of uremic toxin research by mass spectrometry. Mass Spectrometry Reviews 2011;30:510-21.

[12] Grooteman MPC, et al. Effect of online hemodiafiltration on all-cause mortality and cardiovascular outcomes. Journal of the American Society of Nephrology 2012;23:1087-96.

[13] Meert N, et al. Effective removal of protein-bound uraemic solutes by different convective strategies: A prospective trial. Nephrology Dialysis Transplantation 2009;24:562-70.

[14] Meert N, et al. Prospective evaluation of the change of predialysis protein-bound uremic solute concentration with postdilution online hemodiafiltration. Artificial Organs 2010;34:580-5.

[15] Mikhalovsky SV. Emerging technologies in extracorporeal treatment: focus on adsorption. Perfusion 2003;18:47-54.

[16] Furuyoshi S, Nakatani M, Taman J, Kutsuki H, Takata S, Tani N. New Adsorption Column (Lixelle) to Eliminate ß2-Microglobulin for Direct Hemoperfusion. Therapeutic Apheresis and Dialysis 1998;2:13-7.

[17] Winchester JF, Ronco C. Sorbent hemoperfusion in end-stage renal disease: An in-depth review. Advances in Renal Replacement Therapy 2002;9:19-25.

[18] Winchester JF, Ronco C. Sorbent Augmented Hemodialysis Systems: Are We There Yet? Journal of the American Society of Nephrology 2009:in press.

[19] Meyer TW, Peattie JWT, Miller JD, Dinh DC, Recht NS, Walther JL, Hostetter TH. Increasing the clearance of protein-bound solutes by addition of a sorbent to the dialysate. Journal of the American Society of Nephrology 2007;18:868.

[20] Takemoto S, Kusudo Y, Tsuru K, Hayakawa S, Osaka A, Takashima S. Selective protein adsorption and blood compatibility of hydroxy-carbonate apatites. Journal of Biomedical Materials Research 2004;69:544-51.

[21] Yachamaneni S, et al. Mesoporous carbide-derived carbon for cytokine removal from blood plasma. Biomaterials;31:4789-94.

[22] Yushin G, et al. Mesoporous carbide-derived carbon with porosity tuned for efficient adsorption of cytokines. Biomaterials 2006;27:5755-62.

[23] Howell CA, et al. The in vitro adsorption of cytokines by polymer-pyrolysed carbon. Biomaterials 2006;27:5286-91.

[24] Sandeman SR, et al. Inflammatory cytokine removal by an activated carbon device in a flowing system. Biomaterials 2008;29:1638-44.

[25] Ettenauer M, Loth F, Thümmler K, Fischer S, Weber V, Falkenhagen D. Characterization and functionalization of cellulose microbeads for extracorporeal blood purification. Cellulose 2011:1-7.

[26] Thu¨mmler K, Fischer S, Feldner A, Weber V, Ettenauer M, Loth F, Falkenhagen D. Preparation and characterization of cellulose microspheres. Cellulose 2010:1-8.

[27] Weber V, et al. Functionalization and application of cellulose microparticles as adsorbents in extracorporeal blood purification. Macromolecular Symposia;294:90-5.

[28] Weber V, Hartmann J, Linsberger I, Falkenhagen D. Efficient Adsorption of Tumor Necrosis Factor with an in vitro Set-Up of the Microspheres-Based Detoxification System. Blood Purification 2007;25:169-74.

[29] Malik DJ, Warwick GL, Venturi M, Streat M, Hellgardt K, Hoenich N, Dale JA. Preparation of novel mesoporous carbons for the adsorption of an inflammatory cytokine (IL-1). Biomaterials 2004;25:2933-40.

[30] Malik DJ, Warwick GL, Mathieson I, Hoenich NA, Streat M. Structured carbon haemoadsorbents for the removal of middle molecular weight toxins. Carbon 2005;43:2317-29.

[31] Costanzo JA, Ober CA, Black R, Carta G, Fernandez EJ. Evaluation of polymer matrices for an adsorptive approach to plasma detoxification. Biomaterials 2010;31:2857-65.

[32] Sandeman SR, et al. Assessing the in vitro biocompatibility of a novel carbon device for the treatment of sepsis. Biomaterials 2005;26:7124-31.

[33] Feigenbaum J, Neuberg CA. Simplified method for the preparation of aromatic sulfuric acid esters. Journal of the American Chemical Society 1941;63:3529-30.

[34] Tijink MSL, et al. A novel approach for blood purification: Mixed-matrix membranes combining diffusion and adsorption in one step. Acta Biomaterialia 2012;8:2279-87.

[35] Meert N, et al. Novel method for simultaneous determination of p-cresylsulphate and p-cresylglucuronide: Clinical data and pathophysiological implications. Nephrology Dialysis Transplantation 2012;27:2388-96.

[36] Martinez AW, Recht NS, Hostetter TH, Meyer TW. Removal of P-cresol sulfate by hemodialysis. Journal of the American Society of Nephrology 2005;16:3430-6.

[37] Becker JW, Reeke Jr GN. Three-dimensional structure of β 2-microglobulin. Proceedings of the National Academy of Sciences of the United States of America 1985;82:4225-9.

[38] Hedayat A, Szpunar J, Kumar NAPK, Peace R, Elmoselhi H, Shoker A. Morphological characterization of the Polyflux 210H hemodialysis filter pores. International Journal of Nephrology 2012;2012.

[39] Dinh DC, Recht NS, Hostetter TH, Meyer TW. Coated carbon hemoperfusion provides limited clearance of protein-bound solutes. Artificial Organs 2008;32:717-24.

5

Novel membranes for blood contacting applications

M. Tijink
J. Janssen
M. Timmer
J. Austen
Y. Aldenhoff
J. Kooman
L. Koole
J. Damoiseaux
R. Van Oerle
Y. Henskens
D. Stamatialis

This chapter is in preparation for publication

Abstract

Developments in membrane based blood purification therapies often come with longer treatment times and therefore longer blood-material contact, which requires long term biocompatibility. In this study, we develop for the first time membranes using the material SlipSkin™ which is a copolymer made from N-vinylpyrrolidone (NVP) and butylmethacrylate (BMA). Polymer composition, solvent type and solvent evaporation time influence membrane morphology and membranes with sieving properties of cascade filters in plasma fractionation applications are developed. The new membranes have very good biocompatibility. In fact they have low platelet adhesion and equivalently good properties of contact activation, thrombogenicity, leukocyte adhesion, hemolysis, complement activation compared to a membranes used in the clinic and other benchmark membranes.

5.1. Introduction

In blood purification treatments, membranes with optimal separation properties as well as optimal biocompatibility are required. For example, apheresis membranes, plasma separation membranes and hemodialysis membranes have optimized molecular weight cut offs for their application and show good biocompatibility for a few hours of application. New developments in blood purification therapies often require longer durations of the therapies. For example, nocturnal dialysis (where 7.85 hour treatment instead of 3.75h for conventional hemodialysis is applied) leads to improvements on patient survival [1, 2]. However, longer filtration times mean more contact with the membrane material, requiring long term membrane biocompatibility. This holds for wearable and portable artificial kidneys too. Davenport *et al.* reported about a pilot study with a wearable artificial hemodialysis device, however, 2 out of 8 patients had clotting problems and the treatment was discontinued, highlighting the need for improved biocompatible membranes [3].

Currently, blood purification membranes made of synthetic polymers dominate the market. Often polymer blends are used in which a hydrophobic membrane material (e.g. polysulfone or polyethersulfone) is combined with a hydrophilic additive (e.g. polyvinylpyrrolidone (PVP) or polyethylene glycol (PEG)). Also hydrophilic or hydrophilized copolymers are used (poly (ethylene vinyl alcohol) or poly acrylonitrile methallylsulfonate) [4]. Membranes with hydrophilic patches in a hydrophobic membrane matrix are generally thought to be biocompatible [5]. However, the hydrophilic modifier can elute from the dialysis membrane surface into the patients circulation [6]. Another approach is the use of surface modifications such as heparin immobilization on polysulfone membranes [7] or albumin grafting on polyethersulfone based membranes [8]. However, in most of these studies the biocompatibility of blood purification membranes is not fully investigated. Although the effect of biocompatibility of the different membrane materials is hard to show in clinical trials [9], nevertheless, both nurses and physicians prioritize biocompatibility for future innovations on blood purification membranes above efficiency and removal capacity [10].

In this study, we develop for the first time, membranes using the material SlipSkin™ which is a copolymer of N-vinylpyrrolidone (NVP) (hydrophilic building block) and n-butylmethacrylate (BMA) (hydrophobic building block). This material has been used before as a surface coating for several blood-contacting medical devices (catheters and guidewires) and its cytocompatibility and hemocompatibility have been documented [11-13]. We use various polymer compositions in which the molar ratio of the hydrophilic and hydrophobic building blocks is varied and prepare porous flat sheet membranes suitable for plasma fractionation under various process conditions (tailoring solvent type, solvent evaporation time). The biocompatibility of the new membranes is thoroughly investigated based on the ISO guidelines 10993 Biological evaluation of medical devices, part 4 selection of tests for interactions with blood. Following the advice of these guidelines, for external communication devices like hemodialysis equipment, we perform tests in all 5 test categories of thrombosis, coagulation, platelets, hematology and complement system. In all cases we compare the performance of the newly developed SlipSkin™ membranes with several benchmark membranes.

5.2. Materials and methods

5.2.1. Materials

SlipSkin™, copolymer of N-vinylpyrrolidone (NVP, hydrophilic) and n-butylmethacrylate (BMA, hydrophobic) (Figure 1) was used as membrane material and was kindly provided by INterface BIOmaterials BV (Geleen, The Netherlands). Polyethersulfone (PES) (ULTRASON, E6020P) (BASF, Arnhem, The Netherlands) and polyvinylpyrrolidone (PVP) (K90, MW ≈ 360,000) (Fluka, Sigma-Aldrich, Germany) were used as membrane material and additive respectively. Acetone (Biosolve, Valkenswaard, The Netherlands) and extra pure N-methylpyrrolidone (NMP) (Acros organics, Geel, Belgium) were employed as solvents. Ultrapure water, prepared using a Millipore purification unit, was used as non-solvent in the coagulation baths.

a

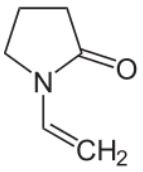

b

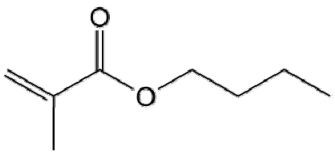

Figure 1. Chemical formulas of **a**) N-vinylpyrrolidone (NVP) and **b**) n-butylmethacrylate (BMA)

Creatinine (113.2 Da), myoglobin (17.8 kDa), bovine serum albumin (BSA) (66 kDa), γ-globulin (150 kDa) and thyroglobulin (670 kDa) were purchased from Sigma-Aldrich and dissolved in ultrapure water.

For the biocompatibility tests, we selected several benchmark membrans for comparison to our Slipskin membranes. PES/PVP blends are often used by the industry for preparation of blood purification membranes [4, 14]. Commercial hemodialysis or plasma fractionation membranes are always in hollow fiber configuration, but for our hemocompatibility testing, flat sheet membranes were necessary. Therefore we prepared flat sheet (home-made) membranes, based on a PES/PVP polymer blend. Besides, commercial flat sheet PES based membranes (14650-47-D, molecular weight cut off=50 000 Da, Sartorius, Nieuwegein, The Netherlands) were selected. A flat sheet polyester membrane which is in clinical use for blood transfusion applications was selected as well and was taken out of blood transfusion filters SQ40SE (PALL, Portsmouth, UK). For the complement activation experiments, two more benchmark materials, regenerated cellulose (RC58, Whatman, Sigma-Aldrich) and DEAE cellulose (DE81 DEAE cellulose, Whatman, Sigma- Aldrich) were used as positive control as described before [15, 16]. Glass coverslips were obtained from VWR (Amsterdam, The Netherlands).

The following reagents for a thrombin generation assay were purchased from Thrombinoscope BV (Maastricht, The Netherlands). FluCa reagent contains 2.5 mM fluorogenic substrate for thrombin (Z-Gly-Gly-Arg-AMC) and 87 mM calcium chloride. The MP reagent contains 24 µM phospholipids at 20:20:60 mole% PS:PE:PC. The thrombin calibrator contains a fixed amount of thrombin-α2-macroglobulin complex. For the second thrombin generation assay, Z-Gly-Gly-Arg-AMC fluorogenic substrate was purchased from Bachem (Bubendorf, Switserland), dimethyl sulfoxide was purchased from Acros Organics (Geel, Belgium), calcium chloride was purchased from Merck (Darmstadt, Germany). For the platelet adhesion assay triton X100 was purchased from Acros Organics, CytoTox

96®non-radioactive cytotoxicity kit was purchased from Promega Madison (USA). Platelets were fixed with glutaraldehyde from Sigma-Aldrich (Zwijndrecht, The Netherlands).

5.2.2. Membrane preparation

SlipSkin™ membranes were prepared from 10 wt% SlipSkin™ in acetone or NMP polymer dopes. Different types of SlipSkin™ co-polymers were used with NVP:BMA molar ratios of 30:70, 50:50 and 70:30. Home-made PES membranes were prepared from 15 wt% PES and 7 wt% PVP in NMP [17]. The solutions were mixed on a roller bank, and afterwards degassed overnight at room temperature. All membranes were prepared by phase inversion. Solutions were cast on a glass plate using a casting knife with a slit of 300 µm for the SlipSkin™ membranes and 150 µm slit for the home-made PES membranes. Casting was immediately followed by immersion in the coagulation bath unless otherwise stated. Coagulation baths of ultrapure water and 60 wt% NMP and 40% ultrapure water were employed for the SlipSkin™ and home-made PES membranes, respectively. In some cases, a solvent evaporation step of 30 seconds, 5 or 10 minutes was performed after which the cast films were immersed into the coagulation bath. After the membrane formation process, the membranes were rinsed and stored in ultrapure water upon further use.

All membranes with accompanying codes and details are described in Table 1. SlipSkin™ membranes are indicated with M, the first number in this code indicates the molar ratio of NVP:BMA building blocks in the polymer composition. When NMP was used as solvent for SlipSkin™, this was also indicated in the code while for the other SlipSkin™ membranes, acetone was used as solvent. Furthermore, the evaporation step was indicated as 'ev' in the code for a solvent evaporation time of 30 seconds, while the solvent evaporation times of 5 and 10 minutes were indicated in the code as ev5 and ev10 respectively.

Table 1. Membrane codes and fabrication information

Code	Manufacturer	Material	NVP:BMA	Solvent	Solvent evaporation time
M30NMP	Homemade	SlipSkin™	30:70	NMP	0
M50NMP	Homemade	SlipSkin™	50:50	NMP	0
M70NMP	Homemade	SlipSkin™	70:30	NMP	0
M30	Homemade	SlipSkin™	30:70	Acetone	0
M50	Homemade	SlipSkin™	50:50	Acetone	0
M70	Homemade	SlipSkin™	70:30	Acetone	0
M50ev	Homemade	SlipSkin™	50:50	Acetone	30 seconds
M50ev5	Homemade	SlipSkin™	50:50	Acetone	5 minutes
M50ev10	Homemade	SlipSkin™	50:50	Acetone	10 minutes
G	VWR	Glass	-	-	-
PESh	Homemade	PES/PVP	-	-	-
PESc	Sartorius	PES	-	-	-
PE	PALL	Polyester	-	-	-
RC	Whatman	Regenerated cellulose	-	-	-
DC	Whatman	DEAE cellulose	-	-	-

5.2.3. Membrane characterization

5.2.3.1. Scanning electron microscopy

For scanning electron microscopy (SEM), membranes were dried overnight in air. To obtain cross sections, the dried membranes were broken cryogenically using liquid nitrogen. These, as well as dried membrane surfaces were put on SEM holder. Then all samples were dried overnight under

vacuum and gold coated (BalzersUnion SCD 040 sputter coater, OerlikonBalzers, Belgium). Membrane cross sections and surfaces were examined using a JEOL JSM-5600LV scanning electron microscope (JEOL, Japan).

5.2.3.2. Membrane transport properties

Clean water permeances were determined using an air-pressurized dead end 'Amicon type' ultrafiltration cell and ultrapure water. Membranes were pre-pressurized at 0.5 or 1 bar and then at least 4 pressure steps were applied for 30 minutes. The clean water flux (J) at each pressure was determined by taking the time and weight of permeated water and membrane surface area into account. The clean water permeance (L_p) of the membrane was calculated from the slope of the linear part of the clean water flux vs. transmembrane pressure relationship and was defined as:

$$L_p = \frac{J}{\Delta \mathrm{P}}$$

Where J represents the clean water flux expressed in $L/m^2/h$, ΔP the transmembrane pressure difference in bar and L_p the clean water permeance in $L/m^2/h/bar$.

The membrane sieving coefficient (SC) was determined using an air pressurized dead end Amicon ultrafiltration cell. The following compounds were dissolved in ultrapure water with initial concentrations of 0.1 mg/mL creatinine, 0.25 mg/mL myoglobin, 1 mg/mL BSA, 0.5 mg/mL γ-globulin and 1 mg/mL thyroglobulin and pressurized through the membrane (active surface area:12.6 cm^2) at 0.5 bar for 30 minutes. Then concentrations of the feed and permeate compartment were analyzed using a photo spectrometer (Varian, Cary 300 Scan UV-visible spectrophotometer) at 230, 409, 278, 278, 280 nm for creatinine, myoglobin, BSA, γ-globulin and thyroglobulin respectively. The SC was calculated as follows:

$$SC = \frac{C_p}{C_f}$$

Where C_p is the concentration of the compound in the permeate and C_f is concentration in the feed. SC=1 means that the compound passes freely through the membrane, while SC=0 means that the membrane rejects the compound completely.

5.2.4. Biocompatibility tests

5.2.4.1. Thrombin generation

Fresh blood was obtained from 3 human healthy volunteers who gave informed consent (donor 1, 2, 3) and collected in Venosafe terumo citrated tubes (final citrate concentration 3.2 w/v%) (Terumo Europe N.V., Leuven, Belgium). Platelet poor plasma (PPP) was prepared by a centrifugation step at 2000 x g for 5 minutes and a second centrifugation step at 10000x g for 10 minutes. PPP was frozen at -80^{o}C until further use. To investigate contact activation, circular membrane pieces (diameter=6 mm) and glass coverslips for 5 repeats were put on the bottom of a flat bottom 96 well plate in ultrapure water. Also empty wells without membranes were used to incubate PPP as blanc. Before addition of 120 µL PPP, the ultrapure water was aspirated. The PPP was incubated at room temperature under gentle shaking conditions for 15 minutes while no calcium ions or phospholipids were present. Then 80 µL of the incubated PPP was aspirated and transferred to round bottom 96 well plates. Also a control of plasma which was not incubated, and a pooled normal plasma internal control were taken into account. 20 µL MP reagent was added to all wells and the plate was pre-warmed at 37^{o}C for 10 minutes. The calibrated automated thrombogram (CAT) assay was performed as previously described [18]. Thrombin generation was started by addition of 20 µL FluCa reagent. The calibration was performed with a mixture of 80 µL plasma and 20 µL of the thrombin calibrator and 20µL FluCa reagent. Fluorescence of the by thrombin splitted fluorogenic substrate was read in a Fluoroskan Ascen reader (Thermo Labsystems OY, Helsinki, Finland) equipped with a 390/460 filter

set. Thrombin generation curves were generated with the Thrombinoscope software (Thrombinoscope BV, Maastricht, The Netherlands). Also the data analysis was performed using this software. Lag time and peak height were calculated from each separate curve.

For the second thrombin generation test, the bottom of the wells of a 96 well plate were covered with the test membranes and glass coverslips. Fresh blood was taken in Vacuette pre-citrated tubes from 3 healthy donors who gave informed consent (donors 4, 5, 6). The whole blood was anticoagulated with citrate (11mM) and platelet rich plasma (PRP) was obtained by a centrifugation step at 200g for 15 minutes. The obtained PRP was aspirated and used within 2h. Fluorogenic substrate was added to the PRP and just before the start of the experiment, PRP was recalcified. 200 µL of this mixture was added to the wells and also empty wells were used as blanc. This thrombin generation test was performed as described before [13]. Fluorescence was measured at 365/460 nm filter set with a SpectaMax M2 microplate reader (Molecular Devices, Sunnyvale, USA). For quantification, the time between the start of the experiment and the moment at which the thrombin concentration first exceeds the 5 nM level was used (thrombin generation time).

5.2.4.2. Platelet adhesion and aggregation and lactate dehydrogenase assay

For these tests PRP was obtained of donor 4, 5 and 6 as described in section 5.2.4.1.

For qualitative platelet adhesion, PRP of two donors was used and membranes and glass coverslips were put on the bottom of a 24 well plate in ultrapure water. Before addition of 100 µL PRP (of donor 5, 6) the ultrapure water was aspirated. The PRP was incubated for 45 minutes at 37^{o}C. Then the PRP was removed. The test membranes and glass coverslips were washed in phosphate buffered saline (PBS) 3 times and then transferred to a clean vial. 900 µL of 2.5% glutaraldehyde was added and incubated for >1h at 4^{o}C. Afterwards, the test membranes and glass coverslips were washed in a 0.1M Phosphate buffer (pH=7.2) and with ultrapure water. After drying, the membranes and glass coverslips were put on a SEM holder, gold sputtered and examined using SEM, as described earlier.

Platelet adhesion was quantified using the lactate dehydrogenase (LDH) assay [19]. Membrane circles (diameter= 6mm) were immersed in ultrapure water (in duplo) in a 96 well plate, and 250 µL PRP (of donor 4, 5, 6) was added and incubated at 37^{o}C for 60 minutes after aspiration of the ultrapure water. Then, the PRP was removed, and the membrane samples were washed three times with PBS to remove non-adherent platelets. The membrane samples were transferred into clean vials, and incubated for 60 minutes at room temperature in 200 µL lysis buffer. 50 µL of the supernatant was transferred in duplo to a 96 well plate and 50 µL substrate mix was added and this mixture was incubated for 30 minutes in the dark. Then, 50 µL stop solution was added and optical density was measured at 490 nm on the SpectraMax M2 microplate reader (Molecular Devices, Sunnyvale, USA). Glass was not used as a control here because of non-accurate estimation of adhered platelets on glass [19]. Platelets were quantified by a standard curve plotted from samples containing known amounts of platelets measured with a Beckman Coulter Ac-T diff analyzer (California, USA).

5.2.4.3. Hematology tests

These tests were adapted, but based on previous literature [20, 21]. Calcium ions are important for leukocyte adhesion, therefore heparin was selected as anticoagulant rather than citrate [22]. Fresh blood was taken from 3 healthy donors (donor 1, 2, 3) in 4 ml sodium heparin tubes (final concentration: 68 IU) (Becton&Dickinson, Franklin Lakes, USA) and per donor pooled together and mixed by decanting. The bottoms of 24 well plates were covered with the test membranes (in triplicate) and 2x washed in sterile physiological saline solution. 600 µL blood was added to each well after aspiration of the saline, and incubated for 1h at room temperature on a gentle shaker.

For the leukocyte adhesion test, also empty wells were taken into account for the incubation of the donor blood. After the incubation, blood was aspirated and analyzed using a Sysmex XE-5000

(Sysmex Europe GmbH, Germany) for leukocytes, basophils, eosinophils, neutrophils, monocytes and lymphocyte counts and hematocrit.

For the hemolysis test, additional wells were taken into account containing 600 µL saline or 600 µL sterile ultrapure water, these wells were used as negative and positive control respectively [23]. After the incubated step, blood was aspirated and centrifuged at 4000 rpm for 6 minutes. Light absorbance was measured at 542 nm on the supernatant to analyze the free hemoglobin concentration. The percentage of hemolysis (H) was obtained as follows:

$$H = \frac{C_s - C_{neg}}{C_{pos} - C_{neg}} \cdot 100\%$$

Where C_s is the concentration of free hemoglobin in the sample (µmole/L), C_{neg} is the concentration of free hemoglobin in the negative control (µmole/L) while C_{pos} is the concentration of free hemoglobin in the positive control (µmole/L).

5.2.4.4. Complement tests

The ISO guideline proposes among others a CH50 test for the complement activation category. To our knowledge in all Dutch hospital laboratories the CH50 test has been replaced by the classical pathway ELISA test. Therefore we used this ELISA test to investigate classical pathway complement activation. Since artificial surfaces are known to activate complement rather via the alternative pathway than the classical pathway, we also performed an alternative pathway complement ELISA test.

The bottom of 24 well plates were covered with 15mm circles of the test membranes in duplo and washed in sterile ultrapure water. Blood was taken from 3 healthy donors (donor 1, 2, 3) and collected in BD Vacutainer SSTII Advance tubes (BD Plymouth, UK) and left to clot for 30 minutes.

Then serum was obtained by a centrifuge step of 2000g for 10 minutes and collected serum was pooled together per donor. The incubation step procedure was based on [20], our own experience and the amount of available serum. Aliquots were immediately frozen for the not incubated serum control. Furthermore, empty wells were taken into account for the blanc incubation of serum. 800 µL serum was added per well and incubated for 1h at 37^{o}C under gentle shaking. After incubation, serum was aspirated and directly analyzed further. The classical and alternative pathway were measured by ELISA using the Wieslab Complement system classical pathway and Wieslab complement system alternative pathway kits (Euro Diagnostica, Malmö, Sweden) according to the instructions of the manufacturer [24]. The internal controls with a normal and pathological pooled serum show results within the valid range confirming the validity of both ELISA tests.

5.3. Results and discussion

5.3.1. Membrane fabrication

Figure 2a shows SlipSkin™ membranes prepared using NMP as solvent and the 30:70, 50:50 and 70:30 copolymers: M30NMP (A, D), M50NMP (B, E) and M70NMP (C, F). Although the mechanical stability of these membranes was not systematically studied, during handling we observed that the M70NMP membranes were very fragile, whereas the M50NMP and M30NMP membranes were less fragile. All these membranes are porous, and below a thin skin layer large macro voids throughout the membrane cross section are present. The mutual affinity (or miscibility) between the solvent-non solvent pair NMP- water is very high, leading to instantaneous demixing and macro void formation during membrane fabrication [25-28]

Figure 2b presents SEM images of membranes formed using polymer dopes of 10 wt% SlipSkin™ dissolved in acetone. The M30 (A) and M50 membrane (B) have a porous sponge like structure. M70 membranes are brittle and a representative SEM picture could not be obtained. The solvent-non solvent pair acetone-water has lower mutual affinity than NMP-water and therefore delayed onset of demixing takes place, leading to macro void free membranes [26]. Similar effects of solvents on membrane structures made from different polymers have been described before. For example, using water as non solvent, a dope of PMMA dissolved in NMP gave finger like macro void structures while a dope of PMMA dissolved in acetone resulted in a symmetric porous sponge like structure [27].

a

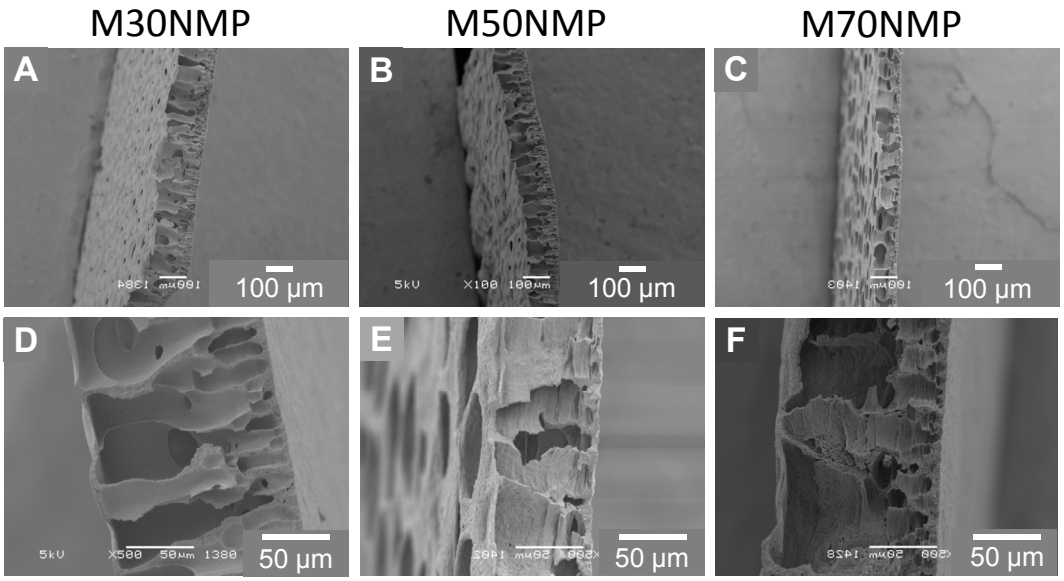

b

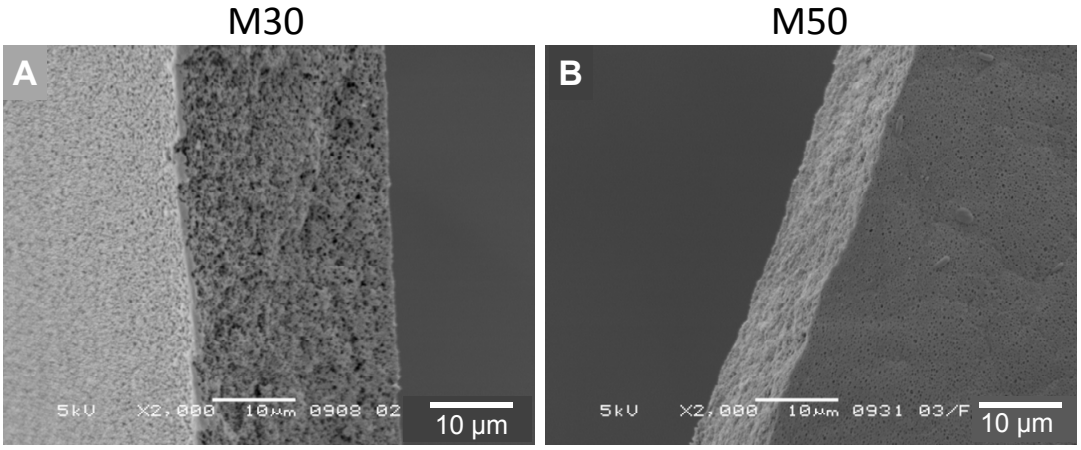

Figure 2. Scanning electron microscopy images of SlipSkin™ based membranes. **a**) Membranes M30NMP (A, D), M50NMP (B,E) and M70NMP (C,F), formed using polymer dopes of 10 wt% SlipSkin™ dissolved in NMP. **b**) Membranes M30 (A) and M50 (B) formed using polymer dopes of 10 wt% SlipSkin™ dissolved in acetone.

c

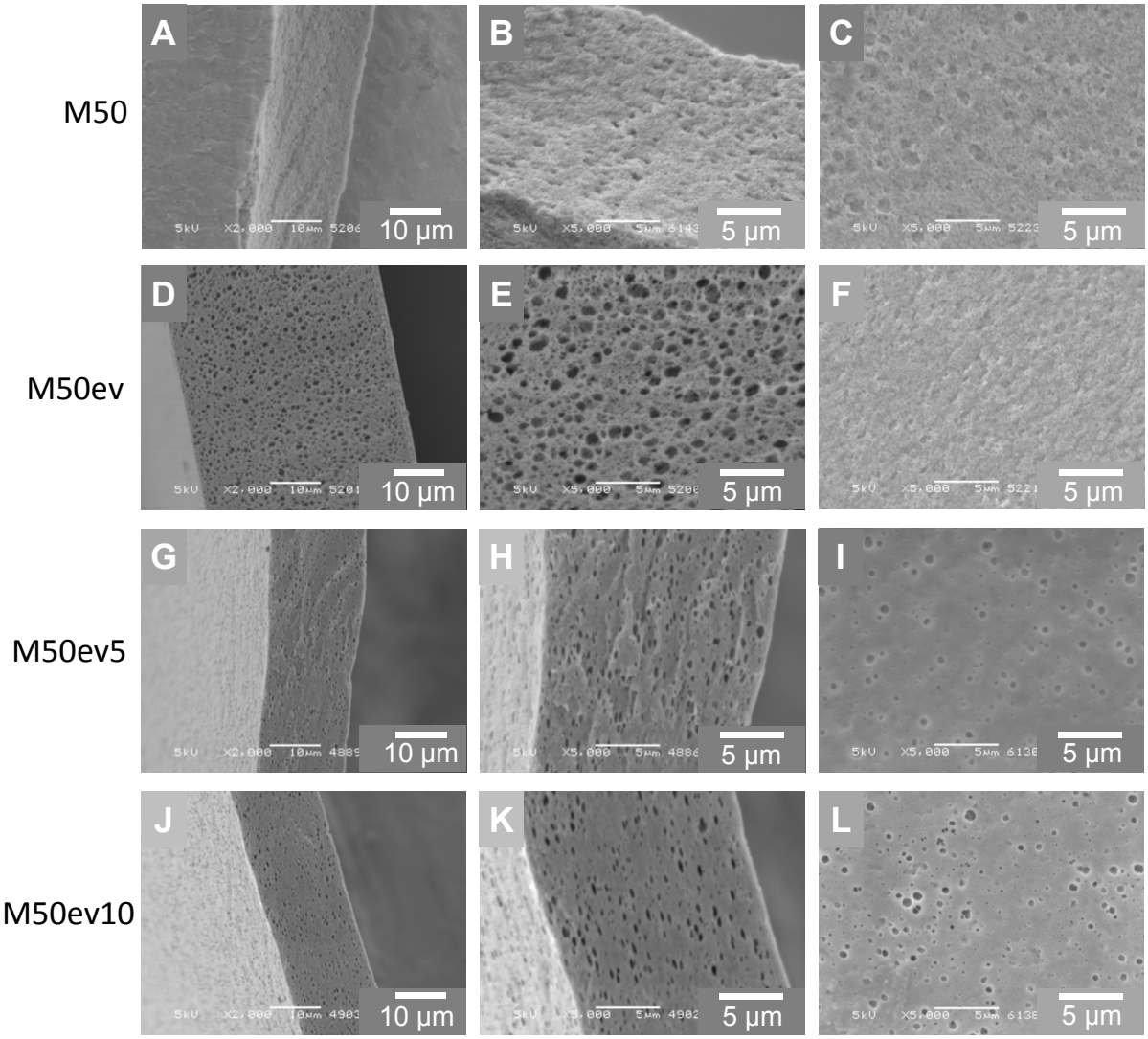

Figure 2. Scanning electron microscopy images of SlipSkin™ based membranes. **c**) Membranes formed from a 10 wt% 50:50 SlipSkin™ in acetone with evaporation steps of 0 seconds M50 (A,B,C), 30 seconds M50ev (D,E,F), 5 minutes M50ev5 (G,H,I) and 10 minutes M50ev10 (J,K,L) with magnifications of 2000x (A,D,G,J) or 5000x (B, C, E, F, H, I, K, L). Images show cross sections (A,B, D, E, G, H, J, K) and top surfaces (C, F, I, L) .

Figure 2c shows SEM images of membranes formed from a 10 wt% 50:50 SlipSkin™ in acetone with no solvent evaporation steps (A,B,C), or solvent evaporation for 30 seconds (D,E,F), 5 minutes (G,H,I) and 10 minutes (J,K,L). All membranes seem to have a porous structure. The M50ev membranes

with 30 second solvent evaporation seem to have bigger pores on the cross section image compared to the M50 membranes. However, the surface images of the M50ev membranes show somewhat smaller pores. Due to the solvent evaporation step the membranes with 5 and 10 minute evaporation step seem to have pores through the membrane thickness but it looks like they are closed cellular pores without good pore interconnectivity.

Macroscopically, shrinkage was observed while drying the membranes in air. Also, the thicknesses on SEM pictures are smaller than the thicknesses of the membranes measured in a wet state using the micrometer, see Table 2. As expected, thinner membranes are formed after longer solvent evaporation. However, there was no difference in thickness between the membranes obtained after the 5 and 10 minute evaporation step.

Table 2. Average membrane thickness

Membrane	Evaporation step	n	Average membrane thickness (µm) ± sd
M50	0 seconds	7	99.9 ± 9.7
M50ev	30 seconds	8	63.8 ± 5.3
M50ev5	5 minutes	5	34.8 ± 3.5
M50ev10	10 minutes	5	33.5 ± 2.5

5.3.2. Membrane transport properties

5.3.2.1. Clean water flux measurements

Figure 3a presents the clean water flux – pressure relationship of the membranes formed using the solvent NMP. The M30NMP membranes have a clean water permeance of 2226 ± 210 L/m^2/h/bar and the clean water flux – pressure relationship is linear. The M70NMP membranes have a clean water permeance in a similar range, 2485 ± 671 L/m^2/h/bar. This clean water permeance is based on the flux – pressure relationship till 0.2 bar since at higher pressures this relationship is not linear. Probably the membrane compacts at higher pressures because of poor mechanical stability. The M50NMP membranes have a lower clean water permeance of 570 ± 121 L/m^2/h/bar with a linear flux – pressure relationship and without any indications of membrane compaction.

Figure 3b presents the clean water flux versus pressure relationship for the M50 and M50ev membranes. The M50 membranes have a clean water permeance of 186 ± 14 L/m^2/h/bar and the flux – pressure relationship is linear. Although the SEM pictures show a porous structure, the M30 membranes show no water permeation after applying a pressure of 1 bar for several hours. The M70 membranes have poor mechanical stability and could not be tested for the clean water permeance. The M50ev membranes have a lower clean water permeance of 112 ± 20 L/m^2/h/bar (p<0.05) compared to the M50 membranes fabricated without a solvent evaporation step probably due to membrane densification. The flux-pressure relationship there is linear. Membranes M50ev5 and M50ev10 fabricated with 5 minute and 10 minute evaporation have no water permeability when these were tested for several hours. This is probably due to the lack of pore interconnectivity, consistent with the SEM analysis of these membranes, which mainly show a closed cell pore structure. Since our target here is to develop ultrafiltration membranes with good mechanical properties we continued further investigation of sieving coefficients and biocompatibility only for the M50 and M50ev membranes.

a

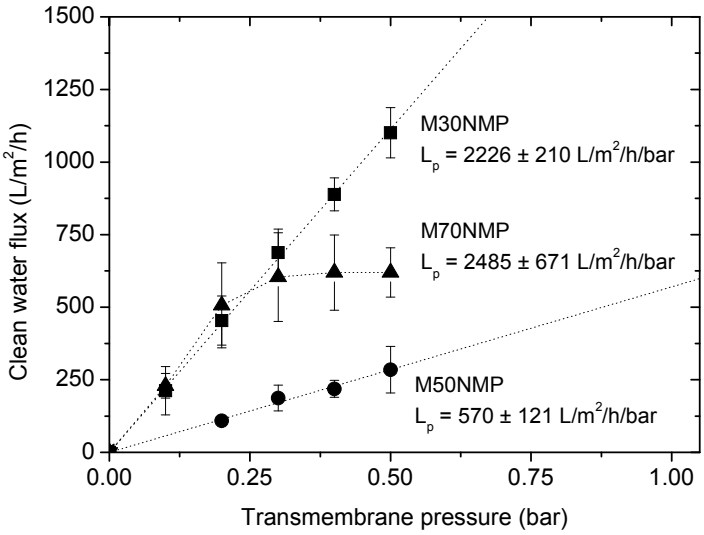

b

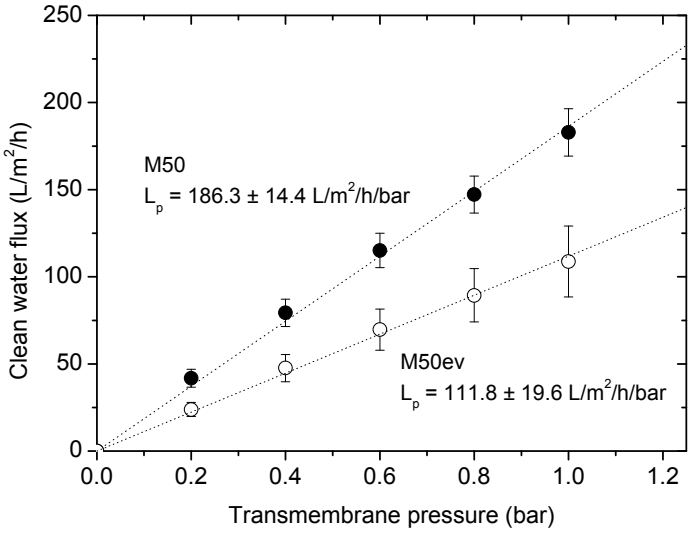

Figure 3. Membrane transport properties. **a**) Average clean water fluxes plotted against transmembrane pressure for the membranes formed from 10 wt% SlipSkin™ dissolved in NMP : M30NMP (n=2), M50NMP (n=2) and M70NMP (n=2) The error bars indicate standard deviations. **b**) Average clean water flux plotted against the transmembrane pressure for membrane M50 (●) (n=5) and M50ev (○) (n=3) formed out of a 10 wt% 50:50 SlipSkin™ dissolved in acetone. The error bars indicate standard deviations.

c

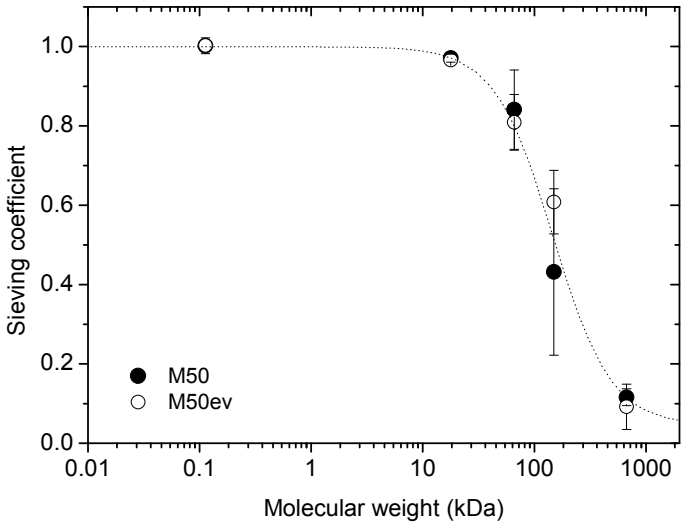

Figure 3. Membrane transport properties. **c**) Average sieving coefficients of molecular weight markers for the membranes M50 (●) and M50ev (○). The following markers were used: creatinine (MW 112.13 Da), myoglobin (MW 17 kDa), BSA (MW 66 kDa), gamma globulin (MW 150 kDa) and thyroglobulin (MW 670 kDa). Sieving coefficients of creatinine were measured in duplo, the other markers were measured in triplo or more. Error bars indicate standard deviations.

5.3.2.2. Sieving curve

Figure 3c presents the sieving curves of the M50 and M50ev membranes. Because of the different clean water permeances of these membranes one would expect also a difference in their sieving curves, since pore size can have a large impact on the water permeability [29, 30]. However, their sieving curves appear to be similar. For the molecules creatinine (113 Da) and myoglobin (17.8 kDa) the SC is approximately 1, while the BSA (66 kDa) is around 0.83. For larger molecules like γ-globulin (150 kDa) and thyroglobulin (670 kDa) the SC is around 0.52 and 0.10 respectively. This may be explained by a decreased number of pores due to the evaporation step for the M50ev membranes, leading to lower clean water permeance while the pore size stays the same, leading to a similar sieving curve compared to M50 membranes. It is also important to note that our M50 and M50ev

membranes have a quite sharp separation curve and separation characteristics similar to some commercial filters in plasma fractionation treatments [31, 32]. For example Evaflux 4A secondary filters show sieving coefficients for albumin of ~0.8 and for IgM (950 kDa) of ~0.1, close to our sieving coefficients (~0.8 for BSA and ~0.1 for thyroglobulin) [33]. Evaflux 4A can be successfully applied for treatment of for example hyperglobulinemia where large globulins are removed such as IgM [34].

For most of the commercial membranes however, there is hardly information available in the scientific literature about biocompatibility. In the next section we investigate extensively the biocompatibility properties of our SlipSkin^{TM} membranes M50 and M50ev and compare this to several benchmark materials.

5.3.3. Biocompatibility results

We performed several biocompatibility tests. The tests are selected based on the ISO guidelines. For the category of coagulation, two different thrombin generation tests were performed. In the category of thrombosis, platelet adhesion and aggregation were analyzed by SEM, while a LDH assay was performed for a quantitative analysis of platelet adhesion in the category platelets. Leukocyte adhesion experiments and hemolysis evaluation were performed for the hematology category. For the complement category, we performed a classical and alternative pathway complement test.

5.3.3.1. Thrombin generation

Thrombin plays a central role in the coagulation cascade, and converts fibrinogen into fibrin so that an actual clot can be formed [35]. Furthermore it influences platelet aggregation and endothelial cell function.

a

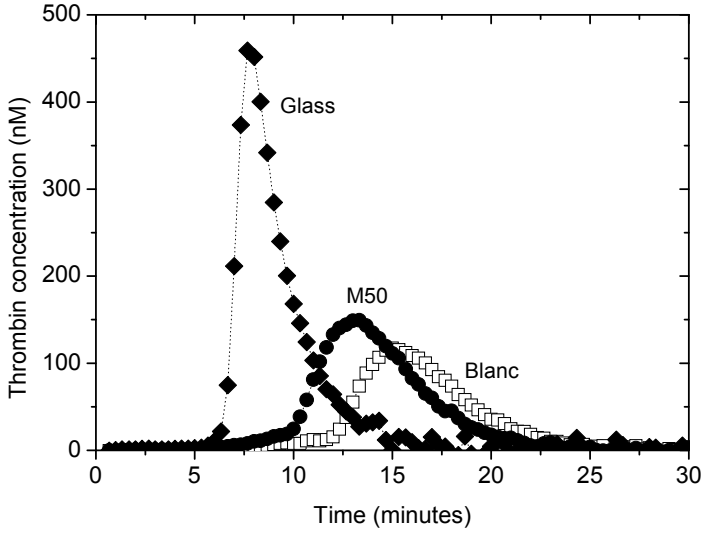

b

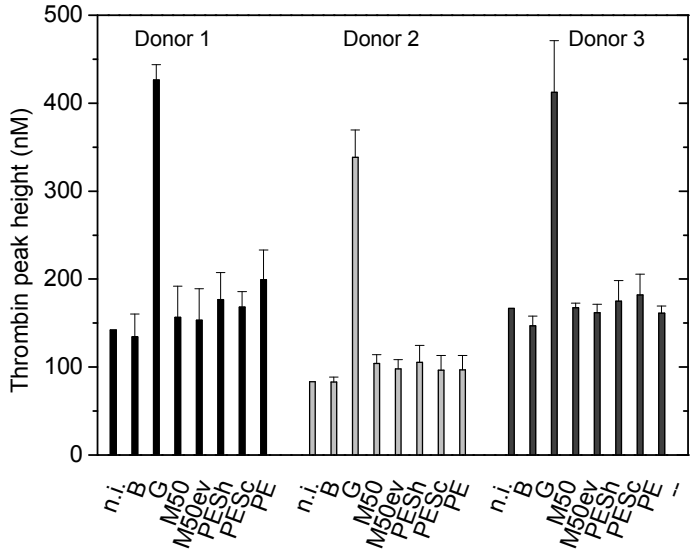

Figure 4. a) Typical thrombin generation curve for blanc (incubated PPP)(□), glass (♦)and a M50 membrane (●). **b**) Average Thrombin peak height presented for the categories: n.i. (not incubated PPP), B (blanc, incubated PPP), glass, M50, M50ev, PESh, PESc and PE for donor 1, 2, 3. Error bars indicate standard deviations.

In this assay, the intrinsic coagulation cascade is responsible for the generation of thrombin, since there is no tissue factor present in the test system. The membrane can lead to contact activation after which the intrinsic coagulation cascade starts. During the incubation period with the membranes there is no calcium or phospholipids present and the coagulation cascade will hold. After addition of phospholipids and calcium ions, the intrinsic pathway will be continued and eventually thrombin will be generated. The peak height of generated thrombin is an indicator for the contact activation caused by the responsible material.

Figure 4a shows typical thrombin generation curves of the positive control glass, M50 membrane and the negative control blanc (incubated PPP). The time till the rapid increase in thrombin concentration (thrombin generation time, TGT) as well as the peak height are analyzed and the peak height gives the most distinguishable and consistent results. The SlipSkin™ membrane M50 peak height is between the peak height values of the positive control glass and the negative control blanc. Figure 4b presents the average peak height of thrombin concentration (nM) of donor 1, 2, and 3. The not incubated PPP shows similar results to the incubated plasma, the blanc. The thrombin peak height of our SlipSkin™ Membranes M50 and M50ev is similar to the benchmark materials and much lower than the glass (positive control) showing that the SlipSkin™ membranes have excellent properties concerning contact activation.

Besides the above, we also measured thrombin generation real time, where PRP was incubated on the membrane in presence of calcium. In this assay, the thrombin generation time was used for further analysis and was an indicator for the thrombogenicity of the material [13, 36]. Figure 5a shows typical results of thrombin generation curves over time for the M50 membrane and negative (blanc) and positive (glass) control. Figure 5b presents the results of the thrombin generation times and again, the SlipSkin™ membranes M50 and M50ev show very good properties, comparable to currently clinical in use PE membranes and other benchmark membranes in terms of thrombogenicity.

a

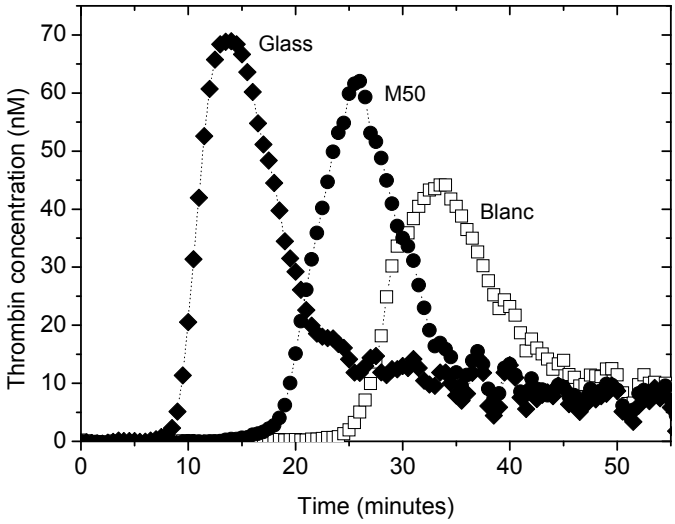

b

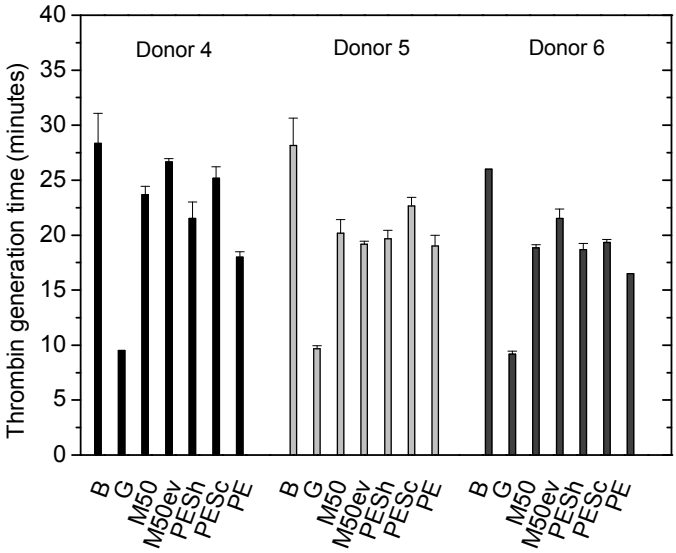

Figure 5. a) Typical thrombin generation curve of glass (♦), M50 (●) and blanc (incubated PRP) (□). **b**) Average thrombin generation times presented for donor 4, 5, 6, for the following materials: B (blanc, incubated PRP), G (glass), M50, M50ev, PESh, PESc, PE membranes. Error bars indicate standard deviations. Thrombin generation times were measured in triplicate for each material and each donor.

5.3.3.2 Platelet adhesion and aggregation

Blood platelets are important during coagulation. They can form a platelet plug to stop bleeding, their presence is necessary for the coagulation cascade and activated platelets can release biologically active compounds [35]. Platelet adhesion and activation on hemodialysis membranes can lead to reactive oxygen species generation by neutrophils [37].

Here, we have performed two tests, SEM image analysis for a qualitative measure for platelet adhesion and aggregation, while quantitative results about platelet adhesion were obtained using the LDH platelet adhesion assay [19]. Figure 6a shows SEM pictures of platelets which adhered onto the tested membranes and glass. Both SlipSkin^{TM} membranes (M50 and M50ev) (C, D, E, F) show little platelet adhesion, no severe cluster formation and the adhered platelets are mostly round with little or no pseudopodia formation. Besides there are hardly any deposits. On glass, single platelets and small clusters are adhered with mostly long pseudopodia and small amounts of deposits (A, B). The PESh membranes (G, H) show deposits on the surface, the platelets are mostly round with small pseudopodia but no clusters are observed. Figure I and J show clusters of platelets with pseudopodia on the PESc surface, and a lot of deposit on the membrane surface. On the PE blood transfusion filter, round, and flat platelets are observed, mostly without pseudopodia. Although some platelets have long pseudopodia (K, L).

a

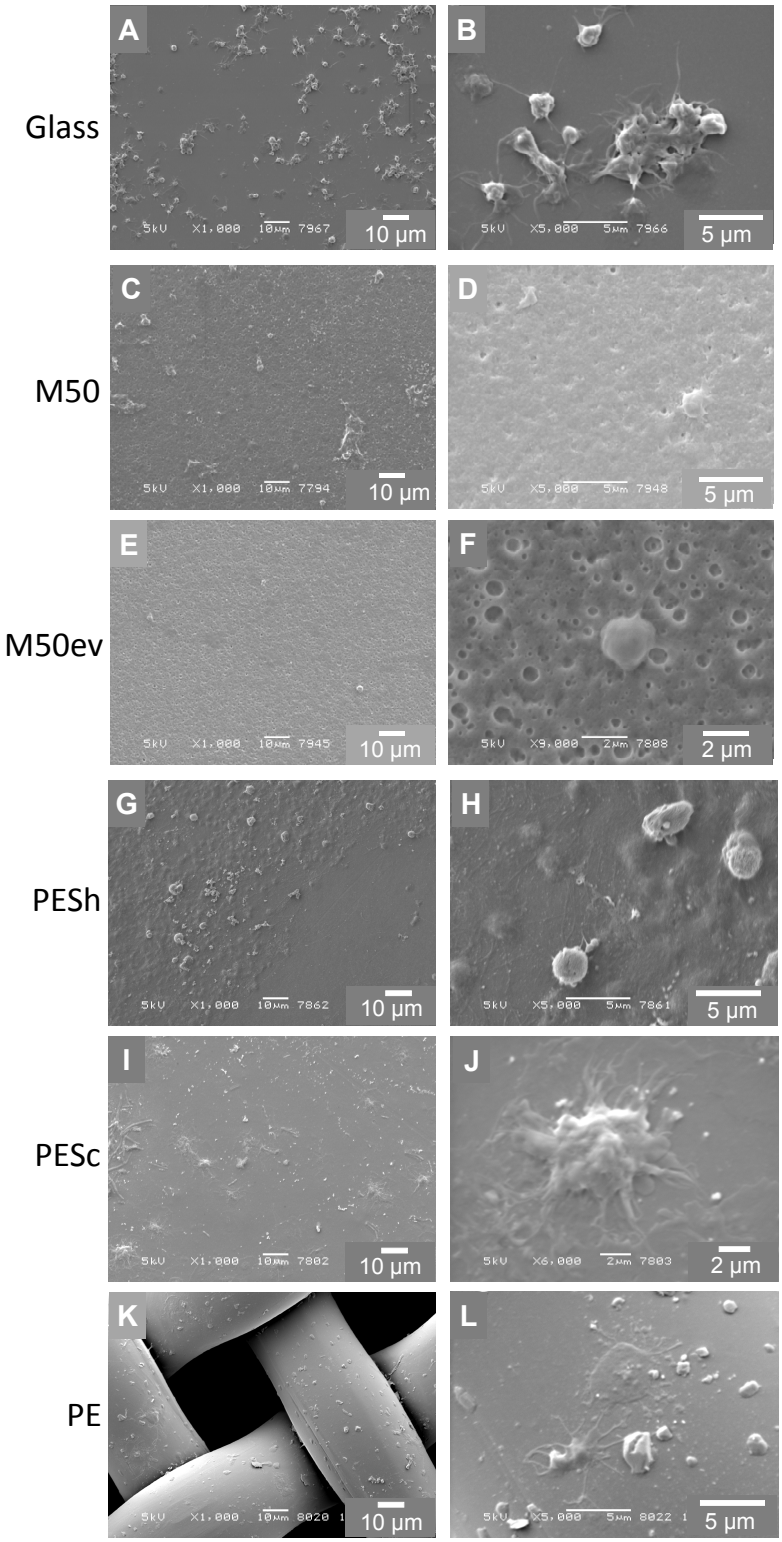

Figure 6. **a**) SEM pictures of adhered platelets on the materials glass (A, B), M50 (C,D), M50ev (E, F), PESh (G,H), PESc (I,J) and PE (K, L).

b

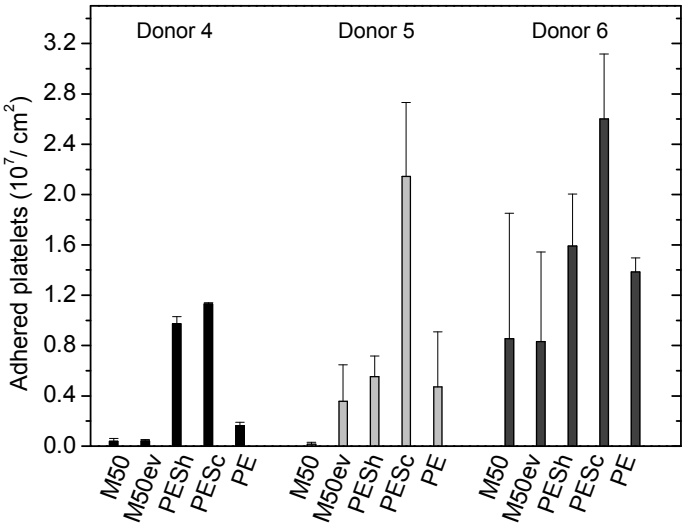

Figure 6. b) Average number of adhered platelets per cm^2 material presented for the following membranes: M50, M50ev, PESh PESC, and PE, for donor 5, 6 and 7. Error bars indicate standard deviations.

Figure 6b presents the average adhered platelets / cm^2 material. In every donor a similar trend can be observed. Only few platelets adhere to the M50 and M50ev membranes, whereas many platelets seem to adhere to the other benchmark materials, especially to the PESc.

5.3.3.3. Leukocyte adhesion

Leukocytes are one of the major players in the inflammatory response, and leukocyte activation can result in release of inflammatory mediators. White blood cells can adhere to the hemodialysis membranes [38] and hemodialysis is associated with production of cytokines by white blood cells [39]. Figure 7 shows the average number of leukocytes left in blood after incubation with the various membranes. The first bar represents the number of leukocytes in not incubated blood. All donors

are in the normal range of leukocyte numbers although donor 1 is on the upper range of the spectrum. The number of leukocytes in blood is similar to the number of leukocytes in blanc which indicates that there is hardly undesired adhesion of leukocytes on the well plate material. Generally, there is hardly any leukocyte adhesion and the M50 and M50ev membranes perform equally good to clinical in use PE membranes and the other benchmark membranes PESh and PESc. Based on the hematocrit levels we conclude that there is no evaporation (data not shown) which could lead to elevated leukocyte concentrations in the blood and misinterpretation of the data. Besides, the following categories of leukocytes were separately analyzed as well: monocytes, basophils, eosinophils, neutrophils and lymphocytes. No major adhesion of any of these cell types were observed for all the membranes (data not shown).

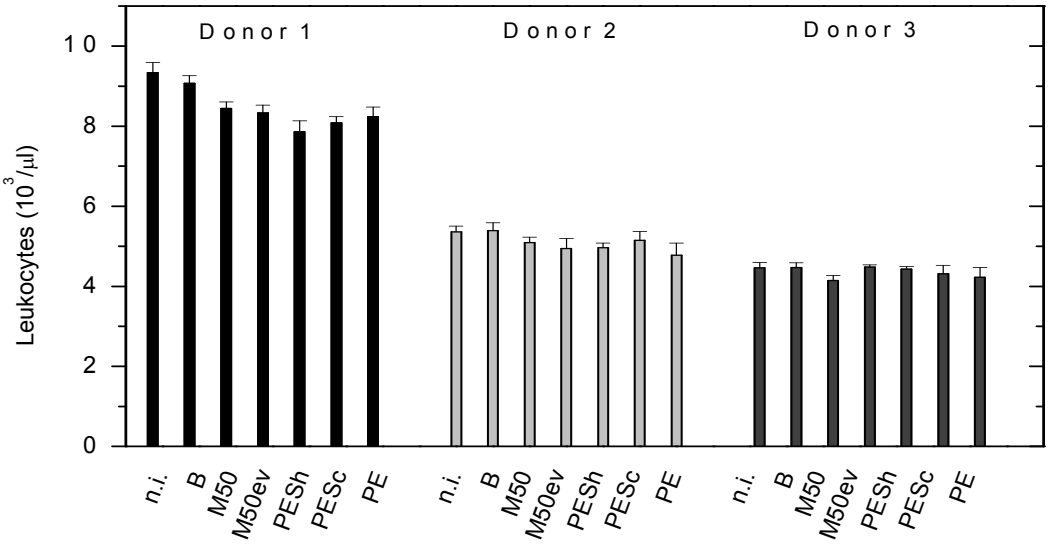

Figure 7. Average number of leukocyte left in blood. For n.i. (not incubated blood), B (blanc, incubated blood), M50, M50ev, PESh, PESc and PE membranes for donor 1, 2, 3. Error bars indicate standard deviations.

5.3.3.4. Hemolysis

Hemolysis is often used as a screening test to assess biocompatibility [40]. Hemolysis less than 5% is regarded as non-toxic according to the ASTM F-756-08 standard [23]. Table 3 presents the average percentage of hemolysis of the tested membranes. The M50 and M50ev SlipSkin^{TM} membranes did not induce toxic levels of hemolysis in this *in vitro* hemolysis screening test and show comparable good results as the benchmark materials PESh and PESc and the clinical in use PE membranes.

Table 3. Average percentage hemolysis (%) ± sd

Membrane	Donor 1	Donor 2	Donor 3
M50	1.7 ± 2.1	1.7 ± 0.4	0.9 ± 0.4
M50ev	0.6 ± 0.5	1.1 ± 0.4	0.8 ± 0.4
PESh	1.5 ± 0.4	1.2 ± 0.3	0.8 ± 0.3
PESc	2.6 ± 2.4	0.9 ± 0.2	0.8 ± 0.5
PE	1.3 ± 0.3	2.0 ± 0.8	0.6 ± 0.3

5.3.3.5. Complement

The complement system is an important part of the body's innate immune system [41]. Three pathways are known for the activation of this system, the classical pathway, alternative pathway and mannose binding lectin pathway. All these pathways eventually cause effect via the formation of opsonisation factors which facilitate phagocytosis, production of leukocyte attracting factors and the production of the membrane attack complex which can lyse e.g. bacteria [41].

Figure 8 shows the average % complement activity of the classical (Figure 8a) and alternative (Figure 8b) pathway of the complement system. The not incubated serum and the blanc (incubated serum),

show similar results in both cases. This indicates that the incubation step itself did not lead to complement activation, therefore a decrease in complement activity in these assays would indicate a relative deficiency of any of the complement components, due to complement activation via the responsible pathway by the membrane. Overall, there was no activation of the classical pathway of the complement system by any of them, see Figure 8a. In donor 1 and 3 all the materials show values close to 100% complement activity. In donor 2, the complement activity for DEAE cellulose seems to be lower than the rest, but this was not observed in the other donors. Activation of the classical pathway usually occurs via immune complexes rather than artificial surfaces. The alternative pathway of the complement system, on the other hand can be activated by artificial surfaces such as

a

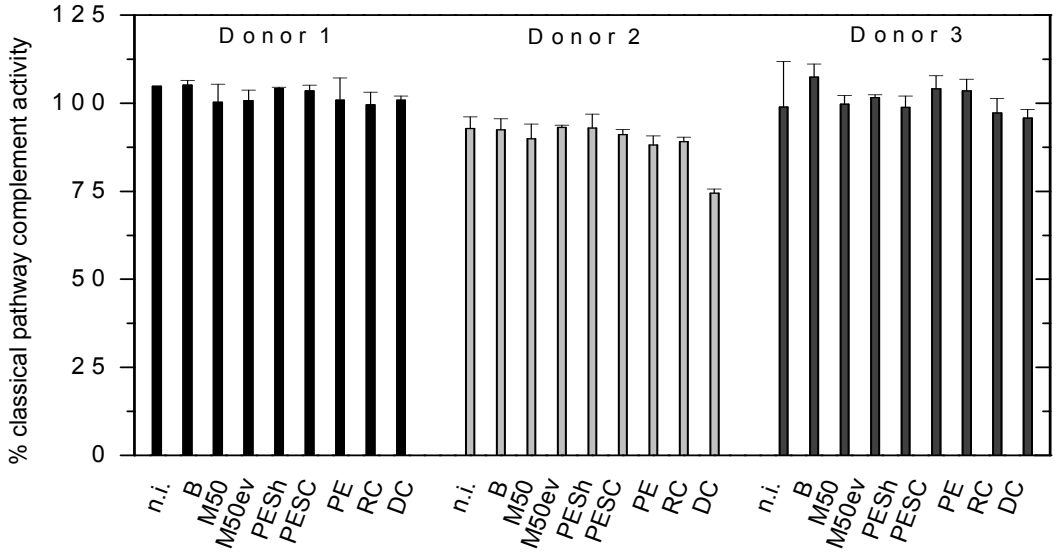

Figure 8. a) Average % classical pathway complement activity in serum. For n.i. (not incubated serum), B (blanc, incubated serum), M50, M50ev, PESh, PESC, PE, RC and DC membranes.

b

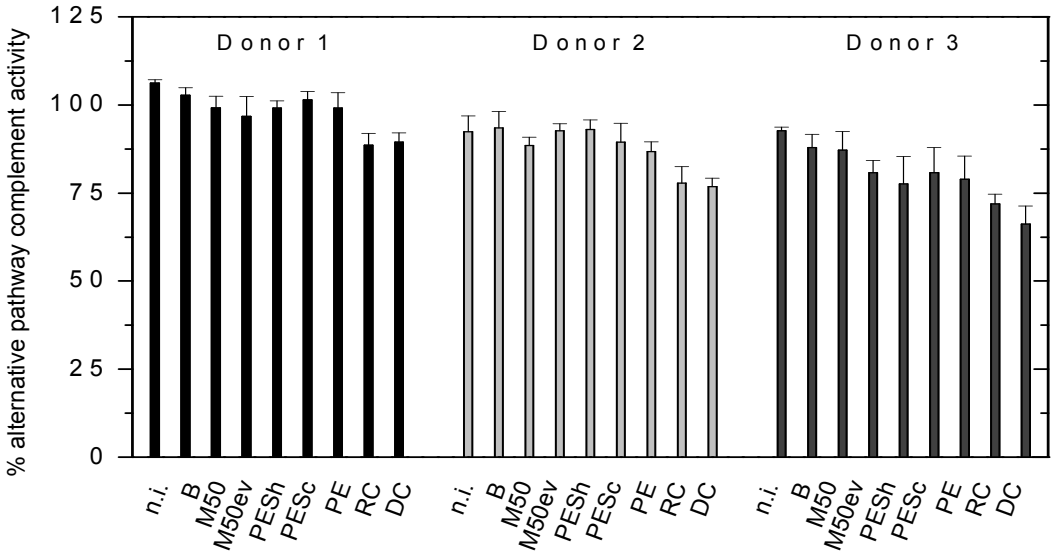

Figure 8. b) Average % alternative pathway complement activity in serum. For n.i. (not incubated serum), B (blanc, incubated serum), M50, M50ev, PESh, PESc, PE, RC and DC membranes. Tested in donor 1, 2, 3. Error bars indicate standard deviations.

5.4. Conclusions and outlook

This work presented the preparation and characterization of SlipSkin™ based membranes with excellent biocompatibility. In our tests these membranes have lower platelet adhesion and have equivalently good properties in relation to contact activation, thrombogenicity based on thrombin generation, leukocyte adhesion, hemolysis and complement activation compared to benchmark materials PESh, PESc and clinical in use PE membranes. The new membranes have a sieving curve similar to cascade filters in plasma fractionation applications.

In the future we plan to develop SlipSkin™ hollow fiber membranes suitable for hemodialysis with a lower molecular weight cut-off so that albumin is retained. Besides membranes purely made from SlipSkin™, this material may be used to coat membranes, so that it can offer its biocompatibility characteristics while the mechanical stability can be provided by a support membrane material. Furthermore, the very promising biocompatibility results of our membranes make it interesting to further investigate their biocompatibility under flow conditions.

Acknowledgements

M. Tijink would like to acknowledge the Dutch Kidney Foundation for the financial support of this project.

Conflict-of-Interest Notification

The authors J. Janssen, Y. Aldenhoff and L. Koole declare that they are shareholders of the company that manufactures and commercializes the SlipSkin™ biomaterial. This is the company INterface BIOmaterials BV (Geleen, the Netherlands; www.interfacebiomaterials.com).

References

[1] Lacson Jr E, et al. Survival with three-times weekly in-center nocturnal versus conventional hemodialysis. Journal of the American Society of Nephrology 2012;23:687-95.

[2] Pauly RP, Gill JS, Rose CL, Asad RA, Chery A, Pierratos A, Chan CT. Survival among nocturnal home haemodialysis patients compared to kidney transplant recipients. Nephrology Dialysis Transplantation 2009;24:2915-9.

[3] Davenport A, Gura V, Ronco C, Beizai M, Ezon C, Rambod E. A wearable haemodialysis device for patients with end-stage renal failure: a pilot study. Lancet 2007;370:2005-10.

[4] Krause B, Storr M, Ertl T, Buck R, Hildwein H, Deppisch R, Göhl H. Polymeric membranes for medical applications. Chemie Ingenieur Technik-CIT 2003;75:1725-32.

[5] Deppisch R, Storr M, Buck R, Go?hl H. Blood material interactions at the surfaces of membranes in medical applications. Separation and Purification Technology 1998;14:241-54.

[6] Matsuda M, et al. Effects of fluid flow on elution of hydrophilic modifier from dialysis membrane surfaces. Journal of Artificial Organs 2008;11:148-55.

[7] Huang XJ, Guduru D, Xu ZK, Vienken J, Groth T. Blood Compatibility and Permeability of Heparin-Modified Polysulfone as Potential Membrane for Simultaneous Hemodialysis and LDL Removal. Macromolecular Bioscience;11:131-40.

[8] Fang B, et al. Modification of polyethersulfone membrane by grafting bovine serum albumin on the surface of polyethersulfone/poly(acrylonitrile-co-acrylic acid) blended membrane. Journal of Membrane Science 2009;329:46-55.

[9] Locatelli F, et al. Effects of different membranes and dialysis technologies on patient treatment tolerance and nutritional parameters. Kidney International 1996;50:1293-302.

[10] Gambro ASA. Dialysis Opinions 2008, focus on innovation, http://www.gambro.com/en/global/About-Gambro/Research--development/Dialysis-opinions/. 2008.

[11] Aldenhoff YBJ, Hanssen JHL, Knetsch MLW, Koole LH. Thrombus Formation at the Surface of Guide-Wire Models: Effects of Heparin-releasing or Heparin-exposing Surface Coatings. Journal of Vascular and Interventional Radiology 2007;18:419-25.

[12] Hanssen HHL, Wetzels GMR, Benzina A, Van Der Veen FH, Lindhout T, Koole LH. Metallic wires with an adherent lubricious and blood-compatible polymeric coating and their use in the manufacture of novel slippery-when-wet guidewires: Possible applications related to controlled local drug delivery. Journal of Biomedical Materials Research 1999;48:820-8.

[13] Stevens KNJ, et al. The relationship between the antimicrobial effect of catheter coatings containing silver nanoparticles and the coagulation of contacting blood. Biomaterials 2009;30:3682-90.

[14] Zweigart C, Neubauer M, Storr M, Böhler T, Krause B. 2.13 - Progress in the Development of Membranes for Kidney-Replacement Therapy. In: Editor-in-Chief: Enrico D, Lidietta G, editors. Comprehensive Membrane Science and Engineering. Oxford: Elsevier; 2010. p. 351-90.

[15] Erlenkötter A, Endres P, Nederlof B, Hornig C, Vienken J. Score model for the evaluation of dialysis membrane hemocompatibility. Artificial Organs 2008;32:962-9.

[16] Muthusubramaniam L, Lowe R, Fissell WH, Li L, Marchant RE, Desai TA, Roy S. Hemocompatibility of silicon-based substrates for biomedical implant applications. Annals of Biomedical Engineering 2011;39:1296-305.

[17] Tijink MSL, et al. A novel approach for blood purification: Mixed-matrix membranes combining diffusion and adsorption in one step. Acta Biomaterialia 2012;8:2279-87.

[18] Hemker HC, et al. Calibrated automated thrombin generation measurement in clotting plasma. Pathophysiology of Haemostasis and Thrombosis 2003;33:4-15.

[19] Tamada Y, Kulik EA, Ikada Y. Simple method for platelet counting. Biomaterials 1995;16:259-61.

[20] Liu TY, Lin WC, Huang LY, Chen SY, Yang MC. Hemocompatibility and anaphylatoxin formation of protein-immobilizing polyacrylonitrile hemodialysis membrane. Biomaterials 2005;26:1437-44.

[21] Uzun L, Yavuz H, Osman B, Ã‡elik H, Denizli A. Poly(hydroxyethyl methacrylate) based affinity membranes for in vitro removal of anti-dsDNA antibodies from SLE plasma. International Journal of Biological Macromolecules;47:44-9.

[22] Van Kooyk Y, Weder P, Heije K, Figdor CG. Extracellular Ca2+ modulates leukocyte function-associated antigen-1 cell surface distribution on T lymphocytes and consequently affects cell adhesion. Journal of Cell Biology 1994;124:1061-70.

[23] Dahe GJ, Teotia RS, Kadam SS, Bellare JR. The biocompatibility and separation performance of antioxidative polysulfone/vitamin E TPGS composite hollow fiber membranes. Biomaterials 2011;32:352-65.

[24] Seelen MA, et al. Functional analysis of the classical, alternative, and MBL pathways of the complement system: Standardization and validation of a simple ELISA. Journal of Immunological Methods 2005;296:187-98.

[25] McKelvey SA, Koros WJ. Phase separation, vitrification, and the manifestation of macrovoids in polymeric asymmetric membranes. Journal of Membrane Science 1996;112:29-39.

[26] Mulder M. Basic principles of membrane technology. Enschede: Kluwer Academic Publishers; 1996.

[27] Jao-Ming C, Da-Ming W, Fung-Ching L, Juin-Yih L. Formation and gas flux of asymmetric PMMA membranes. Journal of Membrane Science 1996;109:93-107.

[28] Xu ZL, Qusay FA. Polyethersulfone (PES) hollow fiber ultrafiltration membranes prepared by PES/non-solvent/NMP solution. Journal of Membrane Science 2004;233:101-11.

[29] Clark WR, Hamburger RJ, Lysaght MJ. Effect of membrane composition and structure on solute removal and biocompatibility in hemodialysis. Kidney International 1999;56:2005-15.

[30] Lysaght MJ. Hemodialysis membranes in transition. ContribNephrol 1988;61:1-17.

[31] Stegmayr BG. A survey of blood purification techniques. Transfusion and Apheresis Science 2005;32:209-20.

[32] Nakaji S, Yamamoto T. Membranes for therapeutic apheresis. Therapeutic apheresis : official journal of the International Society for Apheresis and the Japanese Society for Apheresis 2002;6:267-70.

[33] Sueoka A, Miyahara T, Takakura K, Ueda Y. Study of Filtration Characteristics of EVAL Secondary Filters in Plasma Diseases. Therapeutic Apheresis 2000;4:65-7.

[34] Sueoka A. Therapeutic Apheresis Application Using Membrane Plasma Fractionation Technology: Present Scope and Limitations. Therapeutic Apheresis 2000;4:211-2.

[35] Berne MNLRM. Principles of physiology. Third edition ed: Mosby; 2000.

[36] Stevens KN, Knetsch ML, Sen A, Sambhy V, Koole LH. Disruption and Activation of Blood Platelets in Contact with an Antimicrobial Composite Coating Consisting of a Pyridinium Polymer and AgBr Nanoparticles. ACS Applied Materials & Interfaces 2009;1:2049-54.

[37] Itoh S, Susuki C, Tsuji T. Platelet activation through interaction with hemodialysis membranes induces neutrophils to produce reactive oxygen species. Journal of Biomedical Materials Research - Part A 2006;77:294-303.

[38] Grooteman MP, Bos JC, van Houte AJ, van Limbeek J, Schoorl M, Nubé MJ. Mechanisms of intra-dialyser granulocyte activation: a sequential dialyser elution study. Nephrology Dialysis Transplantation 1997;12:492-9.

[39] Rousseau Y, Haeffner-Cavaillon N, Poignet J-L, Meyrier A, Carreno M-P. in vivo intracellular cytokine production by leukocytes during haemodialysis. Cytokine 2000;12:506-17.

[40] Seyfert UT, Jung F. Criteria and principles of in vitro hemocompatibility testing according to the ISO 10993(4). Infusionstherapie und Transfusionsmedizin 2000;27:317-22.

[41] Walport MJ. Complement. New England Journal of Medicine 2001;344:1058-66.

6

Evaluation and outlook

The field of artificial organs is multidisciplinary and requires understanding of life science principles as well as engineering. Kolff, a medical doctor who liked engineering, constructed a rotating drum dialyzer and saved for the first time a patient's life using this artificial kidney [6, 7]. Ever since this important milestone, many developments have been going on to improve artificial kidneys [8]. The currently available artificial kidneys do treat the patients, but they are definitely not replacing renal functions in a perfect manner. Moreover, the health related quality of life of dialysis patients is low while their mortality is still high [1-3]. This thesis describes preparation and characterization of membranes which offer potential solutions to improve artificial kidney devices.

In **chapter 2** dual layer flat sheet MMM are prepared which combine diffusion and adsorption in one step. Addition of activated carbon particles to the polyethersulfone - polyvinylpyrrolidone membrane matrix influences the membrane formation process and the obtained membrane morphology. The dual layer flat sheet MMM shows good adsorption of creatinine compared to various literature references and shows potential to remove protein-bound solutes. This concept is translated to dual layer hollow fiber mixed matrix membranes in **chapter 3**. Activated carbon particles are embedded in a porous polyethersulfone - polyvinylpyrrolidone mixed matrix membrane layer which is attached to the inner particle free membrane layer. Spinning parameters such as spinneret type, bore liquid and pumping speed of the dope solutions influence the final membrane morphology of the dual layer hollow fiber MMM. The new hollow fiber MMMs combine diffusion and adsorption in one step and remove protein-bound toxins p-cresylsulfate, indoxyl sulfate and hippuric acid from spiked human plasma. This indicates the great potential of this new concept for clearance of the difficult to remove protein-bound uremic toxins. The hollow fiber MMM needs further optimization, the particle accessibility could be improved by better pore interconnectivity or membrane structures with a higher porosity. The adsorption capacity may be further enhanced by increasing the particle proportion. Furthermore, optimal transport properties and sieving characteristics are necessary. Construction of modules containing many hollow fiber MMMs would

be interesting to compare the removal performance of our membranes with for example currently in use artificial kidney membrane modules and adsorption columns.

Developments on wearable artificial kidneys are often based on peritoneal dialysis as well as on hemodialysis techniques, and often the dialysate is regenerated using sorbents [4, 5]. To use MMMs for wearable artificial kidneys, the toxin removal performance, possibilities for miniaturization and time till saturation need to be investigated and optimized. We have shown that MMMs can combine membrane based removal and adsorption in one single step, and this is very interesting to apply for wearable artificial kidneys. Possibly it could enhance protein-bound toxin removal, and it may help to miniaturize the device. It may also be possible to apply MMMs just for the regeneration of the dialysate instead of a column with adsorptive particles so that small adsorptive particles can be used without pressure drop issues in the wearable system. Furthermore, regeneration of the adsorptive particles is interesting for application in wearable artificial kidneys, and washing with hot water could be an option for this, since the adsorption capacity of activated carbon columns could be regenerated and is in development for home hemodialysis systems [6]. Besides, it would be interesting to test if hollow fiber MMMs can prevent endotoxin transport from the dialysate into the blood circulation of the patient because of its adsorptive properties since earlier developed cellulose acetate based MMMs with embedded activated carbon particles can adsorb endotoxins [7]. Another application of MMMs in blood purification could be for treatment of sepsis or treatment of acute liver failure or therapeutic apheresis, and future research may develop MMMs suitable for these applications.

In order to enhance the membrane biocompatibility, coatings can be applied onto the membrane. In a preliminary study, performed in collaboration with J. Van der Vlag and A. Rops, from university medical centre Nijmegen, heparan sulfate was coated on the inside of the dual layer hollow fiber MMM. The new membranes had a higher clean water permeance compared to the uncoated membrane (probably because of the hydrophilic nature of the coating) (Figure 1) as well as a

prolonged clotting time in a modified activated partial thromboplastin time assay (aPTT) indicating improved biocompatibility, see Figure 2.

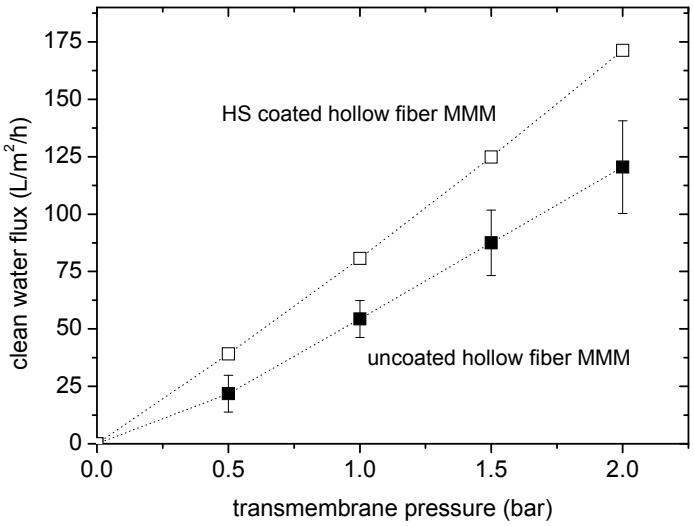

Figure 1. Clean water flux plotted against transmembrane pressure for uncoated hollow fiber MMMs (■) and heparan sulfate (HS) (□) coated hollow fiber MMM. The error bars indicate standard deviations. The dotted lines are plotted to guide the eye.

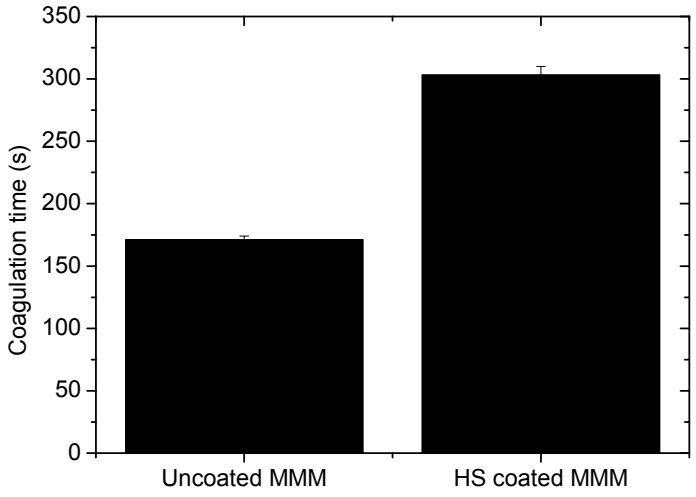

Figure 2. Coagulation time in a modified aPTT (activated partial thromboplastin time) assay, using 5 times diluted plasma flowing through the hollow fiber MMMs with or without a heparan sulfate (HS) coating.

The activated carbon particles used in chapter 2 and 3 are in **Chapter 4** compared to two other adsorptive particles, concerning removal of several uremic retentions solutes. All the selected adsorptive particles adsorb the small molecular weight molecule creatinine and protein-bound toxins p-cresylsulfate, indoxyl sulfate and hippuric acid, and middle molecule β_2-microglobulin although in different amounts. Y-carbon is better for the removal of β_2-microglobulin per gram of adsorbent, whereas Mast carbon and Norit AC seem to adsorb more creatinine and protein-bound toxins. Further investigation of the particles such as adsorption kinetics and surface area are interesting for comparison of these particles as well. Y-carbon seems to be an interesting candidate for embedding in a membrane matrix, since it can adsorb the majority of small water soluble molecules, middle molecules and protein-bound solutes, all three categories of uremic retention solutes.

In **chapter 5** we fabricated SlipSkin™ based flat sheet membranes. Polymer composition, solvent type and solvent evaporation time influence membrane structure and membranes with sieving properties of cascade filters in plasma fractionation with very good biocompatibility were developed. In comparison to clinically used membranes and other benchmark membranes, the SlipSkin™ based membranes have low platelet adhesion and equivalently good properties in terms of contact activation, thrombogenicity, leukocyte adhesion, hemolysis, and complement activation.

Based on these results, it seems very interesting to develop SlipSkin™ based hollow fiber membranes for blood purification (hemodialysis or plasma separation). Preliminary experiments showed that it is possible to spin SlipSkin™ based hollow fiber membranes, see Figure 3. These hollow fiber membranes need to be further optimized concerning mechanical properties and the sieving and transport characteristics. Besides, it would be interesting to develop SlipSkin™ based MMMs.

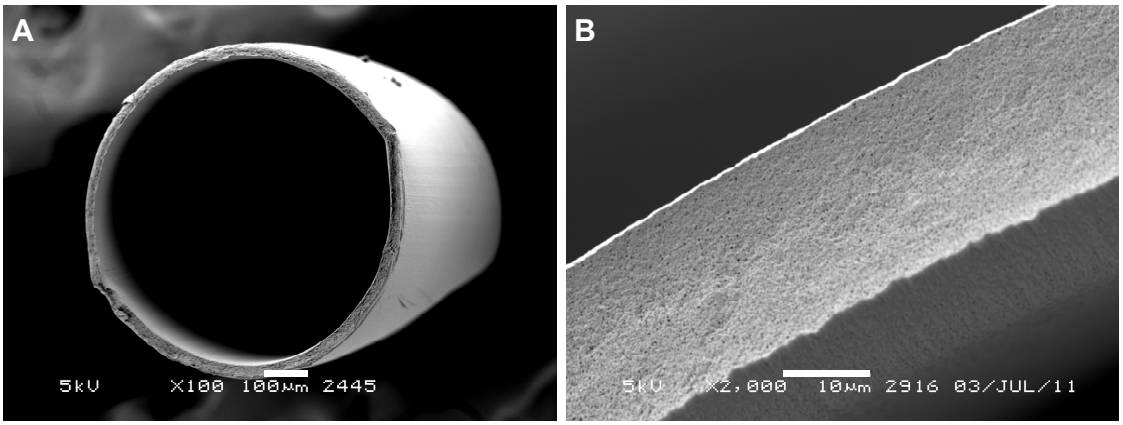

Figure 3. Scanning electron microscopy images of a porous SlipSkin™ based hollow fiber membrane. Scale bars indicate 100 µm in A and 10 µm in B

Preliminary experiments showed that it is possible to develop flat sheet SlipSkin™ MMMs, see Figure 4. In fact, the mechanical stability of these membranes is better than SlipSkin™ membranes without embedded particles, and these membranes showed optimal adsorption for creatinine.

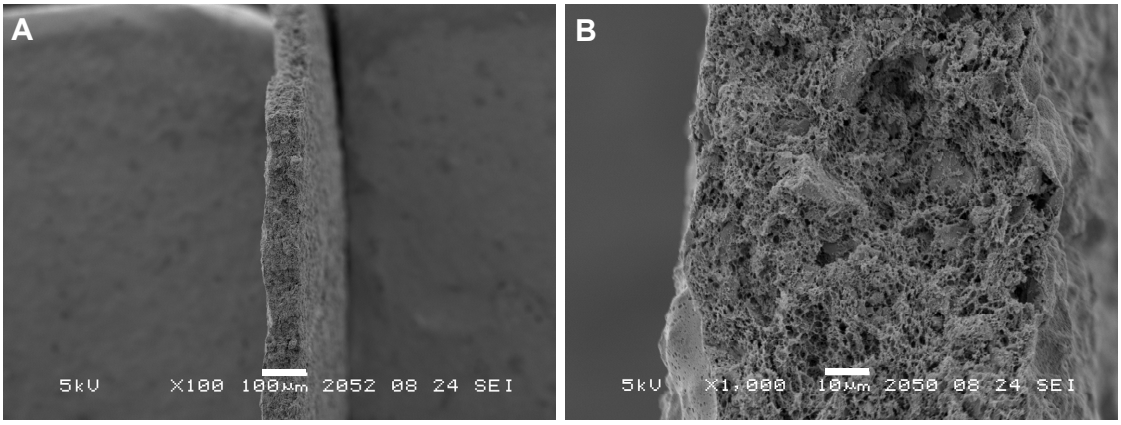

Figure 4. Scanning electron microscopy images of SlipSkin™ based MMMs. Scale bar indicates 100 m in A and 10 µm in B

Overall, this thesis presents results on various membrane developments towards improved blood purification. The dual layer hollow fiber mixed matrix membranes show potential to clear difficult to remove protein-bound toxins from blood. The new SlipSkin™ membranes show less platelet adhesion and good biocompatibility and have potential for long term use application in blood filtration therapies. The adsorptive particle Y-carbon and the SlipSkin™ membrane matrix could be combined to make possibly more effective and biocompatible mixed matrix membranes. Further research could stimulate the application of the mixed matrix membranes either for improvement of the current hemodialysis or apheresis therapies or as an integral part of a wearable artificial kidney.

Acknowledgements

Nazely Diban Gómez is acknowledged for her support with development of SlipSkin™ based hollow fiber membranes. Marco Timmer is acknowledged for his support with development of SlipSkin™ based MMMs. Johan van der Vlag and Angelique Rops, University medical centre Nijmegen, are thanked for the collaboration on the work of heparan sulfate coatings.

References

[1] Mazairac AHA, et al. Changes in quality of life over time-Dutch haemodialysis patients and general population compared. Nephrology Dialysis Transplantation 2011;26:1984-9.

[2] Grooteman MPC, et al. Effect of online hemodiafiltration on all-cause mortality and cardiovascular outcomes. Journal of the American Society of Nephrology 2012;23:1087-96.

[3] Lacson Jr E, et al. Survival with three-times weekly in-center nocturnal versus conventional hemodialysis. Journal of the American Society of Nephrology 2012;23:687-95.

[4] Ronco C, Fecondini L. The Vicenza Wearable Artificial Kidney for Peritoneal Dialysis (ViWAK PD). Blood Purification 2007;25:383-8.

[5] Davenport A, Gura V, Ronco C, Beizai M, Ezon C, Rambod E. A wearable haemodialysis device for patients with end-stage renal failure: a pilot study. Lancet 2007;370:2005-10.

[6] Kim JH, et al. Development of a cold dialysate regeneration system for home hemodialysis. Blood Purification 2009;28:84-92.

[7] Saiful S. Mixed matrix membrane adsorbers for protein and blood purification [PhD Thesis]. Enschede, Netherlands: University of Twente; 2007.

Summary

The research presented in this thesis is about the fabrication and characterization of new membranes for blood purification. An introduction on the topic of this thesis and its scope is presented in **Chapter 1**.

A novel membrane concept for combining diffusion and adsorption in one step to remove uremic retention solutes is presented In **Chapter 2**. A membrane with embedded functionalized particles, a so called mixed matrix membrane (MMM) is developed for this. Flat sheet dual layer MMMs with activated carbon particles embedded in the membrane matrix with a particle free membrane layer on the blood contacting side to improve to improve hemocompatibility and prevent release of particles are developed. The dual layer mixed matrix membranes have high clean water permeance and high creatinine adsorption from creatinine model solutions. In human plasma, the removal of creatinine and of the protein-bound solute para-aminohippuric acid by single and dual-layer membranes is in agreement with the removal achieved by the activated carbon particles alone, showing excellent accessibility of the particles in the MMM under these experimental conditions, and potential to remove protein-bound solutes. This chapter proofs that MMMs can combine diffusion and adsorption of a uremic retention solute in one step.

We translated the novel concept of mixed matrix membranes to a hollow fiber configuration in **Chapter 3**. A dual layer hollow fiber mixed matrix membrane was fabricated with a porous macro void free polymeric inner membrane layer well attached to the MMM outer layer which contains the embedded activated carbon particles. The dual layer hollow fiber MMM has permeation properties in the ultrafiltration range and adsorbs 57%, 82% and 94% of p-cresylsulfate, indoxyl sulfate and hippuric acid respectively from spiked human plasma in 4h. Also under dynamic conditions (in cross

flow experiments with diffusion and convection modes) the dual layer hollow fiber MMM removes the protein-bound toxins. These results indicate great potential for this new type of membranes for clearance of difficult to remove protein-bound toxins.

Three types of adsorptive particles are investigated in **Chapter 4**. Norit activated carbon, Mast carbon and Y-carbon show adsorption of small water soluble molecule creatinine, middle molecule β_2-microglobulin and protein-bound toxins p-cresylsulfate, indoxyl sulfate and hippuric acid. Thus, a broad spectrum of uremic toxins can be removed using adsorptive particles. Y-carbon seems to adsorb more β_2-microglobulin per gram of adsorbent than Mast carbon and Norit activated carbon, while for removal of protein-bound toxins the latter two seem to be a bit better.

In **Chapter 5**, we develop for the first time membranes using the material SlipSkin™ which is a copolymer made from N-vinylpyrrolidone (NVP) and butylmethacrylate (BMA). Developments in membrane based blood purification therapies often come with longer treatment times and therefore longer blood-material contact, and make it interesting to investigate materials with improved biocompatibility. Morphology of SlipSkin™ based membranes is influenced by several parameters such as polymer composition, solvent type and solvent evaporation time. Membranes with sieving properties of cascade filters in plasma fractionation applications are developed and show very good biocompatibility. In fact they have low platelet adhesion and equivalently good properties of contact activation, thrombogenicity, leukocyte adhesion, hemolysis, complement activation compared to a membranes used in the clinic and other benchmark membranes.

In **Chapter 6** the main conclusions of this thesis are discussed as well as interesting future directions for further development of blood purification membranes for improved artificial kidneys.

Nederlandse samenvatting

In dit proefschrift wordt de ontwikkeling van een nieuw type membranen voor de zuivering van bloed beschreven. **Hoofdstuk 1** geeft een introductie over het onderwerp van dit proefschrift.

In **hoofdstuk 2** wordt een nieuw concept beschreven voor membranen die diffusie en adsorptie in een stap combineren om zodoende uremische retentiestoffen uit het bloed te verwijderen. Hiertoe is een zogenaamd mixed matrix membraan ontwikkeld, een membraan met ingebedde deeltjes. Deze deeltjes hebben een adsorberende functie. In dit hoofdstuk wordt beschreven hoe vlakke mixed matrixmembranen (MMMen) bestaande uit twee lagen zijn ontwikkeld. De buitenste laag bevat ingebedde actieve koolstofdeeltjes in de membraanmatrix terwijl de membraanlaag aan de binnenkant (bloedcontactkant) geen deeltjes bevat. Deze binnenste laag kan de hemocompatibiliteit van het membraan verbeteren en tegelijkertijd het lekken van deeltjes naar de bloedcirculatie voorkomen. De MMMen, bestaande uit twee lagen, hebben een hoge schoon waterpermeatie en laten een hoge creatinine-adsorptie uit modeloplossingen zien. De zuivering van creatinine en de eiwitgebonden stof para-aminohippuurzuur uit humaan plasma door membranen bestaande uit een enkele of uit twee lagen is in overeenstemming met de zuivering door pure actieve koolstofdeeltjes. Dit laat een goede toegankelijkheid naar de ingebedde deeltjes in de MMMen zien bij deze experimentele omstandigheden. Daarnaast lijken de MMMen geschikt voor de zuivering van lastig-te-verwijderen eiwitgebonden stoffen. Ten slotte wordt in dit hoofdstuk getoond dat MMMen diffusie en adsorptie in een stap kunnen combineren.

In **hoofdstuk 3** wordt nader ingegaan op de ontwikkeling van holle vezel MMMen bestaande uit twee membraanlagen. De poreuze membraanlaag aan de binnenkant zit vast aan de mixed matrixmembraanlaag aan de buitenkant met ingebedde actieve koolstofdeeltjes. Het holle vezel MMM met twee lagen heeft een schoonwaterpermeatie in het ultrafiltratiebereik en adsorbeert

binnen vier uur respectievelijk 57%, 82% en 94% van de eiwitgebonden toxines p-cresylsulfaat, indoxyl sulfaat en hippuurzuur uit humaan plasma. Ook onder dynamische experimentele omstandigheden (cross flow experimenten met diffusie en convectie modus) zuivert het holle vezel MMM met twee lagen de eiwitgebonden toxines uit humaan plasma. Deze resultaten laten potentie zien van dit nieuwe type membraan voor de klaring van moeilijk te zuiveren eiwitgebonden toxines.

In **hoofdstuk 4** worden drie types adsorberende deeltjes onderzocht. De adsorberende deeltjes Norit actieve koolstof, Mast carbon en Y-carbon laten adsorptie zien van het kleine in water oplosbare molecuul creatinine, middel molecuul β2-microglobuline en de eiwitgebonden toxines p-cresylsulfaat, indoxyl sulfaat en hippuurzuur. De geteste adsorberende deeltjes kunnen dus een breed spectrum van uremische toxines adsorberen. Y-carbon lijkt meer β2-microglobuline te adsorberen per gram adsorberende deeltjes dan Mast carbon en Norit actieve koolstof, terwijl deze laatste twee deeltjes beter lijken te zijn in de adsorptie van eiwit gebonden toxines.

In **hoofdstuk 5** worden voor de eerste keer membranen gefabriceerd van het materiaal SlipSkin™, een copolymeer gemaakt van N-vinylpyrrolidone (NVP) and butylmethacrylaat (BMA). Er zijn ontwikkelingen gaande waarbij bloedzuiveringstherapieën met een langere behandelingsduur gunstige resultaten laten zien. Hierdoor ontstaat er meer intensief bloed-materiaal contact. Dit maakt het interessant om materialen te onderzoeken met een goede biocompatibiliteit. De morfologie van de membranen gemaakt van SlipSkin™ wordt beïnvloed door verschillende parameters zoals polymeercompositie, het type oplosmiddel en de oplosmiddelverdampingstijd. In dit hoofdstuk zijn SlipSkin™membranen met selectiviteitskenmerken van cascadefilters in plasmafractioneringstoepassingen ontwikkeld en deze laten een goede biocompatibiliteit zien. De SlipSkin™membranen hebben lage bloedplaatjes adhesie en gelijkwaardig goede eigenschappen wat

betreft contactactivatie, thrombogeniciteit, leukocytadhesie, hemolyse en complementactivatie vergeleken met membranen welke in klinisch gebruik zijn en andere referentiemembranen.

In **hoofdstuk 6** worden de conclusies van dit proefschrift gepresenteerd en daarnaast worden interessante richtingen voor toekomstig onderzoek beschreven voor de verdere ontwikkeling van membranen voor de zuivering van bloed voor betere kunstnieren.

Acknowledgements – Dankwoord

Plotseling is het voorbij, het project waar ik me vier jaar voor heb ingezet is klaar. Voordat ik verder ga met de volgende stap in mijn leven wil ik graag iedereen bedanken die mij heeft gesteund bij het doen van dit onderzoek en het vervaardigen van dit proefschrift. Een aantal mensen wil ik graag in het bijzonder noemen.

Thank you dr. Dimitris Stamatialis, for the chance you gave me to start with this research on a topic which was completely new for me. I learned a lot from you, especially the 'membrane courses' during meetings on Friday afternoon in the beginning of the project were very good to get into the topic. I enjoyed working with you, especially all the discussions we had during our meetings. However, I cannot be held responsible for all the phone calls which you did not pick up and kept endlessly ringing while we were in meeting. I appreciate the confidence you always had in me and in the results. Dimitris, thanks a lot for your supervision! Ook wil ik prof. Matthias Wessling van harte bedanken voor het vertrouwen dat je in me had en de vrijheid die je me gegeven hebt, ook wil ik je bedanken voor het vervullen van de rol als promotor. Prof. Dirk Grijpma wil ik graag bedanken voor de welkome ontvangst in zijn onderzoeksgroep en het plaatsnemen in de promotiecommissie. I would like to thank my promotion committee for reading and approving the concept of this thesis. Prof. Catapano, dr. Keller, prof. Koole, and prof. Lammertink thank you for taking place in my promotion committee and prof. Van der Steenhoven thank you for being chairmen.

Tijdens het onderzoek heb ik met meerdere onderzoeksgroepen samengewerkt en dit altijd als prettig ervaren. Graag wil ik Maarten bedanken voor onze samenwerking. Naast de metingen die je hebt gedaan, de experimenten die we hebben besproken was ook het doorsturen van alle samples voor mij erg fijn. Karin en Jaap, ook jullie wil ik van harte bedanken voor deze samenwerking. Griet en prof. Vanholder jullie wil ik graag bedanken voor het analyseren van de vele samples die ik gestuurd heb en ook voor het bespreken van de experimentele opzet. Ook wil ik Johan en Angelique

bedanken voor de samenwerking met betrekking tot de GAGs. In Maastricht ben ik altijd zeer welkom ontvangen en hebben we in de relatief korte tijd die ik aanwezig was veel kunnen doen. Hartelijk dank voor de samenwerking, Jorrit, Yvette, Leo, Jeroen, Rene, Jos, Jan en Yvonne. Jasper ook jou wil ik graag bedanken voor de samenwerking binnen het iNephron consortium. Natuurlijk wil ook hier de Nederlandse Nierstichting hartelijk danken voor de financiële ondersteuning van dit onderzoek.

I would like to thank all colleagues from both the Membrane Science and Technology group as well as from the Biomaterials Science and Technology group. Wendy, thank you for your support in the first year of research, I wish you all the best. Jeroen, bedankt voor alle gezellige momenten, ook toen ik niet meer in de MTO groep zat was het erg leuk om koffie te komen drinken en ik vind het fijn dat je mijn paranimf wilt zijn. Anne Corine, bedankt voor de leuke tijden en ik wens je veel succes met de laatste loodjes, you go girl! Sandra I enjoyed our conversations, I wish you the best for your career and personal life. Ook wil ik Bernke bedanken voor alle gesprekken en koppen thee die we gedronken hebben. Karina, I enjoyed our conversations and wish you the best for all your adventures. MTO girls, I enjoyed our drinks dinner dancing evenings Nazely, Geraldine, Oana, Ana, Olga K. (also thanks for the template and Word tip!), Bernke, Sandra and Anne Corine. Zandrie, bedankt dat ik met vragen altijd bij je terecht kon. Harmen, Antoine, Erik, Erik, Herman, Marcel, Ineke, Wika, Lydia, Hetty, Marc, Anita bedankt voor de (technische) ondersteuning. Greet en Karin, hartelijk dank voor de administratieve hulp en ook voor al het andere. John en Zlata, dank jullie wel voor alle bestellingen en ondersteuning. Erwin, de gezamenlijke ervaringen in China vond ik indrukwekkend en mooi om mee te maken en ik vind het fijn dat je mijn paranimf wilt zijn. Jos, ook jij bedankt voor de leuke tijd in China. Lydia dankjewel voor alle leuke gesprekken die we op kantoor hadden. Janine, ook ik vond onze gesprekken over de toekomst altijd leuk! Suvi thank you for the nice conversations, you brought lots of energy into the group! Seb, thank you for all the nice jokes and all the times you made me smile, but please lock the door of the office! Thank you for all nice

moments, Can, Szymon, Katja, Beata, Enver, Zeynep, Gor, Harro, Kitty, Mayur, Matias, Erik, Petra, Hans, Ikenna, Nicolas, Jigar, Kishore, Srivatsa, Giri, Nieck, Louis, David, Jumeng, Susanne,

Al-hadidi, Christina, Henny, Emiel, Mieke, Frank, Marcel, Hammad, Martin, Shariar, Aga, Bade, Frits, Bas, Piet, Vincent, Xiaoling, Andre, Mark, Hans, Niels, Sytze, Tony, Jos, Niels, Rene. I especially look back with a good feeling to all the nice coffee breaks, lunches and conferences and other activities. I would like to thank all my office mates for all the nice moments as well: David, Sander, Izabela, Wojciech, Elif, Joris, Yusuf, Lydia, Suvi, Sebastien. Ook wil ik de studenten Odyl, Pieter, Marco, Anno en Ricardo bedanken voor hun bijdrage aan het onderzoek.

Daarnaast wil ik ook graag een aantal personen bedanken uit mijn persoonlijke kring. BMW-dames, Moniek, Marieke, Marieke TV, Lieke, en Gerrita dank jullie wel voor jullie luisterend oor, gezelligheid en tips op onze dates die me altijd heel goed doen. Sabine en Sanne, ook jullie bedankt voor jullie interesse en gezelligheid. Karen, Lieke, Danielle, Marije, Marieke en Karolien, ook jullie wil ik van harte bedanken voor de gezelligheid in al die jaren dat we elkaar al kennen, laten we zo doorgaan. Raymond & Nicole, Niek & Korien, Laurens & Elles, Dennis & Eline, Huub & Ramona, Paul & Sharon, Jeroen & Marjan, Gert en Bernardo, ook al was het voor jullie misschien niet altijd duidelijk waar ik nou mee bezig was, ik waardeer jullie interesse en gezelligheid van de afgelopen jaren.

Verder wil ik graag mijn familie en schoonfamilie bedanken voor jullie interesse en steun. Gerrit, Suze, Marieke, Harold, Gert-Jan, Monique en Herman dank jullie wel voor jullie belangstelling, steun en tips. Mijn lieve zusjes, Laurien en Carlijn, en natuurlijk ook Patrick en Danny, ik wil jullie bedanken voor alle steun, het altijd klaarstaan, interesse en gezelligheid die we met elkaar hebben. Pap en mam, bedankt voor jullie liefde, interesse en gezelligheid. Bedankt dat jullie er altijd voor mij zijn en ook bedankt voor het vertrouwen en de vrijheid die jullie me altijd hebben gegeven. Lieve Henk, dankjewel voor de liefde die je me geeft, samen met jou is alles nog veel leuker. Ik kijk erg uit naar onze verdere toekomst samen, ik hou van je.

Marlon

About the author

Marlon Tijink was born at February 5th 1985 in Almelo, The Netherlands. In July 2003, she received her VWO diploma (pre-university education) from the Twents Carmel College in Oldenzaal. She started her study Biomedical Sciences in September 2003 at the Radboud University in Nijmegen, and obtained her Bachelor of Science diploma. She continued her studies with the Master Biomedical Sciences and she choose the specializations pathobiology and toxicology and she obtained her Master diploma cum laude. During her studies she performed a study on cryopreservation of bovine ovaries at the University Medical Centre Nijmegen as well as a study on the effects of benzene metabolites on chromosome segregation and spindle positioning at the University of Utrecht in collaboration with the Institute for Risk Assessment Sciences. She finalized her master with an internship at King's College London and St. Thomas' Hospital in London, UK, where she studied the functional impact of diet induced obesity on the uterus. Marlon started her PhD research in January 2009 under supervision of dr. Dimitris Stamatialis and prof. Matthias Wessling and she worked at the Membrane Science and Technology group as well as the Biomaterials Science and Technology group at the University of Twente. The results of her PhD research are described in this thesis. During this multidisciplinary project, she collaborated with other researchers at the University medical center Utrecht, University medical center Nijmegen, University Hospital Gent in Belgium, University medical center Maastricht, and Maastricht University. Furthermore she visited and presented on several international conferences and won two awards. Besides her research project, Marlon participated in the organization of the NanoMemCourse and she was member of the Faculty Council of the Technology and Science faculty of the University of Twente. After finishing her PhD project, Marlon started working at Fresenius HemoCare Netherlands B.V. as product developer.

List of publications

Tijink MSL, et al. A novel approach for blood purification: Mixed-matrix membranes combining diffusion and adsorption in one step. Acta Biomaterialia 2012;8:2279-87.

Tijink MSL, et al. Novel Concept for Artificial Kidney: Mixed Matrix Membranes Combining Diffusion and Adsorption in One Step. Procedia Engineering 2012;44:451-3.

Tijink MSL, et al. Membranes with embedded sorbents for an artificial kidney. International Journal of Artificial Organs 2011;34:653-4.

Tijink MSL, et al. Mixed matrix membranes for toxin removal from blood. International Journal of Artificial Organs 2010;33:460-.

Tijink MSL, et al. Mixed matrix membranes: a new asset to extracorporeal treatments? Submitted.

Tijink MSL, et al. Hollow fiber mixed matrix membranes for removal of protein-bound toxins, in preparation.

Tijink MSL et al. Novel membranes for blood contacting applications, in preparation.